UiT
THE ARCTIC UNIVERSITY OF NORWAY

Faculty of Health Sciences

Production and purification of recombinant C-terminal truncated pro-Matrix Metalloprotease-9

Fatema Rahman

Master thesis in Biomedicine
16th June 2016

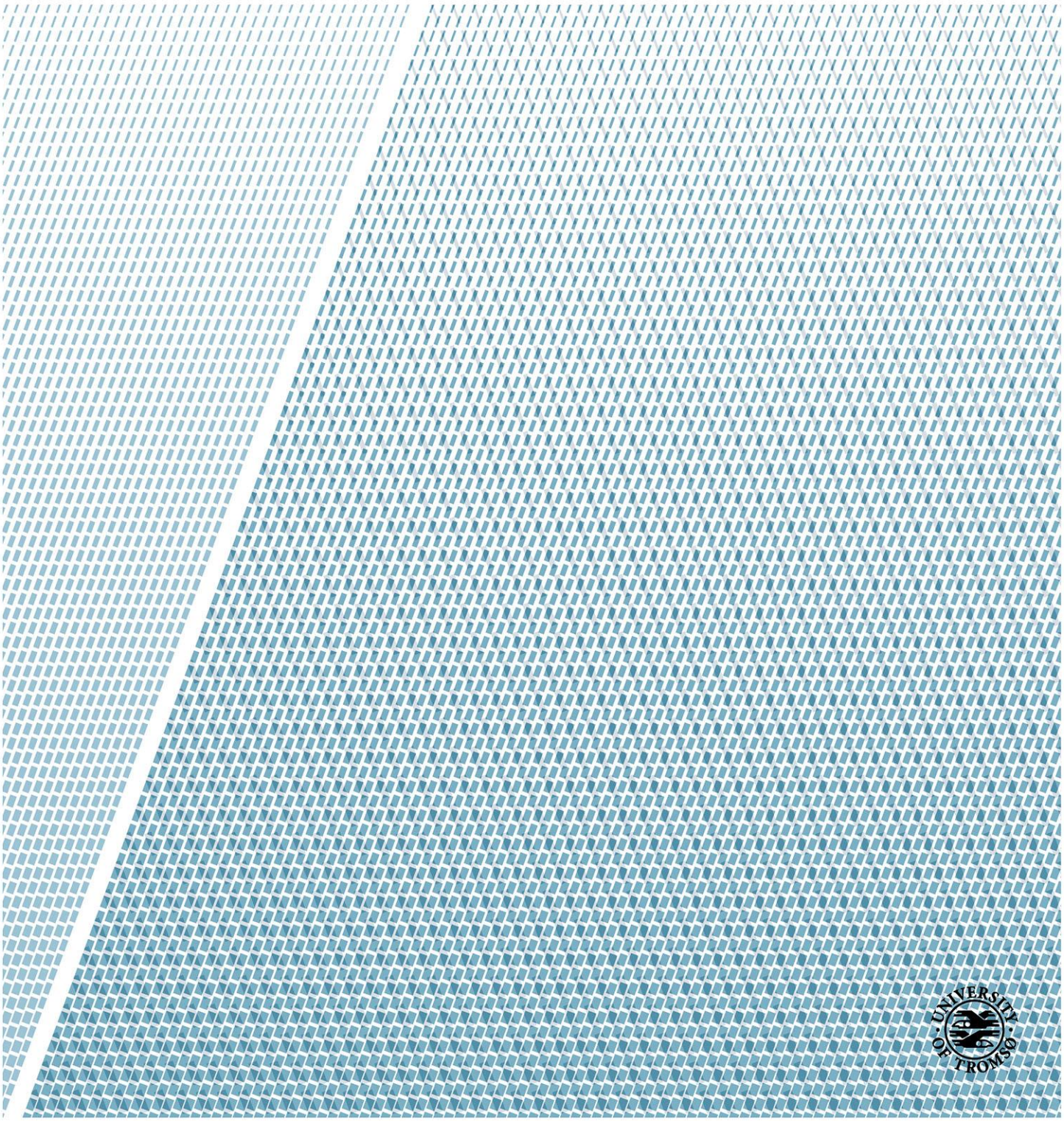

Contents

Acknowledgements

The present work was performed at the Tumour Biology Research Group, Institute of Medical Biology, University of Tromsø from August 2014-January 2015 and from January 2016-May 2016.

First and above all, I praise Allah, the almighty, for giving me the strength and opportunity to carry on this project and granting me the capability to proceed successfully. I also grateful for his blessing with guidance and assistance of many great people in giving the shape of this current thesis.

I express my deepest regards and gratitude to my main supervisor Assistant Prof. Gunbjørg Svineng for her sincere effort, guidance, critical comments and patience throughout the whole stages of bringing this project into light. My sincere gratitude goes to my co-supervisor, Prof. Jan-Olof Winberg for his unlimited encouragement, thoughtful guidance, and correction of the thesis. I have been extremely lucky to have such kind supervisors who really cared so much about my work, and responded to any questions and queries that I had.

I want to express my deep thanks to my esteemed Eli Berg for her constant support in laboratory work as well as her additional care of my health. I will never forget her such motherly responsibilities of making dry food for me in pregnancy period while conducting the experiment in the lab. She was inspiration, energy and full of happiness for me throughout the research work.

I must be indebted to Senior Researcher Nabin Malla for his guidance, support, and valuable suggestions in conducting the critical laboratory work. I would like to thank all members of the Tumour Biology Research Group for their cordial support and cooperation and friendly attitude.

I am grateful to all of my friends specially Yakubu Abudu Princely for his help and suggestions relating to the studies.

I cannot finish without thanking my two beloved boys Saifan and Saihan. Their unlimited dedication and lovely contribution really helped me to make this effort successful. You two are my soul also belong to this achievement. Love both of you so much papa.

I would especially like to express my deepest gratitude to my younger sister, Farhana Rahman, for being around me in taking all family responsibilities throughout writing period of this thesis. Words will not be enough to express my love for her.

Last but not least, I would like to express my very profound gratitude to my husband for his unfailing support and continuous encouragement throughout my years of study. His unmeasurable dedication and inspiration always boosted my confidence. This accomplishment would not have been possible without you my handsome hubby. Love you so much.

May Allah bless you all

Abbreviations

BSA	Bovine serum albumin
DMSO	Dimethyl sulfoxide
DTT	Dithiothreitol
ECM	Extracellular Matrix
HEPES	4-(2-hydroxyethyl)-1-piperazineethanesulfonic acid
HRP	Horse radish Peroxidase
kDa	Kilodalton
MMP	Matrix metalloprotease
MMP-9ΔH-HPX	Hinge and hemopexin truncated MMP-9
PAGE	Polyacrylamide gel electrophoresis
PCR	Polymerase chain reaction
SDS	Sodium dodecyl sulfate
TBST	Tris-buffered saline -Tween
TIMP-1	Tissue inhibitors of metalloprotease-1

Abstract

Matrix metalloprotease-9 (MMP-9) consists of an N-terminal signal peptide, a pro-domain, followed by the catalytic domain that comprises of three fibronectin-like repeats, and a unique hinge region that connects the N-terminal to the C-terminal hemopexin-like domain. Naturally, MMP-9 is secreted by a wide number of cell types. In this study, we produced a truncated proMMP-9 lacking the C-terminal hemopexin domain and the hinge region. We used Sf9 insect cells and the BaculoDirect™ Baculovirus expression system. To produce this truncated variant of MMP-9, site directed mutagenesis was used to generate a point mutation that resulted in a stop codon. We designed two mutagenic primers containing the desired mutation. We changed G to T in the codon GAA code for the amino acid glutamate at the position 448 using a Gateway compatible vector pDONR221-*MMP-9.* The amino acid E-448 is located just after the catalytic domain and in the start of the hinge region. The mutated *proMMP-9ΔH-HPX* and the full length *proMMP-9* were cloned into the Baculovirus genome and by transfecting Sf9 cell with these clones, we produced proMMP-9 and proMMP-9ΔH-HPX.

Both proMMP-9 and proMMP-9ΔH-HPX were purified by employing the Gelatin Sepharose Chromatography and Size Exclusion chromatography. Gelatin zymography revealed the gelatinolytic activity and molecular size of the truncated proMMP-9. The molecular size of the truncated form of proMMP-9 was estimated to be approximately 48 kDa by gelatin zymography, and the purity of the produced protease by SDS-PAGE and Coomassie staining. The identity of the protease was established by Western blot and Mass spectrometry.

Introduction

Extracellular Matrix (ECM)

A complex network of macromolecules presents within all tissues and organs called extracellular matrix (ECM). This non-cellular component provides not only necessary physical support for the cellular constituents but also launch significant biochemical and bio-mechanical stimuli required for tissue morphogenesis, differentiation and haemostasis (Frantz et al., 2010). Each tissue has ECM with a unique cellular composition. Basically, the ECM is composed of water, proteins and polysaccharides. Variation in the relative amount of the different macromolecules and their way of organization in the ECM give rise to an excellent diversity of forms capable of adapting in the functional requirements of the particular tissue. ECM can generate biochemical and mechanical properties of each organ, such as its tensile and compressive strength, and elasticity by changing into calcified form to make bone or teeth, transparent matrix of cornea, basal lamina between epithelial and connective tissue (Alberts B., 2002).

The common thinking used to be that ECM serves mainly for the physical structure of the tissue. However, recent studies revealed its active and complex role in regulating the cell behaviour by influencing their survival, development, migration, proliferation, shape and function (Alberts B., 2002). ECM directs necessary morphological organization and physiological function by binding growth factors (GFs) and interacting with cell surface receptors to stimulate signal transduction and regulate gene transcription (Frantz et al., 2010) (Fig.1).

Molecular composition of the ECM

The ECM is composed of two main classes of macromolecules; proteoglycans (PGs) and fibrous proteins that are secreted locally and assembled into an organized network in close contact with the surface of the cell that produced them (Jarvelainen et al., 2009; Schaefer and Schaefer, 2010). PGs are spectacularly complex macromolecules that each contain a core protein to which various forms of glycosaminoglycan chains (GAGs) are covalently attached (Hay, 1991). PGs in connective tissue form a highly

hydrated gel like ground substance in which the fibrous proteins such as collagen, elastin, fibronectin and laminin are attached (Vakonakis and Campbell, 2007).

Versatile environment of the ECM

ECM dynamics are a feature of tissues undergo radical remodelling and this can result from the changes of altered ECM composition by synthesis or degradation of one or more ECM components. One of the most significant enzyme families involved in ECM remodelling are matrix metalloproteases (MMPs) (Cawston and Young, 2010).

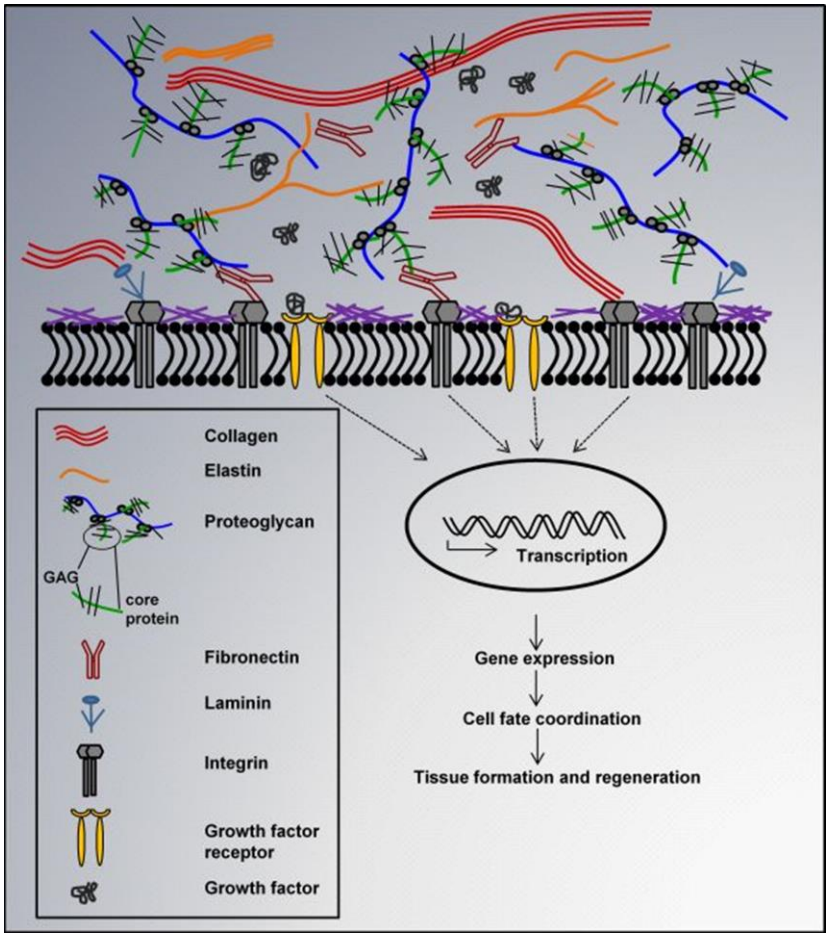

Figure 1. Schematic presentation of major ECM components and their interactions with cells, with permission (Georgia et al., 2012).

MMPs and MMP family members

MMPs are collectively known as matrixins and are zinc-dependent multi domain endopeptidases (Dufour et al., 2008b; Yabluchanskiy et al., 2013). They play a crucial role in morphogenesis, tissue repair, wound healing and tissue remodeling in normal physiological processes and also in response to various injuries (Nagase et al., 2006). These proteases are known to cleave all structural elements of ECM, as well as non-ECM substrates (Massova et al., 1998; Nagase et al., 2006; Yabluchanskiy et al., 2013).

Previously mentioned, the ECM represents a complex and dynamic structure made of different types of proteins molecules which actively interact with cells. It also serves as a reservoir for many biologically active molecules such as cytokines, proteases, growth factors, chemokines, cell factors or growth factor receptors (Sheikh, 2013).

Different types of proteases, for example plasmin and cathepsins, are associated with ECM degradation but the most significant enzymes are considered to be MMPs (Massova et al., 1998; Nagase et al., 2006). The breakdown of ECM molecules or cell surface molecules changes cell-matrix and cell-cell interactions. The release of biologically active molecules, for example growth factors that remain attached to the ECM, makes them available for cell receptors (Jarvelainen et al., 2009) and hence promotes cell differentiation and survival and can lead to many diseases (Fig. 2).

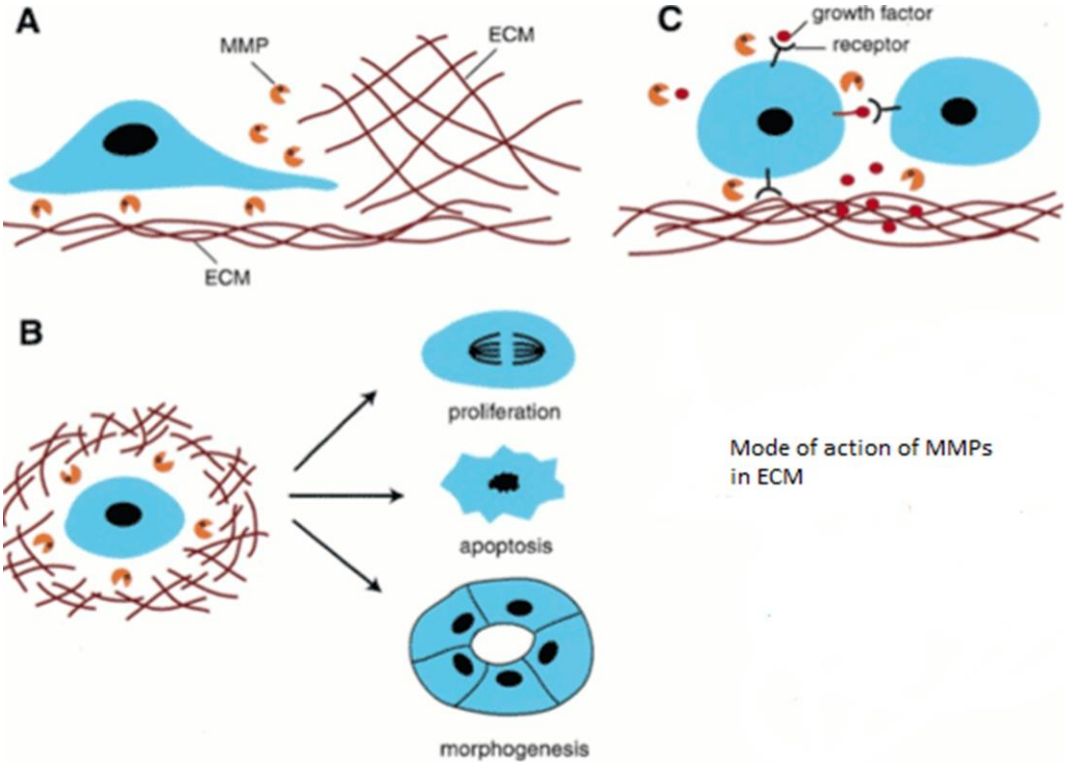

Figure 2. Mode of action of the matrix metalloproteases in the ECM. (**A**) MMPs can affect cell migration by changing the cells from having an adhesive to a non-adhesive phenotype, and also by degrading the ECM. (**B**) MMPs are able to alter ECM microenvironment affecting cell proliferation, apoptosis, or morphogenesis. (**C**) MMPs may modulate the activity of biologically active molecules such as growth receptors and pro-angiogenic factors (VEGF, TGF-b). With permission (Ghulam and Ishfaq, 2013)

To date, 25 family members of MMPs have been identified in vertebrates. Among them, 23 members including duplicated MMP-23 genes are found in human (O'Connell et al., 1994). MMPs are also found in Sea urchins (Hobeika et al., 2007b) and plants like Arabidopsis (Ra and Parks, 2007).

Historically, MMPs were named depending on their preferential action on matrix components. Currently, a classification based on their domain organization is favoured. MMPs are classified into four groups; archetypal MMPs, matrilysins, gelatinases and furin-activated MMPs. Their typical structure consists of a signal peptide (SP), a prodomain, a catalytic domain, a hinge region, and a hemopexin like-domain (Gong et al., 2014) (Fig 3).

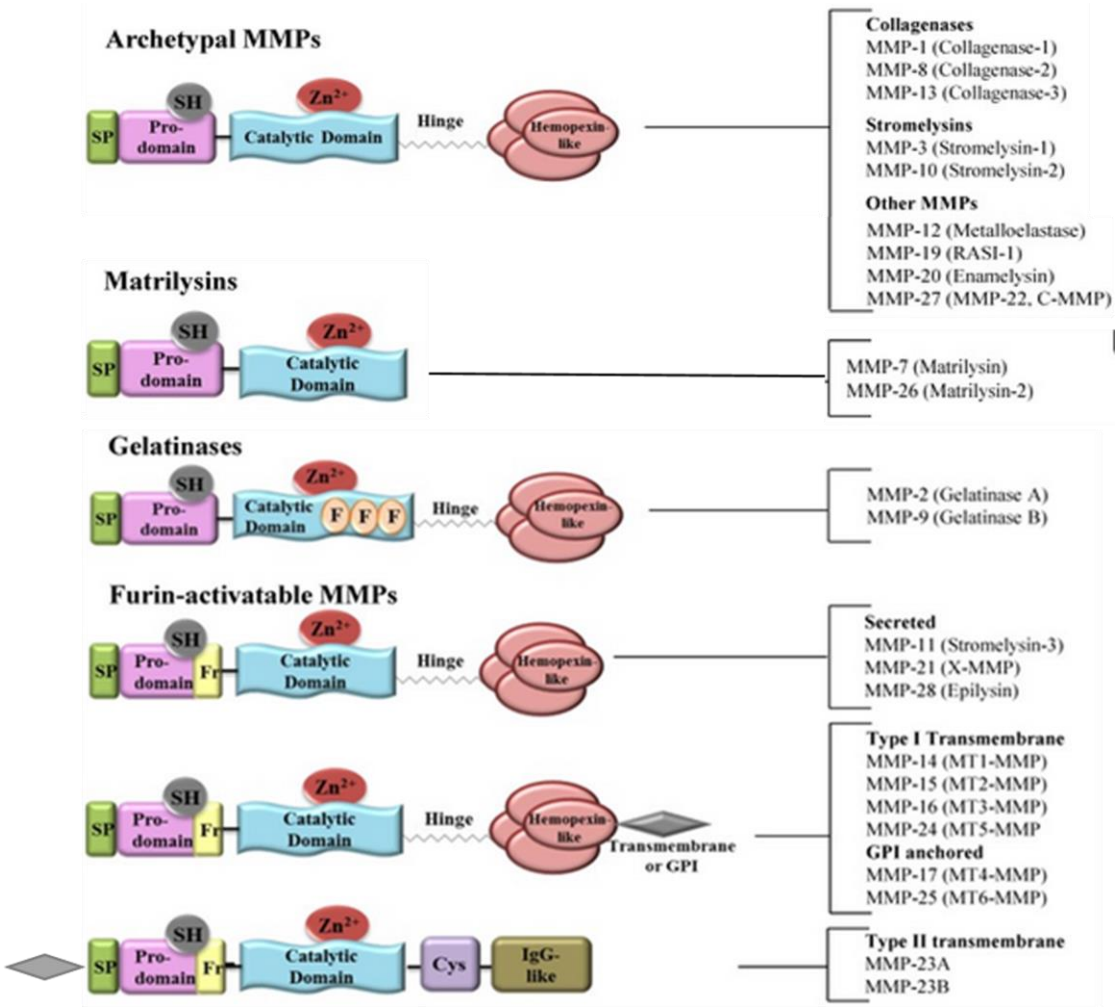

Figure 3. Domain structure and classification of mammalian MMP family members. The archetypal MMPs include collagenases, stromelysins and others based on their substrate specificities. Matrilysins lack the hemopexin domain and hinge region. Gelatinases have fibronectin repeats (Fn) in their catalytic domain. Furin-activated MMPs contain a furin (Fr) recognition motif and this type MMPs include three secreted, six membrane type (MT) and two unusual type II transmembrane MMPs. According to attachment to the plasma membrane, MT-MMPs are divided into type I transmembrane MMPs and glycophosphatidylinositol (GPI) MMPs. Type II transmembrane MMPs do not have the cysteine switch motif in the pro-domain, and the hemopexin domain, instead they have a cysteine array (Cys) followed by an immunoglobulin-like (IgG-like) domain (Gong et al., 2014).

All MMPs, except the two Matrilysins (MMP-7 and MMP-26) and MMP-23 constitute a hemopexin-like domain and a hinge region. The catalytic domain in MMP-2 (gelatinase A) and MMP-9 (gelatinase B) differs from that of the other MMPs as the domain also contain a module of three fibronectin-type II-like repeats. MMP-11 and MMP-28 possesses a furin motif for recognition by furin-like serine proteases. This motif is also present in MMP-21 and in membrane-type MMP (MT-MMP). There are eight different MT-MMPs, four contain a C-terminal type 1 transmembrane domain, two contain a C-terminal GPI anchor while the last two MMP-23 A and MMP-23B contain at the N-terminal a type II transmembrane domain and instead of the C-terminal HPX domain these two MMPs contain a cysteine array and an immunoglobulin-like domain (Gong et al., 2014) (Fig.3).

MMP-2 and MMP-9

The two MMPs, MMP-2 and MMP-9, are known as gelatinases due to their potent gelatin-degrading capacity (Cauwe and Opdenakker, 2010). They are the closest homolog in this family and share four highly homologous domains. The main structural difference between the two gelatinases is the presence of an extremely O-glycosylated hinge region in MMP-9 (Opdenakker et al., 2001b; Van den Steen, 2006).

Degradation properties of MMP-2 and MMP-9 are closely associated with multiple pathologies, including cancer, bone diseases, inflammatory disorders and vascular alterations such as atherosclerosis, aortic aneurysm and myocardial infarction (Hu et al., 2007) and this has in particular attracted biomedical investigators to study MMP-9 to great extent. A long term study on MMPs revealed their importance in the biomedical investigation. From the figure 4, it can be seen that since 1995 the study on gelatinases has grown exponentially. Within the MMPs Pubmed literature, gelatinases were overrepresented and MMP-9 was the top studied with more than 50% of all MMPs literature (Vandooren et al., 2013) (Fig.4).

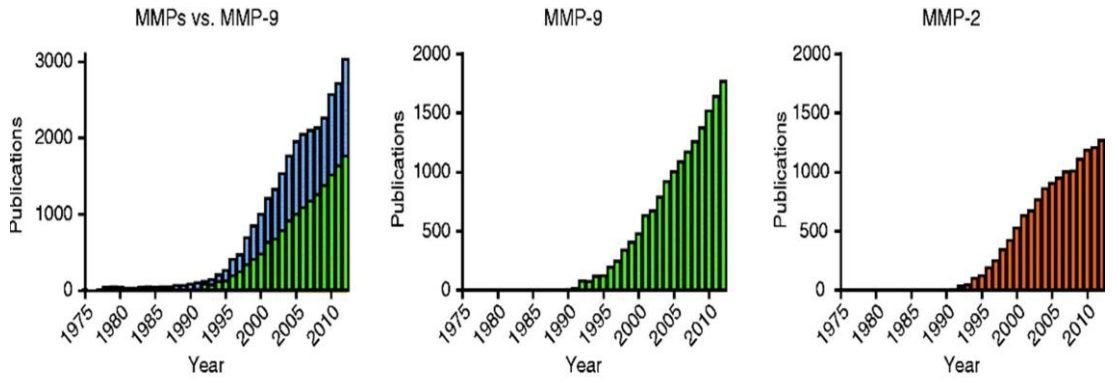

Figure 4. Evolution of the PubMed literature on all MMPs, MMP-2 and MMP-9. MMP-2 and MMP-9 were the most studied MMPs in the past decades. MMP-9 reached top at more than 50% of all MMP literature (Vandooren et al., 2013).

MMP-9 gene

The human MMP-9 gene is located on the long arm (q) of chromosome 20 between positions 11 and 13. This gene consists of 7654 base pair (Homo sapiens Annotation Release 107, GRCh38.p2 (NCBI)) (Fig.5).

Figure 5. Location of human *MMP-9* gene on the chromosome no 20. An arrow showing the position of MMP-9 gene. Modified from Homo sapiens Annotation Release 107, GRCh38.p2 (NCBI).

MMP-9 domains structure and their function

MMP-9 is synthesized as an inactive zymogen referred to as "proMMP-9 (92-kDa)". The domain structure of proMMP-9 consists of an NH_2-terminal pro-domain, a catalytic domain, a hinge domain and a COOH-terminal hemopexin-like domain (Fig. 6A). At the very N-terminal of *preproMMP-9* a signal peptide is located. In the initial phase of translation, this signal peptide directs the growing polypeptide to the endoplasmic reticulum. Next to the signal peptide there is a hydrophobic pro-peptide domain which

consists of approximately 80 amino acids including a highly conserved “cysteine switch” sequence (PRCGXPD). This interacts with the catalytic zinc atom through its side chain thiol group (Massova et al., 1998) and maintain the inactive form of the enzyme (Springman et al., 1990; Van den Steen, 2002b) (Fig.7).

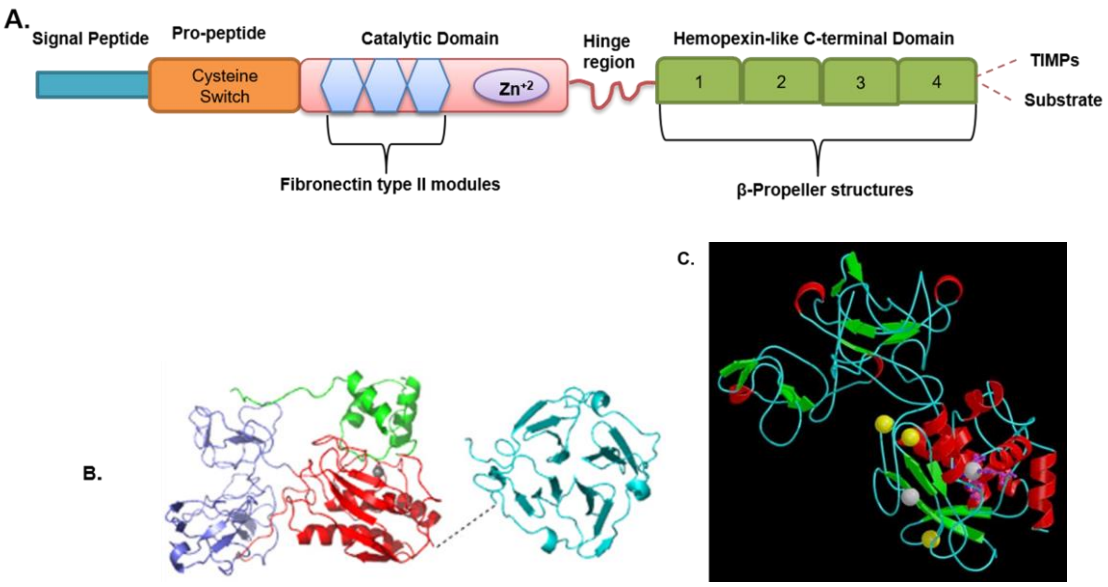

Figure 6. Illustration of domain arrangement of preproMMP-9. **A**. Besides signal peptide in N-terminal region, three domains are the pro-domain, catalytic domain, and the hemopexin-like C-terminal domain connected to the catalytic domain via a flexible hinge region. Inactive MMP-9 or zymogens contains cysteine switch in the pro-domain which must be cleaved to activate the protease. The catalytic domain has three repeats of fibronectin type II module help in binding gelatin. β-propeller structures in the C-terminal domain provide a substrate or TIMP recognition site. **B**. Crystal structures of the N-terminal domains of proMMP-9. The N-terminal pro-peptide (green), three fibronectin type-II repeats (blue), and a catalytic domain (red). A zinc-containing active site in the catalytic domain (grey sphere) (Van den Steen, 2002a). The hinge region (dashed line) contains 64 residues. Crystalization of hinge region in proMMP-9 separately or together with other protein domain has been found difficult due to its built-in bend structure and also its elasticity properties. This region connects the N-terminal domain to the C-terminal hemopexin domain which consists of four propeller blades (cyan) (PDB code: 1ITV) (Cha, 2002; Elkins, 2002). **C**. The catalytic and structural zinc ions are shown as light grey spheres. The structural calcium ions are shown as yellow spheres (PDB code: 1L6J).

MMP-9 has a unique domain inserted into the catalytic domain called fibronectin-like module consisting of three FnII like repeats. This module is homologous to the type II module of fibronectin. The fibronectin-like module is essential for MMP-9 in binding to

denatured collagen (i.e. gelatin) (O'Farrell and Pourmotabbed, 1998). A metal binding site contain a zinc-binding motif that bind catalytic zinc (Fig. 6B and C). The catalytic domain of MMP-9 has additional binding sites for a structural zinc ion and 2-3 calcium ions. These ions are required for the enzymes stability and expression (Fig. 6C). The second zinc ion is located in the catalytic domain around 12 Å away from the catalytic zinc ion (Gupta, 2012).

An elongated linker between the catalytic and hemopexin-like domain is known as the hinge region. This hinge region is around 64 amino acids long and is rich in proline, serine and threonine residues. Previously, the hinge region used to also be called the collagen type V-like domain due to its homology to collagen type V. Later, it was found that the homology with collagen type V was rather low because of its high proline content and the name was no longer used (Wilhelm et al., 1989). The hinge region is an independent protein domain and rich in O-linked glycans and henceforth has also been called the O-glycosylated domain or OG domain (Van den Steen, 2006). The structure of hinge region is unique and important for substrate binding. A number of studies revealed that this domain is crucial for correct MMP-9 function. It has been known that TIMP-1 binds to the C-terminal part of proMMP-9 (Murphy et al., 1991; Oconnell et al., 1994). The hinge region influences the binding of TIMP-1 to the hemopexin domain. Deletion of the hinge region leads to a 10-fold decreased affinity for TIMP-1 and interrupt internalization by the cargo receptors low density lipoprotein-related protein (LRP-1(CD91)) and LRP-2 (megalin) (Van den Steen, 2006). In addition, deletion of this domain also reduces MMP-9-mediated cell migration (Dufour et al., 2008a), and lowers the efficiency of degradation of large gelatinous substrates to great extent (Vandooren et al., 2011). Furthermore, structural studies revealed that this O-glycosylated domain is necessary for proper orientation and for flexibility of proMMP-9 (Rosenblum et al., 2007; Van den Steen, 2006).

The hemopexin like domains in MMPs have structural homology with hemopexin protein that are profoundly present in plasma. Human MMP-9 shares only 25–33% amino acid identity with hemopexin domains from other MMPs (Dufour et al., 2011). Hence revealed the uniqueness of MMP-9 within the MMP family. The C-terminal hemopexin domain of MMP-9 forms a propeller with four blades where the first blade is linked to the fourth one by means of a disulfide bridge (between Cys516 and

Cys704) (Fig.6-7). This covalent linkage is critical for interaction with substrates and binding to cell surface receptors (Fouad A. Zouein, 2015).

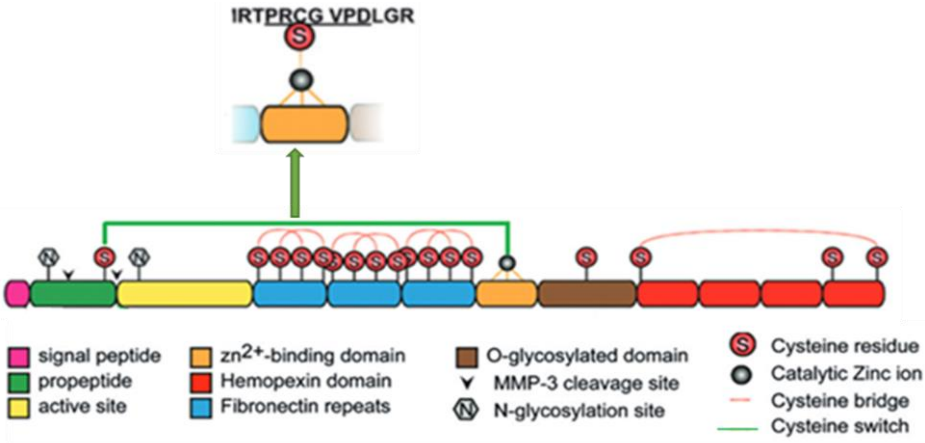

Figure 7. The mechanism of inactivation and cystein bridges of proMMP-9. The proMMP-9 sequence contains 17 cystein residues in which a highly conserved cysteine switch sequence (PRCGVPD) of pro-domain interacts with the catalytic zinc atom through its side chain thiol group to maintain inactive form. Each of the three fibronectin repeats forms two cysteine bridge whereas HPX domain possess one cysteine bridge. Modified from (Vandooren et al., 2013).

Until now, four functions of the hemopexin domain in MMP-9 have been recognized. Those are (i) interaction with substrates, (ii) binding to inhibitors, (iii) binding to cell surface receptors and (iv) induction of auto-activation. The substrates known to bind to HPX of MMP-9 are gelatin, collagen type I, collagen type IV, elastin and fibrinogen (Burg-Roderfeld et al., 2007; Roeb et al., 2002), and their affinity is higher for full-length proMMP-9 than for activated MMP-9 without pro-peptide (Burg-Roderfeld et al., 2007). The HPX domain also interacts with the inhibitors TIMP-1 (Goldberg et al., 1992) and TIMP-3 (Butler et al., 1999), beside binding to several cell surface molecules such as LRP-1, LRP-2 (Van den Steen, 2006), DNA repair protein (Ku) (Monferran et al., 2004), Cell surface glycoprotein (CD44) and Reversion-inducing cysteine-rich *protein* with Kazal motifs (RECK) (Dufour et al., 2008a; Sternlicht and Werb, 2001). In addition, HPX like domain has a role in proper orientation of MMP-9 through the hinge region and in localization of MMP-9 to the membrane by the interaction with the Ku70/Ku80 heterodimer (Monferran et al., 2004). Furthermore, the

HPX domain is found to mediate dimerization or multimerization by noncovalent, and mainly by hydrophobic, interactions at the fourth blade of the domain (Cha et al., 2002b). Recently, HPX domain is discovered to take part in proMMP-9 autocatalysis by binding of heme with hemopexin domain and thereby initiate activation of the enzyme. β-hematin interacts with the MMP-9 HPX domain and bring about autocatalytic processing of proMMP-9 (Geurts et al., 2008). Similarly, a complex of MMP-9 with a chondroitin sulfate proteoglycan (CSPG) is secreted by a macrophage cell line (THP-1) (Winberg, 2000) and is found to be covalently linked via the HPX domain (Winberg et al., 2003).

Amino acid sequence of pre-proMMP-9

The preproMMP-9 consists of total 707 amino acid residues in which 19 amino acid residues in signal peptide, 166 amino acid residues in FnII module and 187 amino acid residues in HPX domain (Fig.8). The domains indication in the figure 8 was done following the information from Vandooren et al., 2013.

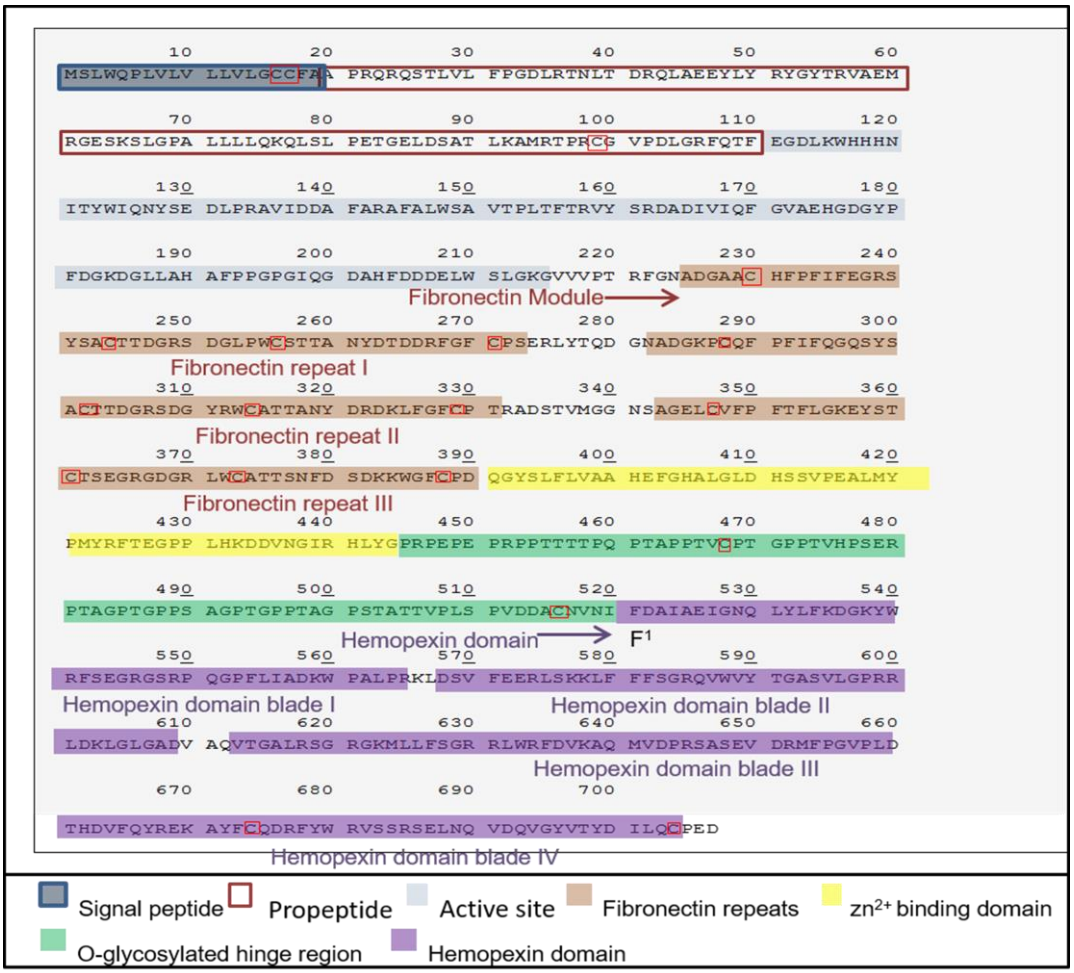

Figure 8. Amino acid sequence of preproMMP-9. The sequence of different domains was indicated by different colours where Cystein residue s were marked in red. The sequence of human preproMMP-9 was taken from the MEROPS database (Rawlings et al., 2014) and the domain indication was done based on the information from (Vandooren, et al., 2013).

Monomer, oligomers, complexes and truncated forms of MMP-9

Besides the monomeric form, MMP-9 is found to forms oligomeric structures and complexes with other molecules, as well as low-molecular weight truncated forms. It is postulated that one intermolecular cysteine bridge is required to form dimer whereas two bridges for trimers and so on. MMP-9 is found to form complexes with Neutrophil gelatinase-associated lipocalin (NGAL) by covalent linkage (Triebel et al., 1992b). Truncated form of MMP-9 is also observed in which different proteases including

MMP-3, kallikrein-related peptidase 7 and meperin-α are involved. MMP-3 generates a 65 kDa form of MMP-9 which lacks NH_2 -terminal pro-peptide and COOH-terminal hemopexin domain (Okada et al., 1992).

Cell expression of MMP-9

MMP-9 is secreted by a large number of cell types, including neutrophils, Polymorpho-Nuclear Leukocytes (PMN), keratinocytes, monocytes, macrophages, osteoblasts, fibroblasts, endothelial cells, and some malignant tumor cell lines including MDA-MB-231 breast cancer, HT-1080 fibro sarcoma and A2058 melanoma cell lines, (Mackay et al., 1992; Opdenakker et al., 2001c; Van den Steen, 2002b).

MMP-9 expression, synthesis and activation

Normally, the expression of most MMPs is low in tissue and it is only induced when remodelling of the extracellular matrix (ECM) is required (Van den Steen, 2002a). The transcription of *MMP-9* gene is initiated with the stimulation of various physiological factors including cytokines and growth factors. Among these factors are interleukins, interferon, Nerve Growth Factor (NGF), Epidermal Growth Factor (EGF), basic Fibroblast Growth Factor (FGF), Vascular Endothelial Growth Factor (VEGF), Platelet Derived Growth (PDGF), and Tumour Necrosis Factor (TNF-a), Transforming Growth Factor (TGF-b), the Extracellular Matrix Metalloproteinase Inducer (EMMPRIN), oncogene product, metal ions, reactive oxygen species or hormones. Many of these factors induce the expression or activation of c-fos and c-jun proto-oncogene products. These products hetero-dimerize and bind to the activator protein-1 (AP-1) sites within MMP-9 gene promoters for expression (Jodele et al., 2006).

Actually, the nature of the stimulus and the cell type normally determine which transcriptional factors will be involved in MMP-9 gene expression. At the position of –79 to –73, the AP-1 most likely is to be considered as the most critical binding motif for MMP-9 transcriptional activity. Maximal expression of MMP-9 by TNF-α through AP-1 requires the association of other transcription factors, such as Sp-1 and NF-κB. Sp-1 located at position –558 to –563 and a NF-κB consensus sequence located at position –601 (Fig. 9).

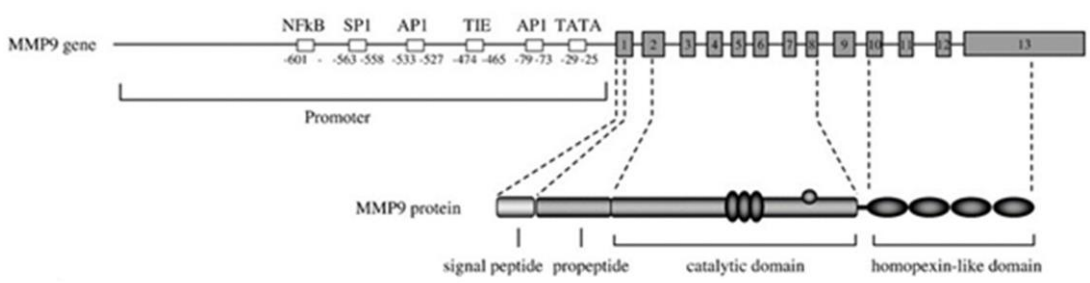

Figure 9. The principal binding motifs of transcription factors in the promotor region of *MMP-9*. Open boxes denote *cis*-elements: NFkB, transcription factor NFkB binding site; SP1, transcription factor SP1 binding site; AP1, transcription factor AP1 binding site; TIE, transforming growth factor β1 inhibitory element, TATA box. Closed boxes denote 13 exons involve in MMP-9 expresion (St-Pierre et al., 2004).

In MMP-9, the transcription factors ETS (Erythroblast Transformation Specific) recognize the purine rich GGAGAGGAAG motif located at position -540 and act synergistically with NF-κB, SP-1 and AP-1 binding sites when cells are activated by the Ras oncogene (Gum et al., 1996). Furthermore, Epidermal Growth Factor (EGF) can also potentiate MMP-9 promoter activation through AP-1 in breast tumor cell lines (Watabe et al., 1998).

However, after transcription the MMP-9 mRNA translated into preproMMP-9 where the pre-domain directs the polypeptide chain to the endoplasmic reticulum where the pre-domain is cleaved off. N-glycosylation occur co-translationally on the nascent protein whereas O-glycosylation occur during later post translational stages in the Golgi apparatus and trans-Golgi when MMP-9 proteins are already folded (Van den Steen et al., 1998). In the ER of the cell, 85 kDa MMP-9 is altered into 89 kDa intermediately glycosylated form and at the end of glycosylation it becomes into 92 kDa after passing through the Golgi complex (Hanania et al., 2012; Olson et al., 2000). Glycosylation is found to have higher impact on the enzyme catalytic efficiency and oligomerization, also on the intra- and inter-domain flexibility (Fouad et al., 2015). In this process of synthesis, proMMP-9 acquires its tertiary structure that is identified by O- glycosylation in the hinge region and seven disulfide bridges (Fig. 7).

Disulfide bond formation between two cystein residues of MMP-9 is the most well-known post translational modification. The MMP-9 translated sequence contains 19 cysteine residues (Fig. 6-8) where two of them are located in the signal peptide (Wilhelm et al., 1989). Upon cleavage of signal peptide during translation, proMMP-9 remains with 17 cysteine residues (Hibbs et al., 1985). Seven disulfide inter-domain bridge is formed by 14 cysteine residues. Six of these disulfide bonds are to be found within the fibronectin-type II repeats of the catalytic domain and are significant for proMMP-9 secretion. (Wilhelm et al., 1989; Khan et al., 2012). The remaining one disulfide bond interconnects blade I and IV within hemopexin domain (Cha et al., 2002a). Out of the rest three cysteine residues, Cys99 in the pro-domain interact with the zinc ion of catalytic domain and thereby keeps the enzyme inactive. The remaining two Cys468 and Cys674 are found within the O-glycosylated and hemopexin domains respectively. It is assumed that these two residues might be involved in intermolecular interaction and MMP-9 multimer formation (Van den Steen et al., 2006).

Activation of pro-MMPs requires the removal of the pro-region by a mechanism called cystein switch. This mechanism depends on a conformational change which results in breaking the bond between the catalytic zinc and cysteine residue in the pro-domain and enables water to interact with the zinc ion in the active site of MMP-9. However, the activation process is accomplished through three different mechanisms: (i) elimination of the pro-domain by direct cleavage by another endoprotease (ii) chemical alteration of the free cysteine followed by autoproteolysis (iii) allosteric re-conformation of the pro-domain (Busti et al., 2010; Ra and Parks, 2007). Intracellular component such as S-nitrosylation or extracellular proteases including tissue kallikrein, plasmin, urokinase-type plasminogen activator, MMP-1, MMP-2, MMP-3, and MMP-7 can all activate proMMP-9 by cleavage of the pro-peptide (Fouad et.al, 2015) (Fig. 10).

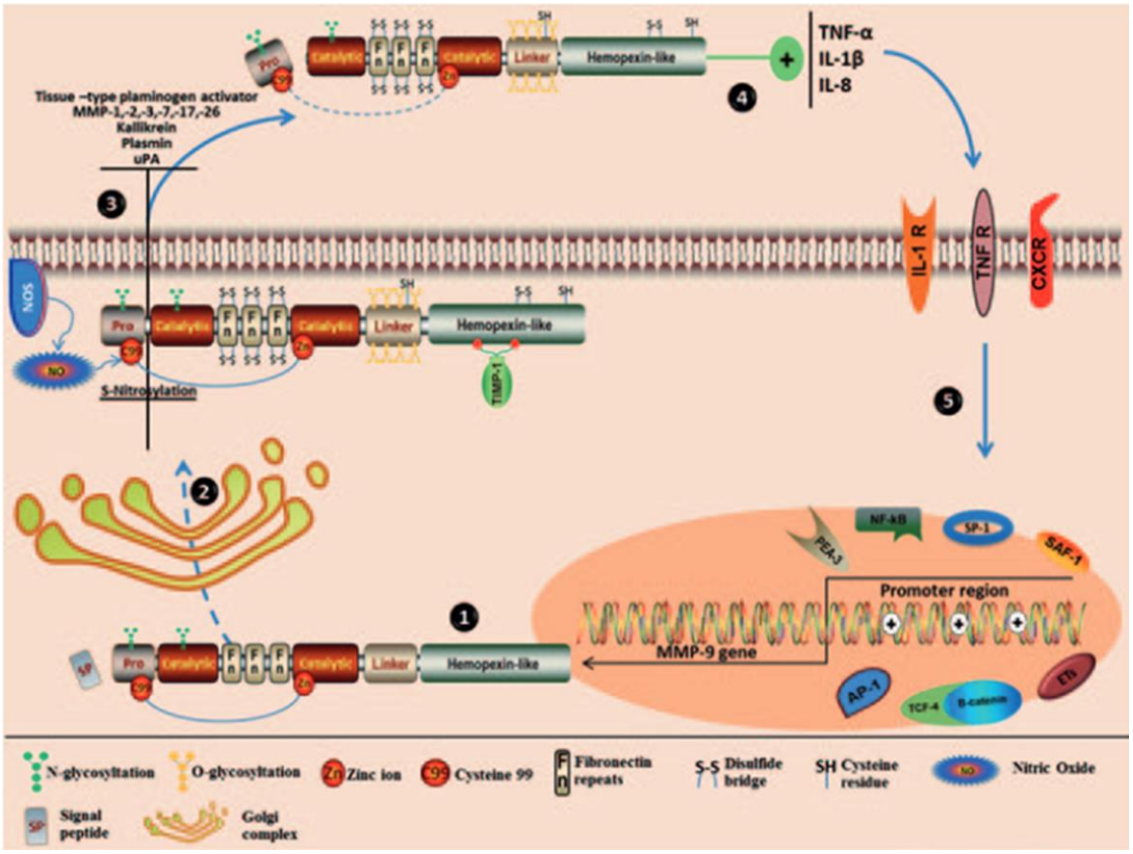

Figure 10. MMP-9 expression, synthesis and activation.**1**. N-glycosylation occur co-translationally at the pro and catalytic domains of proMMP-9. **2**. MMP-9 is processed through Golgi complex and acquire tertiary structure. **3.** Activation of MMP-9 either by intracellular components or extracellular components. **4**. Proteolytic activity on its substrates such as various cytokins and trancription factors. **5**. Binding to the site in the promotor region, Trans-activators stimulate further MMP-9 expression. Permission pending (Fouad et al. 2015).

Autocleavage of the pro-peptide *in vitro* by treating with organo-mercurial compounds, urea, SH reactive reagents, and chaotropic agents, detergents such as SDS which chemically modify the pro-MMP structure can result in auto-activation of MMP-9. Further, an investigation of gelatinase activity of MMP-9 in human placenta *in situ* suggested that the proMMP-9 is enzymatically active with presence of its N-terminal pro-peptide with 10-fold lower activity than fully active enzyme (Bannikov et al., 2002). Thus, through an alternative mechanism involving allosteric activation, pro-MMP-9 can be activated without proteolytic process of the pro-peptide. In this mechanism, binding of proMMP-9 to gelatin or collagen IV, the pro-peptide is distorted away from the active site leaving an open active site that can bind and process substrates. Removal of the binding molecules causes a reversion into an inactive proenzyme (Hadler-Olsen et al.,

2011). Once MMP-9 is activated, it proteolytically processes a wide range of compounds including multiple pro-inflammatory cytokines such as TNF-α, IL-1β, and IL-8. These compounds bind to their receptors and thereby activate them. The activation of the receptors triggers an intracellular signalling cascade that recruits various trans-activators to the binding sites at the promotor region of MMP-9. This in return stimulates to further MMP-9 expression (Fouad et.al., 2015) (Fig.10).

MMP-9 expression regulatory mechanisms

According to past and recent studies, MMP-9 activity is regulated at various levels. A variety of signaling pathways that stimulate or suppress the transcription of the *MMP-9* gene was considered to be the first level of regulation. Second, MMP-9 is regulated at mRNA level and the level of translation into the pre-proenzyme. The final amount of preproMMP-9 is determined by degradation of MMP-9 mRNAs and several signaling pathways are able to stimulate to do so. More importantly, microRNAs were also observed to involve at this level of regulation. Secretion of proMMP-9 from secretory vesicles of neutrophils is might be a third level of regulation. Another level of regulation occurs after secretion, where proMMP-9 needs to go through various mechanisms in the extracellular milieu for activation. Finally, the activity of MMP-9 is regulated by various MMP-9 inhibitors (Vandooren et al., 2013). The mechanism of MMP-9 regulation is described below:

Regulation of MMP-9 gene transcription

At the transcriptional level, MMP-9 is regulated by a number of pathways including the MAPK pathway, the Smad pathway, the NIK/NEMO/IKK pathways, the STAT pathways and nuclear receptor pathways. However, MMP-9 is mainly regulated by ERK1/2 member of MAPK pathways with the interferences of many essential regulatory elements that are mentioned in the previous section 1.5.6. At the initial level of transcription, most of the transcription factors or regulatory elements interfere with the basic MMP-9 promotor activation machinery in order to suppress or repress of MMP-9 expression. The binding of NF-kB and AP-1 factors in the promoter region are often found to suppress MMP-9 transcription. On the other hand, a complex SP2/KLF6 binding to the Sp1 site in the MMP-9 gene promotor is found to repress MMP-9 expression. However, some other factor including Kiss1 (Lee and Welch, 1997) RECK

(Takagi et al., 2009) EGR-1 (Bouchard et al., 2010) were also documented to interfere promotor activity of MMP-9 (Fig.11). In addition, polymorphisms in the gene promoter sequences of MMP-9 have been observed to be associated with the regulation of gene expression (Zhang et al., 1999). The presence of microsatellite d(CA) repeats in the MMP-9 promoter sequence considerably impairs the activity of the MMP-9 promoter in several cell types (Shimajiri et al., 1999). The reason might be the close localization to the transcriptional start site of MMP-9.

In macrophages, the expression of MMP-9 was found to be induced directly by both MMP-1 and MMP-3 by triggering the release of TNF-α. TNF-α induces the expression of COX-2 and PGE2 secretion. Binding of PGE2 to EP4 in the cell membrane stimulates MMP-9 production through MAPK/ERK1/2 signaling (Steenport et al., 2009). Several neurotransmitters and hormones have role in the induction of MMP-9 expression. For example, histamine can induce MMP-9 production in human keratinocytes by signaling through the histamine H1 receptor (H1R). Histamine-induced MMP-9 contribute to the destruction of type IV collagen which is present in the basement membrane of healthy skin (Harvima, 2008). Adrenalin was also observed to induce the production of MMP-9. In a human colon carcinoma cell line, supplementation with adrenalin resulted in increased levels of MMP-9 (Wang et al., 2011). Additionally, noradrenaline induces MMP-9 expression in the mouse neuroendocrine hypothalamus and in nasopharyngeal carcinoma tumor cells (Maolood et al., 2008; Yang et al., 2006). Bile acids were detected to induce MMP-9 production through binding to nuclear FXR which subsequently binds to the MMP-9 promoter region and thereby induces transcription (Vandooren et al., 2013).

Epigenetic regulation where a number of mechanisms involve such as histone modification, DNA methylation and noncoding RNAs (ncRNAs). Depending on the cell type, inhibition of histone deacetylases (HDACs) resulted in either higher (Mayo

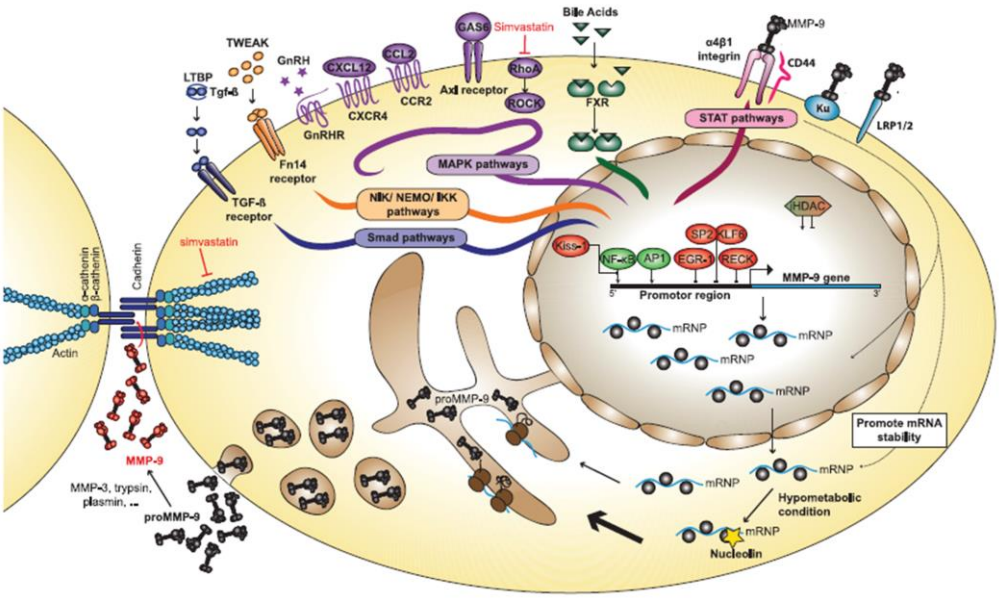

Figure 11. Regulation levels of MMP-9. MMP-9 is regulated by several pathways at transcriptional level. Various regulatory elements, including AP-1 and NF-kB are involved in transcription level by binding to the promoter region of MMP-9. Dynamic mRNP complexes control mRNA degradation and stabilization after transcription with the help of nucleolin. The secreted proMMP-9 is activated into MMP-9 by different proteases such as MMP-3, plasmin and trypsin. Activated MMP-9 binds to several cell surface molecules, e.g. Ku, LRP1/2, integrins and CD44 to form an MMP-9 cell surface complex (Vandooren et al. 2013)

et al., 2003) or lower (Estella et al., 2012) expression levels of MMP-9. The expression of *MMP-9* gene is regulated by DNA methylation. Inhibitors of DNA methylation induce MMP-9 mRNA and protein level of MMP-9 (Sato et al., 2003).

Post transcriptional and post translational regulation of MMP-9

After transcription, the final amounts of mRNA are determined by stabilization and destabilization regulation upon binding of noncoding (ncRNAs) RNAs and RNA-binding proteins to the mRNA cis-acting elements (Wu and Brewer, 2012). A dynamic complex of mRNA with proteins called ribonucleoprotein complexes (mRNPs) are found to act as mediators of post-transcriptional events such as capping, splicing, quality control and trafficking (Hieronymus and Silver, 2004). The 3'UTR of *MMP-9* gene was found to be a crucial region for post-transcriptional regulation. A study of

RNA or protein interaction showed that the elevated binding of nucleolin to the 3'UTR of the MMP-9 transcript might be significant for the increased efficiency of MMP-9 translation (Fahling et al., 2005).

Noncoding RNAs are not translated into proteins consist of many other types of RNA. Based on function and features, they are numerous. However, only miR-4915q has been found to be correlated with the expression of MMP-9 in glioblastoma multiforme (GBM) disease (Yan et al., 2011).

Glycosylation event is very crucial in the activities of protein macromolecules and their interactions with inhibitors or substrates (Kotra et al., 2002). Unlike other glycoproteins, the addition of N-linked oligosaccharides takes place co-translationally in the endoplasmic reticulum (ER) together with the folding of MMP-9 (Dwek, 1996). These N-linked sugars have been found to be associated with correct protein folding (Kotra et al., 2002). O-linked oligosaccharides are sequentially attached by specific sugar transferases when the N-glycosylated folded proteins travel to the Golgi apparatus and the trans-Golgi (Van den Steen et al., 1998). However, correct folding and intramolecular disulfide bonds in the fibronectin domain are a prerequisite for the MMP-9 secretion (Arnold and kaufman, 2003).

Regulation of MMP-9 secretion

Neutrophils do not constitutively produce MMP-9. An inflammatory stimulus is needed for MMP-9 secretion (Van den Steen, 2002b). The MMP-9 produced by neutrophils is TIMP-1 free and it was demonstrated to be pro-angiogenic. However, a study showed that a GTPase like Rab27a co-localize with neutrophil MMP-9, regulating the secretion of the MMP-9 (Brzezinska et al., 2008). Secretion of MMP-9 differs with timing between macrophages and neutrophils. The mature neutrophils store MMP-9 in granules and release it upon stimulation within minutes, while in macrophages, it takes several hours as macrophages rely on the process of *de novo synthesis* of MMP-9 prior to secretion. MMP-9 is not stored in macrophages but instead directly secreted after synthesis (Opdenakker et al., 2001a).

MMP-9 inhibition

As mentioned before, MMP-9 is secreted as zymogen where pro-domain coordinates with Zn^{2+} of catalytic domain to suppress the MMP-9 activity. Till now three different activation mechanisms of MMP-9 have been identified, those were described earlier. Once MMP-9 is secreted, its protease activity is tightly controlled to keep the physiological balances in the host. Both monomers and multimers of MMP-9 are inhibited by endogenous inhibitor TIMP-1. The main TIMP-1 binding site of proMMP-9 is located in the hemopexin domain (O'Connell et al., 1994). Olsen et al. also reported that proMMP-9 multimers have two high affinity binding sites for TIMP-1, both most likely localized in the hemopexin domain (Olson et al., 2000). Polyunsaturated fatty acids can efficiently inhibit the activity of MMP-9. A study revealed that Zn^{2+} chelation is not the way of inhibition by fatty acid instead it is linked to the fact of mimicking the natural sequence of the pro-domain of MMP-9 (Hu et al., 2005).

Chemical inhibitors such as tetracyclines and chemically modified tetracyclines (CMTs) exert diverse inhibitory effect on MMP-9 synthesis and activation. The proposed mechanism of action of these inhibitors results from their ability to bind Ca^{2+} and Zn^{2+} which are required by MMP-9 to maintain its proper conformation and hydrolytic activity. By chelating Zn^{2+} at the binding site in the catalytic domain of active MMP-9, leads to disruption of the normal conformation of the protein structure and thereby result in a non-functional and inactive MMP-9 (Golub et al., 1991; Salo et al., 2006).

MMP-9 substrates

Even though MMP-9 has high activity against denatured collagens (gelatin), it also degrades native collagen, elastin, fibronectin, aggrecan core protein, vitronectin, laminin (Bourguet, 2012). Besides some mentioned above, the Non-ECM molecules including transforming growth factor (TGF)-β (Yu and Stamenkovic, 2000) and monocyte chemo-attractant protein (MCP)-3 are also degraded by MMP-9 (McQuibban et al., 2002).

The role of MMP-9 in diseases

MMP-9 has been reported to be associated with many physiological and pathological conditions. The ability to degrade ECM and non-ECM components suggest that this enzyme can be a potential oncogenic factor for different type of tumour initiation, promotion and genetic instability (Fig. 12).

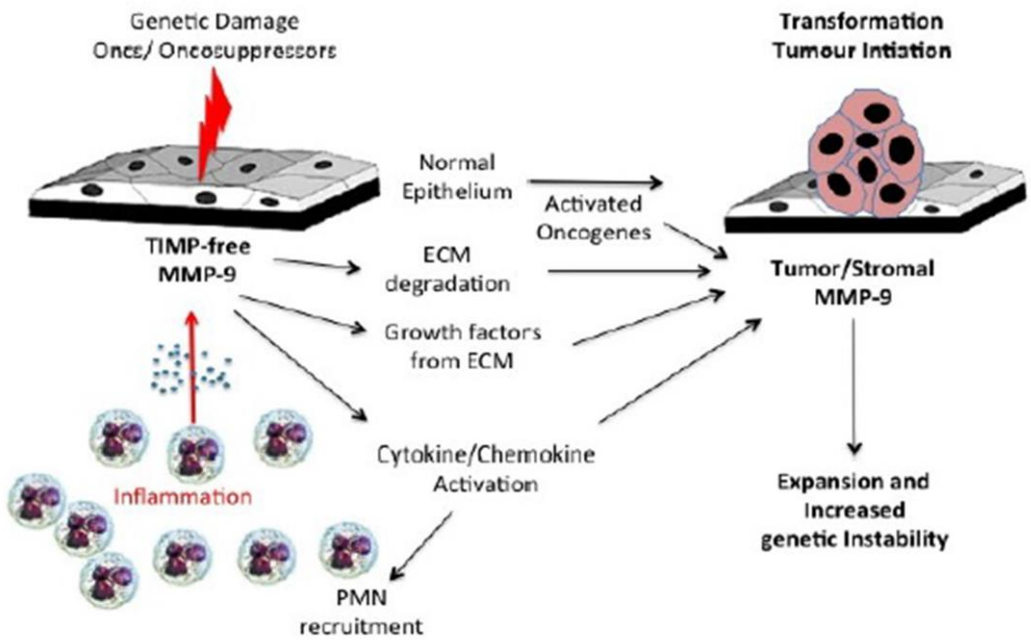

Figure 12. The role of inflammatory polymorphonuclear leukocyte (PMN)-derived tissue inhibitor of metalloproteinase (TIMP)-free MMP-9. The free MMP-9 degrades extracellular matrix (ECM) components such as cytokines, chemokines and growth factors. The release and activation of those components initiate tumour and promote genetic instability. With permission (Farina and Mackay, 2014).

Since uncontrolled MMP-9 activity can easily destroy the network of multidirectional communication within cells and tissues, MMP-9 is considered an important regulator of tissue homeostasis and the immune response.

An increased expression of MMP-9 is associated with numerous disorders or diseases in human body. MMP-9 has been reported to be involved in cardiovascular diseases, periodontal disease and it is common with other MMPs in different type of cancers including breast cancer, skin and oral epithelial cancer, lung cancer, pancreas cancer,

bladder cancer, cervical cancer, ovarian cancer, colorectal, prostate cancer and brain cancer (Giraudo et al., 2004; Lamar et al., 2008; Mehta et al., 2003; Roy et al., 2009; Sier et al., 2000).

MMP-9 has been found to be associated with numerous pathological processes and different domains of MMP-9 has been implicated as prominent players in these processes. Therefore, understanding of MMP-9 physiology including structure, regulation and activation is crucial in order to design potential inhibitors of MMP-9. To date, several studies has been recorded that aimed to explore MMP-9 structure and function. The information provided by Protein Data Bank (PDB) shows that in most cases an *E. Coli.* expression system was used to produce recombinant MMP-9 only with catalytic domain, which lacked the FnII module. This has been used for X-ray crystallization with inhibitors in high through put inhibitory studies. Crystallization of entire MMP-9 at a time has been found difficult because of its very long and flexible hinge region. Another method Bac-N-Blue ™ DNA (Invitrogen) was used to produce recombinant proMMP-9 in Sf9 insect cells. Among the proMMP-9 variants produced with this method was two deletion variants, one lacks the HPX domain and the other lacks both the hinge and the HPX domain (Van den Steen et al., 2006). In the present master thesis, we used BaculoDirect ™ Baculovirus expression system and Sf9 cells to produce recombinant MMP-9 lacking both the hinge and HPX domains. Before describing the potentiality of Baculovirus as a vector for protein expression, a brief introduction on Baculovirus life cycle is summarised below:

Baculovirus

Baculovirus life cycle

Baculoviruses are a group of arthropod-specific virus that contain large, circular, supercoiled double stranded DNA molecule with a size ranging from 80 to over 180 kbp and encoding 90 to 180 genes (George, F.R. 2011). The name “Baculovirus” is derived from the latin “*baculum*” meaning the rod-shaped nucleocapsids which is 230–385 nm in length and 40–60 nm in diameter. Baculoviruses predominantly infect insect larvae of Lepidoptera (butterflies and moths) along with Hymenoptera (sawflies) and Diptera (mosquitoes). The most widely studied Baculovirus is *Autographa californica*

multiple nucleopolyhedrovirus (AcMNPV) for which the complete genome sequence has been determined (George, F. R. 2011). AcMNPV has two phenotypes: budded virions (BVs) and occluded virions (OVs) (Fig.13). These two types of virions vary in their origin and composition of envelopes and their functions in the virus life cycle. BVS consists of a single rod shaped nucleo-capsid envelope enriched in virally-encoded membrane fusion protein GP64. This protein is incorporated into the BV particles during virus budding and release. In the later stage of infection, large number of occlusion virions (OVs) or polyhedral are formed. The orally infectious OVs are enclosed in a para-crystalline matrix forming occlusion bodies (OBs). The major component of OVs is occlusion protein polyhedrin which is a virus-encoded protein produced by transcriptional activity of the polyhedron gene promoter. This protein protects the virus in the natural environments and permits virus particle to survive outside of their natural host and thereby allow virions to remain infectious for very long period of time. BVs spreads the infection within the insect host while occlusion-derived virus between hosts.

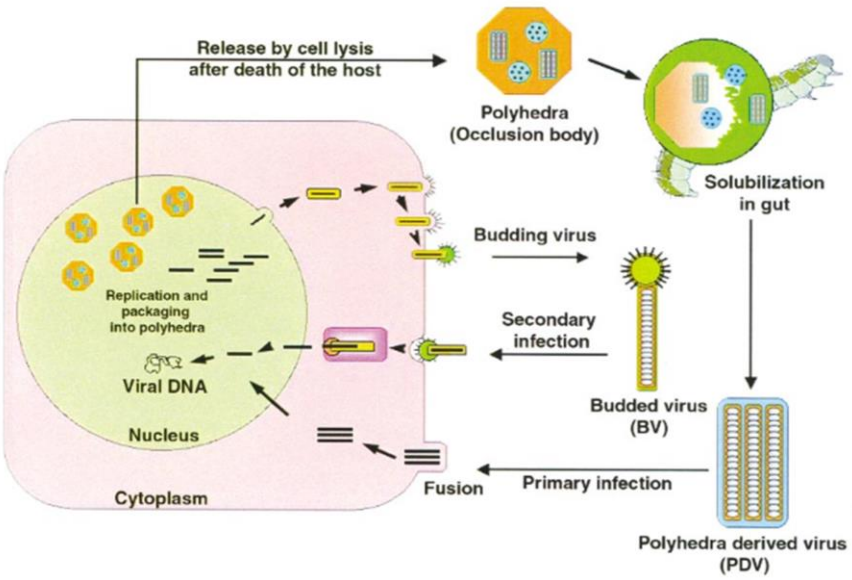

Figure 13. Bi-phasic AcNPV replication cycle. Upon ingestion, the polyhedra are dissolved inside the gut of the larvae to release occlusion derived virions or polyhedral derived virus (PDVs). The PDVs then fuse with midgut epithelial cells and enter the cell's nucleus through primary infection. The viral DNA is uncoated and viral transcription initiated. The uncoated nucleocapsid are then transported to the plasma membrane where they bud from the host cell acquiring an envelope derived from the host cell membrane to produce BVs that in turn cause secondary infection. Also, the progeny viruses get embedded into OBs which are released from the cell upon cell death (Ghosh et al., 2002).

Gene transcription of Baculovirus

The gene transcription of baculovirus has four phases: immediate early, delayed early, late and very late phase. Immediate early genes are identified by host transcription factors and viral proteins are not necessary at this stage. Transcription of delayed early genes require activation with the products of immediate early genes. The delayed early phase is followed by the synthesis of DNA and the late gene products of the virus (Hefferon and Miller, 2002). It is believed that there is a close relationship between these two events of DNA synthesis and late gene product of virus. The late transcription phase occurs following the initiation of viral DNA replication. In this phase nucleocapsid structural proteins including glycoprotein GP64 are synthesized which play a crucial role in the horizontal infection by infectious BV (Whitford et al., 1989). During the very late phase the production of BV is greatly reduced. The process of occlusion of nucleocapsids occurs by the very late viral

protein-polyhedrin. As occlusion proceeds, fibrillar structures comprising mostly of a very late protein p10 (Vanderwilk et al., 1987).

Baculovirus as expression vector

The massive expression of the very late genes has been exploited to design the vector for foreign gene expression based on Baculoviruses. Since early 1980's this expression system has become one of the most popular method for production of large quantity of recombinant protein within eukaryotic cells because of safety (not harmful to non-target organisms) and easy handing in the laboratory. Baculoviruses have several attractive features including easy manipulation, able to carry large (at least 38 kb) (Cheshenko et al., 2001) and multiple DNA inserts (Bieniossek et al., 2012). BV can also be readily produced and purified at high titers. A Baculovirus expression vector (BEV) is a genetically modified recombinant Baculovirus used for the expression of a foreign gene. BEVs are sustainable in insect cell culture and sometimes in larvae. However, it depends on the Baculovirus genes deleted in the process of the recombinant virus generation. In BEVs, the foreign gene coding sequence is usually placed under the transcriptional control of viral promoter. This is why viral factors are required for the transcription of the foreign gene. The most successful strategy for cloning recombinant Baculovirus is the use of a linearized parental genome of Baculovirus. The principle of this technique is illustrated in the method section.

Sf9 insect cells

The traditional cell lines for Baculovirus-directed protein expression system are Sf21 and Sf9 cells. These two cell lines were originally derived from the pupal ovarian cells of *Spodoptera frugiperda* (fall army worm) termed IPLB-Sf-21 cells, with Sf9 cells (IPLB-Sf21-AE) being a clonal isolate of Sf21 cells. Sf9 cells are considered a suitable host for expression of recombinant protein from Baculovirus expression systems because Sf9 cell lines are normally simple to maintain compared to mammalian cell lines (O'Reilly et al., 1992). Additionally, Sf9 can grow in serum-free media containing amino acids, carbohydrates, vitamins and lipids essential for insect cell growth that reduce the effect of rate-limiting nutritional restrictions or deficiencies that are present within serum-supplemented media. Serum-free media is also observed to support

rapid cell doubling times and permit cell growth to higher densities compare to serum-supplemented media facilitating higher virus titres or protein yields. Furthermore, the eukaryotic-Sf9 Baculovirus expression system has advantages over prokaryotic and yeast expression system as recombinant protein expressed in Sf9 cells are post translationally modified and thereby producing protein similar to their native counterparts (Zhang et al., 1994).

Aim of the study

The hinge and hemopexin domain have been found crucial for the proper structural orientation and function of MMP-9. In order to study their role in MMP-9 function it is important to compare a full length version of MMP-9 with a truncated version where the hinge and HPX domain are lacking. In the present study, our aim was to produce recombinant human proMMP-9-ΔH-HPX protease by Sf9 cells and establish a purification protocol.

To reach the goal we performed the following experiments:

1. Site directed mutagenesis to generate a point mutation introducing a stop codon in the hinge region.
2. LR recombination reaction for cloning pDONR221- *MMP-9ΔH-HPX* into the Baculovirus DNA.
3. Transfection of Sf9 cells with the recombinant Baculovirus to produce proMMP-9ΔH-HPX protease.
4. Modified Gelatin Sepharose Chromatography and Size Exclusion Purification performed for the proMMP-9ΔH-HPX protease purification.

Materials and methods

Materials

Chemicals and reagents

Name	Producer (company)
Ammonium sulphate, Magnesium sulphate, bovine serum albumin (BSA), Magnesium chloride ($MgCl_2$), Sodium acetate, Glacial acetic acid, SDS, Glycerol, Bromophenol blue, Gelatin bloom 300, TEMED, Glycine, Acetic acid (HAc), Methanol, Sodium chloride (NaCl), Brij-35, EDTA, Pefabloc, DTT, E64, HEPES, Streptomycin (10 mg streptomycin per ml in 0,9% NaCl), Trypan Blue, Tween 20	Sigma-Aldrich Chemical Co.
TRIS hydrochloride (TRIS-HCl), DMSO, Coomassie Blue stain, Potassium chloride, Triton X-100, Calcium chloride dihydrate	Merck (Darmstadt, Germany)
EDTA	BDH (Poole, UK)
Agarose	Cambrex Bio-sciences, Denmark
Dpn I restriction enzyme (10 U/µl)	Invitrogen
NuPAGE-4-12%, Bis-Tris Gel 1.0 mm x 12 well SDS-PAGE gel	
PfuUltra High- Fidelity DNA polymerase (2.5 U/µl)	Agilent Technologies
Western Blotting Luminol Reagent	Santa Cruz Biotechnology Inc.
GelRed™ Nucleic Acid Gel Stain	Biotium
Biotinylated Protein Ladder Detection Pack	Cell Signaling Technology, Inc
Kanamycin	Thermo Scientific (Rockford, IL, USA)
SeeBlue®Pre-stained Standard	
Spectra™ Multicolor High Range Protein Ladder	
Fetal Bovine Serum	Biochrom AG,

XL1-Blue supercompetent cells	Agilent Technologies
P-250 kDa protein Ladder	New England Biolabs
1 kb DNA ladder (Cat. No. N3232S)	
Agarose, Low melt preparative Grade	BIO-RAD
Non-fat milk powder	MolecoNestle® Molico instant, Norway

Kits list

Name	Producer (Company)	Cat. No.
QuikChange II XL Site-Directed Mutagenesis Kit	Agilent Technologies	200523
BaculoDirect™ Transfection kit	Invitrogen	12562-062
BaculoDirect™ Expression kit		12562-054
QIAprep Spin Miniprep Kit	QIAGEN®	27106
BigDye® Terminator v3.1 Cycle Sequencing Kit	Applied Biosystems	4337456

Buffers and solutions used for the different methods

TRIS-HCL	
1 M Tris-HCl, pH 8.0	<u>To make 1 Liter:</u> 121.1 g Tris-base (MW: 121.14) dissolved in Milli-Q water pH adjusted to 8.0 with HCl Volume adjusted to 1 L with Milli-Q water
Preparation of Primer stock	
TE buffer	10 mM Tris-HCl, pH 8.0 0.1 mM EDTA
QuikChange II Site- Directed Mutagenesis	

10x reaction buffer	100 mM KCl 100 mM $(NH4)_2SO_4$, 200 mM Tris-HCl, pH 8.8 20 mM MgSO4 1% Triton®X-100 1 mg/ml nuclease-free bovine serum albumin (BSA)
Plasmid purification (Qiagen Kit Buffers)	
Buffer P1	50 mM Tris-HCl pH 8.0 10 mM EDTA 100 µg/ml RNaseA
Buffer P2	200 mM NaOH 1% SDS
Buffer N3	4.2 M Gu-HCl 0.9 M potassium acetate pH 4.8
Buffer PB	5 M Gu-HCl 30% isopropanol
Buffer PE	10 mM Tris-HCl pH 7.5 80% ethanol
Buffer EB	10 mM Tris-Cl, pH 8.5
DNA sequencing	
5x sequencing buffer	400 mM Tris-HCl, pH 9.0 10 mM $MgCl_2$
Agarose gel electrophoresis	
50x TAE (Tris (2 M)-Acetate (1 M)-EDTA (50 mM) buffer stock solution (working solution 1x)	<u>To make 1 liter of 50x TAE:</u> 242 g Tris-base disolved in 700 ml H_2O 57.1 mL glacial acetic acid 100 ml of 500 mM EDTA (pH 8.0) solution Add H_2O to 1 liter
1% agarose	<u>To make 100 ml:</u> 1 g agarose 100 ml 1x TAE buffer

5x loading buffer	0.25 M Tris-HCl pH 6.8 10% SDS 50% glycerol 0.5% Bromophenol blue
Gelatin Zymography	
Gelatin (2%)	<u>To make 10 ml:</u> 0.2 g Gelatin bloom 300 10 ml Milli-Q water
Concentrating gel buffer	0.5 M Tris-HCl, pH 6.8 0.4% SDS
Separating gel buffer	1.5 M Tris-HCl, pH 8.8 0.4% SDS
Separating gel (7.5% acrylamide)	<u>To make 4.507 ml:</u> 1.120 ml Separating gel buffer 0.225 ml of 2% gelatin 2.266 ml Milli-Q Water 0. 874 ml of 40% Acrylamide 7 µl TEMED 15 µl 10% Ammonium persulfate
Stacking gel (4% acrylamide)	<u>To make 1.498 ml:</u> 0.186 ml Stacking gel buffer 1.145 ml Milli-Q water 0.155 ml 40% Acrylamide 4 µl TEMED 8 µl of 10% ammonium persulfate
Electrophoresis Buffer, pH 8.3 (10X)	<u>To make 1 Liter:</u> 30 g Tris-HCl 144 g Glycine 10 g SDS (final conc. 1%) 1 litre Milli-Q water pH adjusted to 8.3 with conc. HCl
Staining solution stock	<u>To make 200 ml:</u> 0.4 g Coomassie Brilliant Blue

	120 ml Methanol 80 ml Milli-Q water
Staining solution	20 ml Staining solution stock 20 ml of 20% acetic acid Staining stock solution is first filtered and was mixed with 20% acetic acid.
Washing buffer	<u>To make 400 ml:</u> 10 ml Triton X-100 (warm) 390 ml Milli-Q water
De-staining solution	<u>To make 400 ml:</u> 120 ml Methanol 40 ml of 100% Acetic acid 240 ml Milli-Q water
Developing or incubation buffer 10x	<u>To make 1 liter:</u> 12.1 g Tris-base (MW:121.14 g/mol) 63.0 g Tris-HCL(MW:157.60 g/mol) 117 g NaCl (MW:58.44 g/mol) 7.4 g $CaCl_2$-$2H_2O$ (MW: 147.02 g/mol) 6.7 g 30% Brij-35 Milli-Q water added to give the total volume of 1 liter. pH 7.8
EDTA (10 mM)	1 ml of 0.5 M EDTA in 50 ml washing buffer. 500 µl of 0.5 M EDTA in 25 ml Incubation buffer
Pefabloc (1 mM)	100 µl of 0.5 M pefabloc in 50 ml washing buffer 50 µl of 0.5 M pefabloc in 25 ml incubation buffer
E64 (10 µM) (3.2 mM E64 in DMSO)	156 µl of 3.2 mM E64 in 500 ml washing buffer 78 µl of 3.2 mM E64 in 25 ml incubation buffer
0.5 M DTT	80 µl 5x Sample buffer 20 µl 2.5 M DTT
Gelatin Sepharose Chromatography assay	
Equilibrium or binding buffer	<u>To make 500 ml:</u> 11.9 g HEPES (MW:238.30) pH 7.5

	0.186 g $CaCl_2$ (MW:74.56) Milli-Q water added to give the total volume 500 ml PH adjusted with NaOH
Washing buffer	<u>To make 100 ml:</u> 2.38 g HEPES (MW:238.30) pH 7.5 0.0372 g $CaCl_2$ (MW: 74.56) 5.8 g NaCl (MW: 58.44) Milli-Q water added to give the total volume 100 ml. pH adjusted with NaOH
Elution buffer	<u>To make 10 ml:</u> 9.25 ml equilibrium buffer, 0.75 ml DMSO (100%) pH 7.5
Western blotting	
1xTBST	<u>To make 1 Liter:</u> 30 ml 5 M NaCl 20 ml 1 M Tris, pH 8.0 1 ml Tween 20 Volume adjusted to 1 L with Milli-Q water
Blocking buffer	<u>To make 150 ml:</u> 7. 5 g 5% Non-fat milk powder 150 ml 1x TBST
1xNuPAGE Running Buffer (MES-SDS)	<u>To make 600 ml:</u> 30 ml MES-SDS running buffer (20x) 570 ml Milli-Q water
Blotting buffer	<u>To make 1 liter:</u> 5.8 g Tris-base (MW: 121.14) 29 g Glycine (MW: 75.07) 800 ml Milli-Q water 200 ml Methanol (20%) pH 8.6

Antibiotics

Antibiotic	Working Concentration (µg/ml)	Method
Streptomycin/Penicilin	50 µg/ml/50 IU/ml	Sf9 cell culture
Kanamycin	50 µg/ml	Bacterial culture

Antibodies

Antigen	Antibody description (dilutions)	Manufacturer, Cat. number
MMP-9	Rabbit Polyclonal anti-MMP-9 (1: 2500x of 5.1 mg/ml stock)	Custom made by Eurogenetic in 2008
Human and mouse immunoglobulins	Horseradish Peroxidase (HRP) conjugate goat Anti-Rabbit IgG (1:2000x of 1 mg/ml)	Southern Biotech (Birmingham, AL, U.S.A) Cat. no 4050-05

Primers

Oligonucleotide name	Sequences (5′-3′)	Manufacturer
Forward primer for mutagenesis	*GGCATCCGGCACCTCTATGGTCCTCGC CCTTAACCTGAGCCACGGCCTCCAACC*	Sigma-Aldrich
Reverse primer for mutagenesis	*GGTTGGAGGCCGTGGCTCAGGTTAAGG GCGAGGACCATAGAGGTGCCGGATGCC*	
M-13 (-20) Forward primer	*GTAAAACGACGGCCAG*	
M-13 (-24) Reverse primer	*AACAGCTATGACCATG*	
Forward primer for sequencing mid-part of MMP-9	*GCGTCGTGGTTCCAACTCGGTTTGGAA ACG*	

Polyhedrin ForwardPrimer (-20)	*AAATGATAACCATCTCGC*	**Invitrogen**
V5 Reverse Primer	*ACCGAGGAGAGGGTTAGGGAT*	

Insect cells and growth media

Cells/Medium	Amount	Composition	Company	Cat. no
Sf9 frozen cells,		$1x10^7$ cells in 1 ml 60% Grace's Media, 30% heat inactivated FBS, and 10% DMSO	Invitrogen	B825-01
Growth medium for Sf9 cells	Grace's Medium, Unsupplemented	Sterile-filtered medium contains L-glutamin		11595-030
	Grace's Medium, supplemented	Lactalbumin hydrolysate (LAH) and yeastolate, and supplemented with 10% Fetal Bovine Serum (FBS), 1% glutamin (if media is older than 3 months),1% Streptomycin		11605-094
	Grace's complete medium	Grace's Medium, supplemented, 1% streptomycin (50 µg/ml) 10% FBS1% glutamin (200 nM)		
Bacterial growth media	LB broth media	To make 1 liter: 10 g Peptone 140, 5 g Yeast Extract 5 g NaCl.		Made locally at the laboratory

	SOC	2% tryptone, 0.5% yeast extract, 10 mM NaCl 2.5 mM KCl 10 mM $MgCl_2$, 10 mM $MgSO_4$ 20 mM glucose.	Thermo-fisher Scientific	.
LB Agar plate		1 Litre: 15 g agar,1000 ml distilled water, 5 g yeast extract, 10 g NaCl, 10 g Bacto-pepton, pH 7.5		

Instruments and software

Instrument	Description and software	Manufacturer
LEICA DFC320	Light Microscope	Leica Microsystems Inc.
Lumi-Imager F1™	Blot Analyzer with LumiAnalyst software	Mannheim Boehringer GmBH
Image Quant LAS 4000 image reader	Digital Imaging system with the ImageQuant LAS 400 software	General Electric health care Bio-science AB (Uppsala, Sweden)
NanoDrop 2000 Spectrophotometer	Thermo Software IQ	Thermo Fisher Scientific
Western blot electrophoresis (powerEase 500) for SDS-PAGE		Invitrogen Life Technologies (California, USA)
Software for alignment	Bioedit sequence alignment editor 7.2	http://bioedit.software.informer.com/7.2
MEROPS	Peptidase database	merops.sanger.ac.uk
ExPASy	SIB Bioinformatics Resource Portal	https://www.expasy.org/
Speed Vac concentrator (2211 superrac), hydrostatic pump		Savant Instruments Inc (Farmingdale, N.Y, USA)

Methods

Site-directed Mutagenesis

Mutagenesis is a method to change or delete the nucleotides of DNA. Several methods can be used to generate mutations into the DNA sequence. Random mutagenesis generates a variable amount of unspecific mutations into different sites of the DNA sequence (Glick, 2010). In contrast, Site-directed Mutagenesis create a specific and targeted mutation in the known DNA. A commercial kit called QuikChange® site-directed mutagenesis (Agilent technologies) can be used for oligonucleotide-directed or site-directed mutagenesis. In this technique, a point mutations can be inserted into DNA which results in a mutation in the amino acid of a protein that the gene code for. This technique does not require specialized vectors, unique restriction sites or multiple transformations. However, the basic procedure does require a dsDNA vector containing the gene of interest and two synthetic oligonucleotide primers which contain the desired mutation. Typically, site-directed mutagenesis is performed using a PCR-based method. In the PCR, the plasmid is first denatured and then the reverse and forward primers are allowed to anneal to their complementary nucleotide bases in the template strand. The primers are extended by PfuUltra high-fidelity (HF) DNA polymerase and thereby generate a mutated plasmid containing staggered nicks. This method uses PfuUltra HF DNA polymerase instead of Taq DNA polymerase because pfuUtra high-fidelity (HF) DNA polymerase has 18-fold higher fidelity in DNA synthesis than Taq DNA polymerase.

The PCR product is then treated with Dpn I endonuclease which target sequence is 5´-GATC-3′. It is used to digest the parental DNA template and to select for the newly synthesized mutated DNA. After digestion of the methylated template strand, the XL1-Blue supercompetent bacteria are transformed with the nicked newly synthesized mutated DNA. After transformation the supercompetent bacteria repair the nicks in the mutated plasmid (Fig.14)

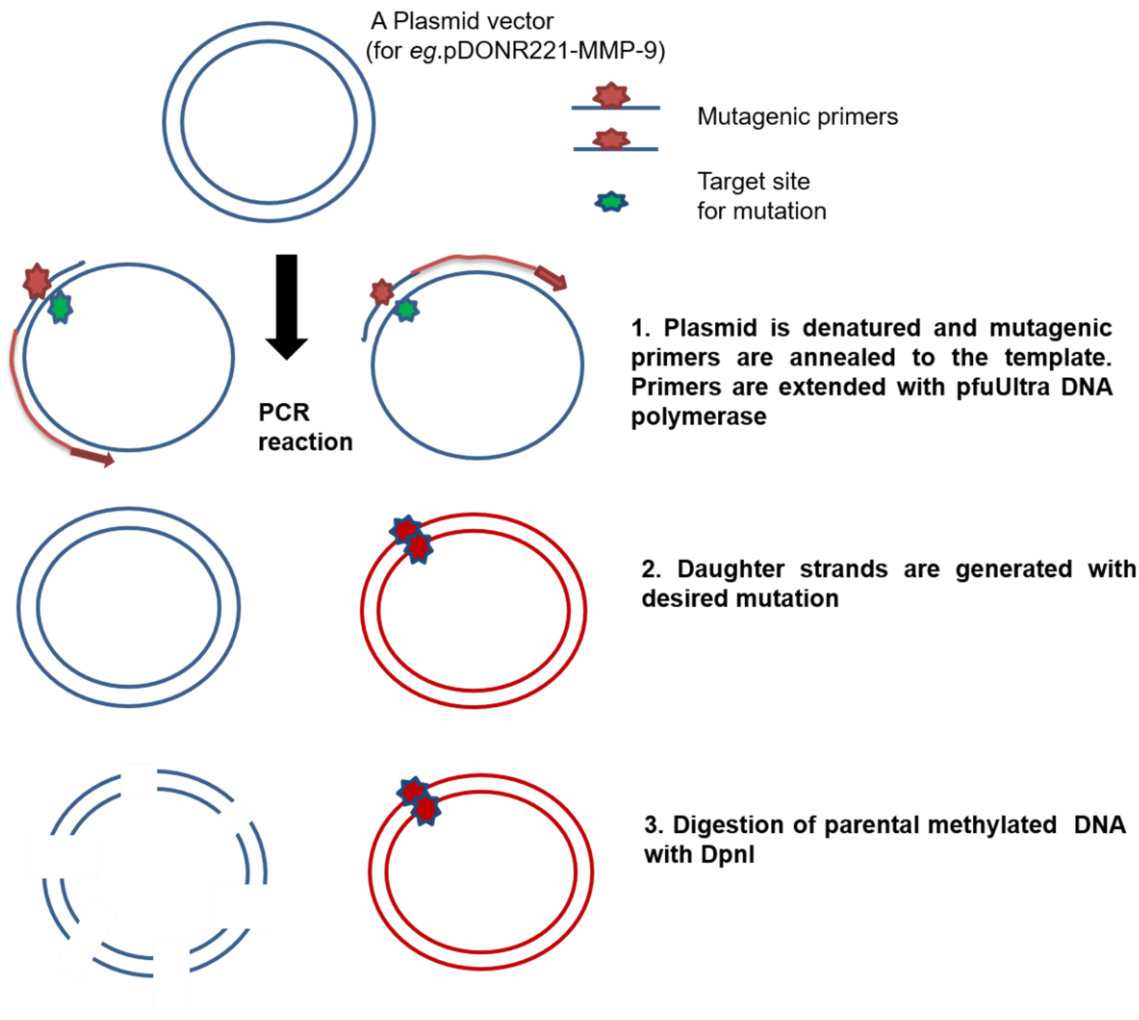

Figure.14 Overview of the Site-Directed Mutagenesis. PCR is performed to generate mutation in the target site. Plasmid is denatured and mutagenic primers containing mutation are annealed into the plasmid. Primers are extended by pFuUltra DNA polymerase. Daughter strand contain the desired mutation and methylated template strands are digested by DpnI restriction enzyme.

Designing of mutagenic primers

Primers were designed with 54 bp in length with a melting temperature more than 78ºC.The desired mutation was almost in the middle of the primers with around 25 bases of correct sequence on both sides. The GC content was more than 40% and both primers terminated with two C's. Both of the mutagenic primers contained the mutated nucleotide. The codon GAA coding for the amino acid glutamate (E) at position 448 (E448) of MMP-9 was mutated into the stop codon TAA by replacing the G with a T.

PCR Primer Stocks preparation

Before opening the tube containing the lyophilized (freeze-dry) primer, the tube was centrifuged for 1 minute at 13.000 rpm in a table top centrifuge to ensure that the powder was collected in the bottom of the tube. In order to prepare 100 µM stock solution of the mutagenesis primer, the information in the technical datasheet that was provided along with primer tube by the company was used. 108 ul of 1x TE buffer was added to the pellet and mixed properly by inverting the primers tube gently. The primer stock solution was stored at -20ºC. This tube was used further to make working solutions when needed. To generate 10 µM working solution of the primers, 10 mM Tris, pH 8.8 was used.

Polymerase chain reaction (PCR)

PCR is a process by which a DNA fragment is amplified many times to yield huge number of copies of that particular DNA or gene. In PCR, a pair of synthetic oligonucleotides, called primers, are used to initiate DNA synthesis. Furthermore, a heat stable DNA polymerase and a reaction buffer containing nucleotides are required. A commonly used DNA polymerase is the Taq enzyme, originally isolated from the bacterium *Thermus aquaticus*. This enzyme produces a new DNA strand by elongating the strand from the primers by incorporation of deoxyribonucleotides triphosphates (dNTPs) in an order based on the template DNA strand. For producing sufficient copies of the PCR product, the reaction mixture undergoes a cycle of temperature changes. A denaturation step that causes the DNA strands to separate or melt at high temperature of 94-98ºC for a few seconds. During an annealing step the primers bind to the target sequence in the template. At this step the temperature is lowered according to the melting temperature (Tm) of the primers. Normally the annealing temperature is around 50-70ºC. An extension step is where the Taq DNA polymerase uses the primers as a starting point to create a complimentary strand by adding dNTPs to the 5’ end of the primers. These three steps are repeated for 30-40 cycles. Provided that there are sufficient reagents, at the end of one PCR cycle the number of starting target sequences is doubled.

Donor vector pDONR221- MMP-9

The vector pDONR221-*MMP-9* was provided by Dr. Nabin Malla in our research group. In brief, the construct was generated using Gateway®technology (Invitorgen, Van Allen Way, USA) where a BP recombination reaction between attB-flanking DNA fragment containing the gene encoding human MMP-9 and attP-site in the donor vector pDONR221 gave rise to attL-flanked pDONR221-*MMP-9*. The attB-flanked human *MMP-9* gene in the pEZ-02-vector was purchased from GeneCopoeia, Rockville, MD (cat. no EX-F0125-M02). The reaction was catalysed by BP Clonase™ enzyme (Fig.15).

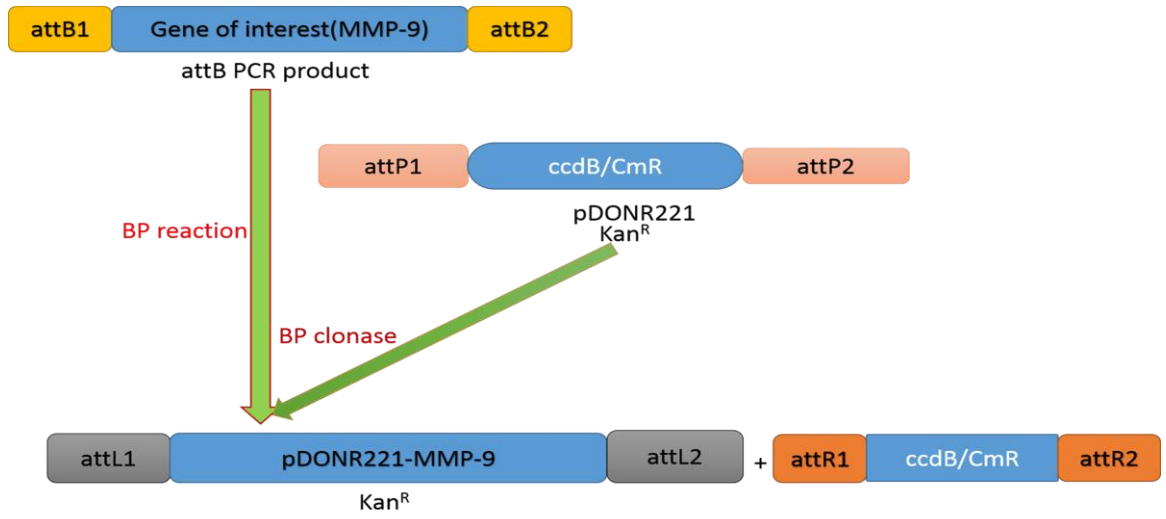

Figure 15. Generation of the pDONR221-*MMP-9* construct using Gateway®technology. The gene of interest (*MMP-9*) is inserted by BP recombination reaction between a donor vector pDONR221 and attB flanking MMP-9 DNA. The reaction was catalysed by the BP clonase enzyme.

Site directed mutagenesis of MMP-9

Using the template pDONR221-*MMP-9*, mutagenesis was performed according to the protocol for the QuikChange II site directed mutagenesis kit. The reagents and the PCR program used for PCR is shown in table 1 and 2, and the mutagenic primers is listed in table of primers.

Table 1. Setup for the mutagenesis reaction

Reagent	Amount (one sample)
10X reaction buffer	5 µl
Template pDONR221-MMP-9 (50 ng/µl)	1 µl
Mutagenic forward primer (125 ng/µl)	1 µl
Mutagenic reverse primer (125 ng/µl)	1 µl
dNTP mix (10 mM)	1 µl
ddH_20	40 µl
PfuUltra HF DNA polymerase (2.5 U/ µl)	1 µl
Total	**50 µl**

Table 2. PCR programme for the QuikChange II Site-Directed Mutagenesis

Segment	Cycle	Temperature	Time
1	1	95ºC	30 seconds
2	12	95ºC	30 seconds
		55ºC	1 minute
		68ºC	7 minutes

*elongation at 68ºC is estimated to be 1kb/min, thus since pDONR221-MMP-9 is 6.54 kb, the time was set to 7 minutes.

Dpn I Digestion of the Amplicon (Amplified product)

Previously mentioned that Dpn I digest the DNA methylated template and thereby reduce the probability of false positive colonies in the transformation.

The following procedure was conducted:

1. 2 µl of DpnI restriction enzyme (10 U/µl) was added directly to 50 µl amplification reaction.
2. The mixture was mixed gently and thoroughly by pipetting the solution up and down several times then span down in a table top microcentrifuge for 1 minute at 12000 rpm.

3. The mixture was then incubated for 1 hour at 37ºC.

Transformation of XL1-Blue supercompetent bacteria

After digestion of the parental methylated DNA strand, the newly synthesized mutated DNA was transformed into XL1-Blue supercompetent bacteria. The bacteria repair the nicks in pDONR221-*MMP-9ΔH-HPX* DNA. As the pDONR221-*MMP-9ΔH-HPX* plasmid contain a kanamycin resistant gene that code for a protein and therefore, only XL1-Blue supercompetent bactria that successfully has taken up the mutated plasmid will be kanamycin resistant and survive on LB agar plate containing (50 µg/ml) kanamycin. In contrast, those XL1-Blue supercompetent bacteria that has not taken up the mutated plasmid pDONR221-*MMP-9ΔH-HPX* are killed with kanamycin.

The following procedure was conducted for the transformation:

1. 50 µl of XL1-blue cells were gently thawed on ice.
2. 2 µl of Dpn I treated DNA was mixed with 50 µl XL1-blue cells and incubated for on ice for 30 minutes.
3. The bacteria were heat-shocking by incubation in a water at 42ºC for 45 seconds, followed by immediate transfer on ice for 2 minutes.
4. 500 µl pre-warmed SOC medium (Super Optimal Broth with catabolite repression) was added to the transformation reaction and incubated at 37ºC for 1 hour with shaking at 225-250 rpm.
5. To be sure to get single colonies, two different volume of transformation mixture (300 µl and 100 µl) was plated on agar plate containing kanamycin (50 µg/ml) by spreading them out using a sterile glass rod.
6. The agar plates were incubated for overnight at 37ºC.
7. The number of single colonies were recorded and the plates were wrapped in plastic to avoid drying out and stored at 4ºC until further processing of the colonies.

QIAprep Spin Miniprep Kit Protocol

The cells were harvested and used for plasmid DNA extraction. The concentration of the purified plasmid was determined by NanoDrop technique. The purification procedure is based on lysis of bacterial cells under alkaline conditions. The lysate is

subsequently neutralized and adjusted to high-salt binding in one step, the crude lysates and denatured and precipitated cellular components are loaded directly onto the TurboFilter membrane. RNA, cellular proteins, and metabolites are all removed by filtration through the TurboFilter membrane. This is followed by adsorption of plasmid DNA onto silica in the presence of high salt. Endonucleases are efficiently removed by a brief washing step with Buffer PB. This step was necessary to remove high carbohydrate content and trace nuclease activity. Salts are efficiently removed by a brief washing step with Buffer PE. High-quality plasmid DNA is then eluted from the QIAprep column with Buffer EB. The purified DNA is ready for immediate use.

The procedure conducted were as follows:

1. Eight single colonies from the transformations were picked using a sterile pipette tip and each single colony was transferred to 3 ml LB media with kanamycin and followed by incubation at 37^0C overnight.
2. The 3 ml of overnight bacterial culture was pelleted by centrifugation at 13,000xg for 1 minute and supernatant was discarded.
3. Pelleted bacterial cells was re-suspended in 250 µl Resuspension Buffer P1 (with RNase A) by pipetting up and down.
4. 250 µl Lysis Buffer P2 was added to the tube and the tube was inverted gently 4–6 times until the solution becomes viscous and slightly clear. This reaction step proceeded for maximum 5 minutes.
5. 350 µl of Neutralization Buffer N3 was added to the tube and the tube was inverted immediately 4–6 times in order to avoid localized precipitation. The tubes were centrifuged for 10 min at 12,000 rpm in a table top microcentrifuge resulting in a white pellet containing cellular materials.
6. The supernatant was collected and applied to the QIAprep Spin Column by pipetting and centrifuged it for 1 minute and then the flow-through was discarded.
7. 500 µl PB Buffer was added on to the QIAprep Spin Column and centrifuged it for 1 minute. The flow-through was discarded.
8. The QIAprep Spin Column was then washed by adding 750 µl Wash Buffer PE and centrifuged for 1 minute at 12000 rpm.
9. The flow-through was discarded followed by another centrifugation of 1 minute to remove residual wash buffer.

10. The column was transferred to a new 1.5 ml micro-centrifuge tube and 50 µl of elution buffer EB was the added to the column and centrifuged at 12000 rpm for 1 minute.

Determining the purified pDONR-MMP-9ΔH-HPX DNA concentration and yield

The purified plasmid DNA was determined by using NanoDrop spectrophotometer at A_{260nm}. NanoDrop technology is based on absorbance measurements of the molecules to be measured. The molecules like Nucleotides, dsDNA, ssDNA, RNA all absorb light at a specific wavelength. Nucleic acids have a peak absorbance of UV light at 260 nm where proteins and phenolic compounds have a strong absorbance at 280 nm. Several organic compounds have strong absorbance at around 225 nm. Chaotropic salts, TRIzol, phenol, and peptide bonds in proteins absorb light between 200 and 230 nm.

For DNA, absorbance readings are performed at 260 nm where DNA absorbs light maximally. The NanoDrop spectrophotometer calculates concentrations and records them as ng/µl. DNA concentration can be estimated based on the following equation

$1OD_{260}$ unit = 50 µg/ml (A260 of 1.0 = 50 µg/ml pure dsDNA).

Concentration (µg/ml) = the absorbance at 260nm × dilution factor × 50 µg/ml

DNA yield (µg) = DNA concentration × total sample volume (ml)

However, other molecules can absorb UV light at 260 nm. RNA also has an absorption maximum at 260 nm. The aromatic amino acids present in protein absorb at 280 nm, if those are present in the DNA solution, will contribute to the total measurement at 260 nm. In addition, the presence of guanidine results in higher 260 nm absorbance. Therefore, evaluation of DNA purity is necessary. The most common purity calculation is the ratio of the absorbance at 260 nm divided by the absorbance at 280 nm. For pure DNA and RNA, A260/280 ratios should be somewhere around 1.8, and 2.1 respectively. A lower ratio indicates the sample is contaminated with protein. On the other hand, the A260/230 ratio is used as a secondary measure of nucleic acid purity. The A260/230 ratio are commonly expected to be in the range 2.0-2.2. The value

below 1.8 are considered to have a significant amount organic compounds or contaminants.

Procedure:

1. First, the upper and lower optical surfaces were cleaned with deionized water and wiped off both surfaces with laboratory dry wiper.
2. The software was opened and nucleic acid module was selected.
3. A blank measurement was performed by pipetting 1 µl elution buffer on the lower optic surface.
4. After the measurement of the blank appeared zero, the optical surfaces were wiped off.
5. 1 µl of undiluted purified plasmid DNA was pipetted on the lower optical surface.
6. The DNA concentration was determined by NanoDrop spectrophotometer automatically.

PCR-based DNA sequencing

DNA sequencing is a process of reading the precise order of nucleotides in a DNA molecule. There are two principle methods of determining the sequences, Maxam-Gilbert chemical method and the Sanger's method, which is also referred to as dideoxy sequencing or chain termination method. Sanger's method, is based on the use of labelled dideoxynucleotides (ddNTP's) in addition to the normal nucleotides (NTP's) found in DNA. Fluorescently distinguished fluorophores are covalently attached to each of four ddNTP`s. The PCR based DNA sequencing is an automated sequencing system based on the principle of Sanger's method. Dideoxynucleotides are basically the same as nucleotides except them contain a hydrogen group on the 3' carbon of the pentose instead of a hydroxyl group (OH). These modified nucleotides, when integrated into a sequence, prevent the addition of further nucleotides. These molecules terminate DNA chain elongation because they cannot form a phosphodiester bond between the dideoxynucleotide and the next incoming nucleotide.

For performing the sequencing reaction, a single strand template, single primer (forward or reverse complimentary to the template strand), a mixture of a particular ddNTPs each labelled with Fluorescent dye, normal dNTP, and a thermostable DNA polymerase are required. When the mixture is heated, the two complimentary strands in the DNA molecule separates. Then the temperature is lowered so that the primer finds its complimentary sequence in the template DNA, and then allowing the polymerase to add nucleotides to extend the primer using the single stranded DNA as template. The DNA polymerase makes no distinction in adding dNTP or labelled ddNTPs, once a ddNTP is incorporated, the synthesis stops. The strand can be terminated at any position and resulting in a collection of labelled single stranded DNA differing with one nucleotide in length. A laser within an automated DNA sequencing machine is used to analyze the DNA strands produced. The results are depicted in the form of a chromatogram which is a diagram of colored peaks representing each nucleotide for each location in the sequence. A successful sequencing reaction depends significantly on DNA purity, sequencing buffer concentration, amount of template and the DNA polymerase used.

The following procedure was conducted to sequence purified pDONR221-*MMP-9ΔH-HPX* plasmid:

1. According to protocol 3 µl of 5x BigDye sequencing buffer was taken in total volume of 20 µl reaction mix.
2. The amount of template 270 ng was used as recommended in the protocol.
3. Three different primers used for the full sequencing of pDONR221-*MMP-9ΔH-HPX.*
4. M-13 forward primer to anneal the M-13 priming site of pDONR221.
5. Second forward primer for the sequence of middle part of mutated *MMP-9ΔH-HPX* in forward direction.
6. M-13 reverse primer sequence from the end of *MMP-9ΔH-HPX* in reverse direction.
7. The sequencing reaction mixture for each reaction was added into the PCR tubes on ice and run by the program.

The reagents and PCR program used for sequencing is shown in table 3 and 4. After the PCR was done, the tubes were sent to the DNA sequencing core facility of Arctic

University hospital northern Norway to resolve the actual sequencing by genetic analyzer.

Table 3. Setup for pDONR221-*MMP-9ΔH-HPX* plasmid sequencing

Program	Reagent	Volume (one reaction)
PCR	5x BigDye sequencing buffer	3 µl
	Template (540 ng/µl)	0.5 µl
	Primer	0.5 µl
	BigDye terminator v3.1mix	0.5 µl
	dH_20	15.5 µl
	Total	**20 µl**

Table 4. PCR program for sequencing the pDONR221-*MMP-9ΔH-HPX*

Step	Number of cycle	Temperature	Duration
1	1	96ºC	5 minutes
2	25	96ºC	10 seconds
		50ºC	5 seconds
		60ºC	4 minutes
3	1	4ºC	∞

BaculoDirect™Baculovirus Expression System

By using BaculoDirect™Baculovirus Expression System (Invitrogen, cat.no.12562-054), any gene of interest can be transferred directly into the Baculovirus genome *in vitro* without the need for extra cloning or recombination in bacteria or insect cells. The resulting recombinant Baculovirus DNA is then directly transfected into insect cells for generating recombinant virus and to screen for expression. In this system, attR1 and attR2 sites in the BaculoDirect™ linear DNA serves as the recombination cloning sites for the gene of interest from a Gateway entry clone. In order to generate recombinant Baculovirus DNA, LR reaction is performed using LR Clonase®II. Gateway LR Clonase enzyme mix promotes *in vitro* recombination between attL of an entry clone

and attR-containing BaculoDirect™Linear DNA (destination vector) to create an attB containing expression virus. The actual crossover occurs between homologous 15 bp core regions on the two sites but surrounding sequences are also needed as they contain the binding sites for the recombination protein (Landy, 1989). The LR reaction result in a recombinant Baculovirus DNA containing the gene of interest.

The procedure of LR Recombination Reaction was as follows:

1. 10 µl (30 ng/µl) Baculovirus linear DNA was mixed with pDONR221-*proMMP-9* (100 ng/µl) (positive control for protein production) in a tube
2. 10 µl (30 ng/µl) Baculovirus linear DNA was also added to another tube containing sample or entry clone pDONR221-*MMP-9ΔH-HPX* (541.7 ng/µl).
3. 1x TE buffer was added to the both tubes to give the final volume of 16 µl.
4. 4 µl LR Clonase® II Enzyme Mix was added to the both positive control tube and sample tube. These were mixed well by tapping the tubes several times and incubated for 18 hrs at room temperature.

As a control, LR recombination reaction product was amplified in PCR. To do this 1 µl aliquot of LR reaction was used as template. The reagents and PCR program used for the DNA amplification are summarized in the table 5 and 6.

Table 5. The setup for the PCR of LR reaction product

Program	Reagent	Volume (one reaction)
PCR	dH_20	15.5 µl
	Polyhedron forward primer (10 µM)	1.5 µl
	V5 reverse Primer (10 µM)	1.5 µl
	Template (LR reaction)	1 µl
	10x reaction buffer	5 µl
	dNTP mix (10 mM)	0.5 µl
	Taq DNA polymerase	0.5 µl
	Total	**25 µl**

Table 6. The programme used for the PCR for the LR reaction product

Step	Number of cycle	Temperature	Duration
1	1	95ºC	5 minutes
2	25	94ºC	45 seconds
		52ºC	1 minute
		72ºC	1.5 minutes
3	1	72ºC	10 minutes

The amplified LR product was analysed by performing agarose gel electrophoresis.

Agarose Gel electrophoresis

Gel electrophoresis is a method for separating and analysing the macromolecules DNA or RNA and their fragments based on their size or and charge. Nucleic acids are separated by applying an electric field to move the negatively charged molecules through an agarose matrix towards the positive pole. The shorter molecules move faster and migrate further than longer ones because shorter molecules migrate more easily through the pores of the gel.

The following procedure was conducted:

1. A 1% agarose gel was prepared by weighing out 0.5 g of agarose into a 250 mL conical flask.
2. 50 mL of 1x TAE buffer was added to the agarose and swirled to mix properly.
3. The mixture was then microwaved for about 1 minute to dissolve the agarose.
4. The gel was poured slowly into the gel tank. The bubbles if any was removed using a disposable tip.
5. The comb was inserted into the gel and the gel was left for 1 hour to become solid.
6. The comb was carefully removed from the gel and the gel was submerged into the gel tank with 1x TAE buffer.
7. 2 µl of PCR amplified LR recombination reaction product was loaded into one well and a molecular standard 1 kb ladder (NEB cat.no N3232S) was also loaded in another well.
8. The electrode position was checked before running the gel.

9. The gel was run at 90 V for 1 hr or until the dye of sample buffer is approximately 75-80% of the way down the gel.
10. The gel was then stained with GelRed staining solution.

Staining with GelRed

GelRed™ is a sensitive, stable, environmentally safe fluorescent nucleic acid dye. It is designed to replace the highly toxic ethidium bromide for staining dsDNA, ssDNA or RNA in agarose or polyacrylamide gels.

The procedure conducted was as follows:

1. 3x GelRed staining solution was prepared by adding 12 µl of GelRed™ 10,000x stock solution to 40 ml water for a single gel.
2. 1.6 ml of 2.5 M NaCl was added to the 40 ml GelRed solution to enhance the staining sensitivity.
3. The gel was placed in a suitable polypropylene staining container and the gel was submerged by sufficient amount of 3x GelRed staining solution.
4. The tray was placed in a shaker to agitate the gel gently at room temperature for 30 minutes.
5. Destaining was performed by placing the gel into a plastic dish and washed with water at shaking condition.
6. The gel was photographed by Image Quant LAS 4000 image reader.

Sf9 insect cells culture

The Sf9 (*Spodoptera frugiperda)* insect cells was provided with the BaculoDirect™ Transfection and Expression kits (Invitrogen, B825-01). Before performing the transfection procedure, we needed Sf9 cells ready to be transfected. Normally, this cell line was cultured in two separate manners for two purposes:

1. Purpose of Suspension cultures: Suspension culture was maintained to continue the passaging of the Sf9 cell line in insect growth medium. Viable cells are determined before each culture. For generating the sub-culture of Sf9 cells in suspension, approximately $2x10^6$ to $4x10^6$ cells/ml were used in suspension with supplemented Grace's Insect growth medium. The seeding densities for the cultures throughout the experiment allowed for 3-4 days' subculture schedule and a cell viability

of 90% was observed by trypan blue technique. Sf9 cells were maintained in a non-humid incubator at 26-28ºC for its most optimal growth.

2. Purpose of Adherent culture: Adherent cells were required for the periodic passaging and adherent condition of the cells were required for the transfection procedure. When cells were observed to have 90% confluent (a monolayer culture), transfection procedure was conducted.

Viable Cells counts using Trypan Blue

Trypan blue is a dye that can only penetrate the plasma membrane of dead cells. Hence, only dead cells appear blue under light microscopy. Counting both viable and non-viable cell, the viability of the cell culture can be calculated.

The procedure of staining was as follows:

1. The Sf9 cells were diluted in complete medium without serum to an approximate concentration of 1x 10^5 to 2x 10^5.
2. 10 µl of that cell suspension was placed in a screw cap test tube and 10 µl of 0.4% Trypan Blue stain was added to the tube. These was mixed thoroughly and left for 7 minutes for staining the non-viable cells.
3. With a cover-slip in place, 10 µl of Trypan Blue suspension mixture was transferred to the chambers of hemocytometer for cell counting.
4. Under microscope, non-viable cells were observed to be stained and viable cells excluded the stain.
5. The blue and non-blue cells within 4 separate squares with triple lines were counted and recorded.
6. The counting system is illustrated in the figure 16

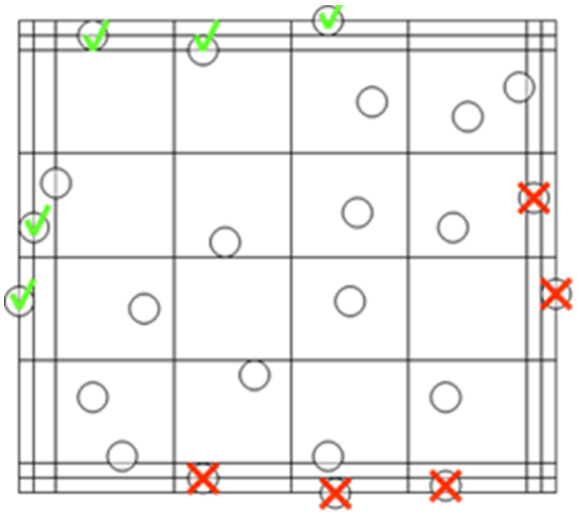

Figure 16. Cell counting system in Hemocytometer. Cells lying within squares and touching the upper and left-hand centre lines are counted. The cells touching the bottom lines and right hand lines are not counted

Each square of the hemocytometer represents a total volume of $0.1mm^3$ or 10^{-4} cm^3. Since 1 cm^3 is equivalent to approximately 1 ml, the subsequent cell concentration per ml is 10^4. Therefore, cells per square were determined by following the equation:

Cells/ml = the average count per square x dilution factor x 10^4

Total cell = cells per ml x the original volume of mixture from which cell sample was removed.

Cell viability = total viable cells (unstained) / total cells (stained and unstained) x 100

Transfection of Sf9 cells

DNA transfer into a new cell is called transfection. Cellfectin®II Reagent is used in BaculoDirect™ Expression system for transfection of Sf9 insect cells, it is called lipid-mediated transfection. Once virus particles enter into the insect cells, they prepare the infected cells for viral replication. Actual viral synthesis occurs 0.5 to 6 hours after infection following either a lysogenic phase or a lytic phase. In the lysogenic phase, the virions enter the nucleus of Sf9 cells, and within 6 hours of infection early-phase

proteins are produced. In a lytic phase many new phage of viral DNA within the Sf9 cell are produced and when the number of phage increases within Sf9 cells it damages the cells and exits, and subsequently infects other Sf9 cells. Within 20 to 36 hours after infection, recombinant gene product is evident. In a recombinant Baculovirus, polyhedrin gene is replaced with *MMP-9ΔH-HPX* gene. During the very late phase of infection, the inserted heterologous *MMP-9ΔH-HPX* gene is placed under the transcriptional control of AcNPV polyhedrin promotor. Thus the way, instead of polyhedrin protein, recombinant protein is produced.

The procedure of transfection was as follows:

1. Around 8x 10^5 Sf9 cells were plated in the 6-well plate allowing cells attach for 15 minutes at room temperature in the hood.
2. Two transfection mixture (A and B) were prepared for both the sample (*MMP-9ΔH-HPX*) and positive control (*proMMP-9*).
3. Transfection mixture A contained Cellfectin®II reagent and un-supplemented Grace's Insect Medium whereas transfection mixture B contained LR recombination reaction and un-supplemented Grace's Insect Medium.
4. The transfection mixture A and B were mixed together for positive control (*proMMP-9*).
5. The mixture A and B for the sample (*MMP-9ΔH-HPX*) was also mixed together and were incubated at room temperature for 25-35 minutes.
6. The transfection mix from 1 and 2 were added drop wise onto the adherent Sf9 cells and incubated for 4 hrs at 27ºC.
7. The transfection mixture was removed from the well after incubation and replaced with 1.8 ml complete growth medium containing 100 µM ganciclovir which inhibit the replication of non-recombinant virus within Sf9 cells (Kovacs et al., 1991).
8. The plates were then sealed with a plastic bag and incubated for 72 hours at 27ºC.
9. 2 ml of grace's insect medium from both positive control well and sample well were collected in a sterile 15 ml tubes.
10. The tubes were centrifuged at 3,000 rpm for 5 minutes in order to remove cells and large debris.

11. The supernatant of both positive control and sample were then transferred to fresh 15 ml tubes and stored at -20ºC until further use. These samples are referred to as the P1 viral stocks.
12. 1 ml from P1 viral stock was used for further transfect the fresh Sf9 cells and to continue the passages of viral stock P2, P3, P4.

Sodium dodecyl sulfate-polyacrylamide gel electrophoresis (SDS-PAGE)

Gel electrophoresis is used for analysing the mixture of proteins based on their physical properties such as charge or molecular mass. When polyacrylamide gel contains anionic detergent sodium dodecyl sulfate (SDS), it is called SDS-PAGE. Normally amino acids that make up proteins might be positive, negative, neutral, or polar in nature. Therefore, the overall charge of a protein depends on the sum of the charges on the individual amino acid side chains. The SDS-PAGE technique where proteins are coated by SDS in a proportion to its total molecular mass and give rise to rod-like overall negatively charged complexes. When an electric field is applied, the negatively charged complexes are separated based on the differences of their molecular masses. Two different gel 'Stacking' and 'Separating' are used in SDS-PAGE. The pH of those two gels and buffer is very important for the proteins mobility. During electrophoresis, the protein-SDS complexes are concentrated into a narrow zone in the stacking gel (pH 6.8) and only effective separation occurs when the complex reaches the separating gel (pH 8.8). The pH prevailing in the separating gel allow the protein-SDS complexes to move in a uniformed buffered (pH 8.3) electric field to separate from each other according to their size and charge (Walker, 1984). When an electric field is applied, the uniform negatively charged protein travel from concentrating gel through the polyacrylamide matrix based on their molecular size. The larger protein molecule travel slower through the polyacrylamide matrix than the smaller one.

This technique can be carried out under reducing condition in the presence of a reducing agent DTT, or without reducing agent. Reducing agent DTT breaks off disulfide bonds of already denatured protein by SDS, which only disrupts the non-covalent bond between amino acids. Removing the last traces of tertiary and quaternary structure of protein by DTT, protein appears as an unfolded simple primary

structure. Hence, the unfolded protein complex under reducing condition travel more slowly in the gel than unfolded compact protein complex under non-reducing conditions. Comparing reduced and non-reduced samples, molecular size of a protein subunit and the information about monomeric or oligomeric forms of protein can be obtained. In the current experiments we performed SDS-PAGE both under reduced and non-reduced conditions.

The procedure was as follows:

1. 20 µl protein sample were mixed with 6 µl 5x sample buffer (0.5 M DTT or without DTT) and boiled for 4 minutes.
2. The sample tubes were centrifuged for 30 seconds at 12000 rpm and then loaded in 4-12% NuPAGE ready-made gel along with P-250 kDa protein ladder.
3. 600 ml MES-SDS running buffer was added to the electrophoresis try.
4. 200V was set for electrophoresis for 35 minutes.
5. The gel was removed from the plastic cover and was shake for 5 minutes putting in a shaker. This step was repeated twice for 10 minutes.
6. The gel was stained with 20 ml imperial Coomassie protein staining solution in a warming condition in the micro-oven until any band was visible.
7. De-staining step was accomplished with water and the gel was imaged by Quant LAS 4000 image reader.

Gelatin zymography

Gelatin zymography, an electrophoretic technique where gelatin has been incorporated in the gel in order to detect the enzymatic activity of a gelatin degrading protease. This technique is commonly based on sodium dodecyl sulfate-polyacrylamide gel electrophoresis (SDS-PAGE). In order to perform gelatin zymography, two different types of gel are required; the stacking or concentrating gel and the separating gel. The separating gel contains a higher concentration of polymerized and cross-linked acrylamide compared to that of the concentrating gel. This along with the different pH in the two gel compartments allows for the separation of proteins. Concentrating gel concentrate protein in narrow bands. Gelatin

zymography is always performed under non-reducing conditions in order to avoid inactivation of the enzymes.

When SDS is removed from the protein in washing step, protein refolds. During the refolding, the pro-domain (for *eg.* MMP-9) refolds back to the catalytic domain. Instead of refolding back to the correct position, it binds to the catalytic site as a substrate. Hence, the pro-domain is cleaved off leading to auto-activation of the MMP. Gelatin Zymography, a precise and very sensitive tool to detect gelatin degrading enzymes like MMP-9.

Enzyme degradation of the gelatin substrate appears as transparent bands against a deep blue background after staining the gel with Coomassie Blue. Using gelatin zymography, semi-quantitative measurement of the amount of a protein in a sample can be determined. In addition, the molecular weight of the protein and discrimination between latent and active species can be identified (Dwek et al., 2012; Snoek-van Beurden and Von den Hoff, 2005). The major limitation of this technique is that the net proteolytic activity of gelatinases is not obtained as TIMP that inhibits the activity of the enzyme is dissociated from the enzyme during SDS-electrophoresis. Moreover, the refolding of MMPs after electrophoresis recovers only the part of its original activity.

The following procedure was conducted:

1. Zymography apparatus including glass plates was cleaned with 96% ethanol.
2. A 7.5% separating gel mix were prepared using the reagent were shown in the table 2.1.3 and 0.1% gelatin was incorporated into the separating gel allowing for the detection of MMP-9 through its degradative capacity.
3. 7.5% separating gel mix was pipetted between the glass plates avoiding bubbles.
4. The plates were filled about 80% way up leaving space for the stacking gel and comb.
5. A small amount of distilled water was overlaid on top of separating gel to achieve a completely flat interface between separating gel and stacking gel. The separating gel was allowed to polymerize for about 10 minutes.
6. A 4% stacking gel mix were prepared using the reagent were shown in the material section.

7. The excess water was poured off from polymerized separating gel.
8. The stacking gel mix was poured avoiding bubbles and comb was inserted.
9. The comb was removed carefully after the stacking gel was polymerized.
10. The gel was assembled onto the electrode section of the gel apparatus.
11. Central well of the gasket was filled with 1x running buffer and the bottom of the tank with 1x running buffer.
12. Samples were pipetted into wells by using gel loading tips.
13. 150V and 18 mA was set and the gel was run for 2 hours at 4ºC until the dye front reaches the end of the gel.
14. The apparatus was disassembled and gel was gently placed into a plastic dish and washed two times for 15 min in approximately 100 ml 2.5% Triton-X-100 in order to remove SDS from the gel.
15. The gel was incubated with 50 ml incubation buffer at 37ºC overnight.
16. The next day the incubation buffer was discarded and the gel was stained with 50 ml Coomassie blue staining solution in a shaker for 1 hour.
17. The gel was de-stained with de-staining buffer until the background appeared as blue due to presence of gelatin and white bands where the gelatin has been degraded.
18. The gel was then photographed by Quant LAS 4000 image reader.

Protein purification by Gelatin Sepharose Chromatography

Affinity chromatography technique for protein purification depends on a reversible interaction between proteins or group of proteins and a specific ligand which remain coupled to a chromatography matrix. This technique is considered to be an ideal technique for protein purification with high selectivity and several thousand-fold high recovery of active material. In addition, by using this technique a target molecule can be separated from complex biological mixtures, native forms can also be separated from denatured forms of biological molecules. In order to perform this affinity technique, a bio-specific ligand that can be covalently attached to a chromatography matrix is necessary. Additionally, the coupled ligand must retain its specific binding affinity for the target protein (molecule) and more importantly, the binding between the ligand and target molecule must be reversible, allowing the target molecules to separate in an active form in the elution step. In our case the technique was referred

to as Gelatin Sepharose Affinity Chromatography, where the ligand is gelatin which is attached covalently to the Sepharose matrix. The ligand gelatin has affinity to the fibronectin type domain of MMP-9. Hence MMP-9 bind to the gelatin reversely and MMP-9 can be eluted from the column using a buffer containing 7.5% DMSO. We have used this technique to isolate full length proMMP-9 (positive control) and the deletion variant of MMP-9 (proMMP-9ΔH-HPX) from the viral stocks (P2-P4).

The following procedure was conducted:

1. 1 ml column for both sample and positive control were prepared by setting small glass wool filter rolls in the bottom of the column.
2. 200 µl gelatin sepharose was applied on the top of wool filter. The columns were then vertically fixed on a stand.
3. 5 ml washing or binding buffer used 3-4 times in order to wash the column.
4. 1 ml sample was applied to the column.
5. 1 ml positive control was applied to another column.
6. The flow through was collected from the column in 1.5 ml Eppendorf tube.
7. 500 µl aliquot of the 1.5 ml washing buffer was also collected to verify unbound protein material.
8. An additional pre-elution step was applied where the buffer contained 0.1% DMSO.
9. 300 µl of elution buffer containing 7.5% DMSO was applied for the final elution.
10. Eluted protein was collected in three separate tubes, 100 µl in each.

Concentration of purified proteins and removal of impurities with molecular size less than 10 kDa

In order to concentrate the eluted protein, a spin column with a cut off of 10 kDa (Millipore) was used to concentrate the protein molecules that are bigger than 10 kDa.

The procedure was as follows:

1. 100 µl of proMMP-9 and proMMP-9ΔH-HPX sample were added to the spin column and centrifuged at 45000 rpm until it reached 20 µl remaining volume.
2. With 300 µl of 0.1 M HEPES buffer, the samples were centrifuged at 45000

rpm. This was repeated 4-5 times in order to remove DMSO from the samples.

3. After centrifugation, the final volume of 20 µl was expected to be DMSO free.
4. The amount of protein in the concentrated samples was determined spectrophotometrically by determining the absorption at 280 nm and then using Beers law the concentrated proMMP-9ΔH-HPX proteas was then determined.

Beers law $A=\varepsilon*c*l$

Where A= Absorbance at 280 nm, ε = extinction coefficient (for *eg.* the extinction coefficient of MMP-9 is 114.36 $mM^{-1}cm^{-1}$ (Murphy and Crabbe, 1995) and MMP-9ΔH-HPX is 73.06 $mM^{-1}cm^{-1}$ c = concentration and l = optical path length in cm. Therefore, if ε is known, measurement of A gives the concentration directly. The value of l depends on the path length of the cuvet. A rapid way to calculate the extinction coefficient is by using the ProtPARAM tool from ExPASy with target protein's amino acid sequence, which was done for MMP-9ΔH-HPX. In the case of the full length proMMP-9, this theoretical calculation (ε=112.73 $mM^{-1}cm^{-1}$) is close the experimental value obtained by Murphy and Crabbe (see above).

Size exclusion purification

The process of Size Exclusion Chromatography uses a matrix consists of porous particles and where molecules separation is achieved according to molecular size and shape of the molecules. For separating molecules of different sizes, normally molecular sieve properties of different sizes porous matrix are utilized. The SEC matrix consist of a range of beads with slightly different pore sizes where the separation process depends on the ability of different proteins to enter all, some or none of the channels in the porous beads. The length of the column (cm) is a significant parameter as it affects the resolution and also time used to elute the sample. In addition, the rate of the flow of eluent is another factor to be considered, as it affects the speed at which separation of the molecules are obtained. When three different molecules are separated using the chromatography where large protein molecules are not able to enter into the smaller cavities they pass quickly between the beads and come out of

the column in void volume (V_0). In contrast, smaller protein molecules enter into the cavities and take the longer path around the beads. They come out in what is called the elution volume (V_e). Very small particles like potassium dichromate enter also the smallest cavities of the beads and these particles are used to define the total volume of the column (V_t). In the present investigation a Sephadex G-75 column was used. This column can separate proteins with molecular sizes that ranges from 3 to 80 kDa and the protein molecule larger than 80 kDa enter in the void volume.

The procedure was as follows:

1. 6 ml Sephadex G-75 gel was packed in 10 ml pipet.
2. 2 column volume of equilibrium buffer was used to wash the column.
3. To get an idea of the separation properties (V_0 and V_t) of this column with G-75, Blue dextran 2000 (150 µl) and potassium dichromate (100 µl) were used.
4. The first 2 ml only contained buffer and was discarded.
5. Blue dextran 2000 came in void volume (V_0) and was determined to 2.5-4 ml. Potassium dichromate was collected in the total volume (V_t) and was determined to 4-5 ml.
6. Based on the idea above, 100 µl concentrated protease sample was added to the Sephadex G-75 column and 16 fractions of 500 µl was collected.
7. 100 µl gelatin sepharose was added to each 500 µl protease sample and left them for 10 minutes.
1. The gelatin sepharose beads was then washed with washing buffer.
2. Purified protease was eluted with 100 µl of elution buffer containing 7.5% DMSO.

Mass spectrometry

Mass spectrometry is an analytical chemistry tool that measures the molecular masses of individual compound, chemicals, or atoms precisely by converting them into gas-phase to ionic species. There are three main section in any mass spectrometer; ionization source, the mass analyser and the detector. During ionization event of spectrometer, by electron impact that leads to break down the covalent bonds in the target molecules leading to generation of high amount of characteristics fragment ions. These ions are then accelerated, so all the ions are of same kinetic energy. The charged ions are separated and sorted out on the basis of their mass-to-charge ratio.

This is done with the help of mass analysers. The detection of the beam of those ions while passing through the machine is detected electrically. The obtained information is stored and analysed depending on the type of investigation from which the data are formed (Feng et al., 2008).

Western blot analysis

Western blot also known as protein immunoblot is an extensively used analytical technique to detect specific proteins from a complex mixture of proteins that are extracted from tissues or cells, or secreted from cells into culture media. This technique involves three major steps; protein separation by size or charge, protein transfer to the blotting membrane and finally detection of the protein by using specific primary and secondary antibodies to recognize the target protein.

The separation of protein from the mixture is attained according to the length of polypeptide (molecular weight) or charge through electrophoresis. The separated proteins are transferred to the membrane made of nitrocellulose or positively charged nylon Polyvinyl Dene Fluoride, (PVDF) by applying an electrical current that induces the proteins to migrate from the gel to the membrane. The transferred protein is immobilized on the membrane. Thereafter, the protein has been attached to the membrane. The membrane is washed with blocking buffer made from non-fat milk powder or BSA. This step is necessary to prevent any unspecific binding of primary antibodies to the surface of the membrane. The membrane is then incubated with a dilute solution of primary antibody which is specific for the protein of interest. After which the membrane is washed with TBST to remove unbound primary antibody. The membrane is then incubated with blocking buffer containing a diluted secondary antibody usually conjugated with a biotin or a reporter enzyme most commonly Horse Reddish Peroxidase (HRP) as probe to recognizes the primary antibody. The membrane is washed again to remove unbound secondary antibodies. Luminal reagents are then added with HRP conjugated antibodies. The enzyme linked to secondary antibody convert the luminal reagents to a fluorescent product by which antibodies are detected. The thickness and intensity of the band is proportional to the amount of the protein present in the sample (Dwek et al., 2012).

The procedure followed was as follows:

1. A readymade 4-12% NuPAGE SDS-PAGE gel was washed with milli-Q water and the white tape set in the bottom of the gel and comb were taken out carefully.
2. The gel was rinsed with 1xNuPAGE running buffer and was set in the mini-cell rack orienting inward.
3. In case of one gel, a dam gel was used as gel number two.
4. The electrophoresis inner camber was filled with 1xNuPAGE running buffer. It was necessary to first to check for any buffer leakage.
5. The outer chamber was filled with 1xNuPAGE running buffer. 10 µl sample along with 8 µl multicolor protein marker and 7 µl biotin-labelled molecular weight protein standards were loaded into the gel.
6. The gel was run for 35 minutes at 200V.
7. PVDF- membrane was cut in the same size of the gel and kept them in methanol for 3 seconds followed by 10 seconds in water and then in blotting buffer for more than 5 minutes.
8. The gel was removed from the casket by breaking the sides of the casket using a gel – knife and the lowest part of the gel was cut off and discarded.
9. The pre-wetted PVDF-membrane was placed on the top of gel while the pre-wetted filters were on the top of PVDF-membrane.
10. Air bubbles were removed by rolling a glass rod over the membrane slowly.
11. The pre-wetted pads and filter-paper were placed in the cathode core for blotting. The inner chamber of cathode core was filled with blotting buffer while outer chamber with water for cooling.
12. Setting the lid in the proper way, the blotting program was run and the membrane was washed keeping inside a tube containing 5 ml 1X TBST for 5 minutes in a rotating wheel.
13. The membrane was then blocked with 5 ml blocking buffer for an hour and then the membrane was incubated with 5 µl 1000x diluted Rabbit anti-MMP-9 primary antibody overnight at 4^{o}C.
14. The gel was washed with 1x TBST for three time each 5 minutes and followed by incubation with HRP conjugated 2.5 µl 2000x diluted goat anti-rabbit IgG secondary antibodies for an hour at room temperature.

15. The membrane was washed for three times with 5 ml 1X TBST each five minutes.
16. 1:1 ratio of luminal reagents (A and B) for antibody detection was added to the membrane and left for 1 minute.
17. The image was obtained by using luminescent image analyzer Lumi-Imager F1^{TM}.

Results and Discussions

Generating a truncated variant of proMMP-9, the proMMP-9ΔH-HPX

Structural and domain analysis has shown that proMMP-9 is composed of several domains including a hinge region and hemopexin-like domain. (Figure 17A). In order to produce a proMMP-9 that lacks the hinge region and the hemopexin domain, a point mutation was introduced at the beginning of the hinge region by site-directed mutagenesis using the QuikChange II Site-Directed Mutagenesis Kit (Agilent Technologies). The vector pDONR221-MMP-9 containing the full length human *preproMMP-9* open reading frame (ORF) was provided by Dr. Nabin Malla in our research group and used as template in the site-directed mutagenesis reaction.

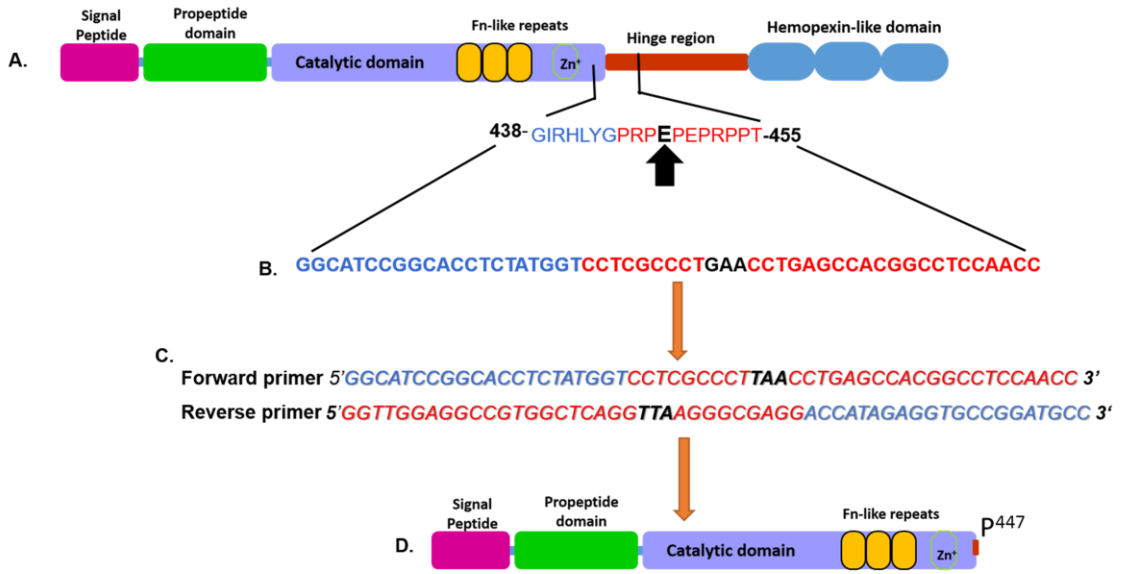

Figure 17. proMMP-9ΔH-HPX truncated variant from the full length proMMP-9. A. Domain representation of full length preproMMP-9. Amino acid sequences highlighted in blue color (normal) are the end part of catalytic domain and red in color are some part of hinge region. The amino acid **E**448 in the hinge region was mutated by site directed mutagenesis is displayed in black color (bold) and it is indicated by a black arrowhead. **B.** The corresponding nucleotide sequences of amino acids (438-455) were used for primers design where triplet codon GAA for amino acid E was mutated and it is indicated in black (bold). **C.** The resulting stop codon (*TAA*) is shown in the sequence (5`-3`) of both primers. **D.** The domains structure of the truncated variant proMMP-9ΔH-HPX.

As site-directed mutagenesis is a PCR based method, we needed a set of two primers; forward primer and reverse primer. For introducing the mutation, primers were designed with the nucleotide sequences from 438-455 surrounding E448 amino acid (Fig.17B). In both primers, G in the GAA codon was replaced by T resulting in a stop codon and thereby producing a proMMP-9 of 447 amino acids long lacking the hinge region and hemopexin-like domain instead of the wild-type 707 amino acid protein (Fig.17D).

Transformation of site directed mutagenesis product into XL1-Blue supercompetent bacteria and Sequencing

After transforming the DpnI treated mutagenesis product (pDONR221-*MMP-9ΔH-HPX*) into XL1-Blue supercompetent bacteria, the transformation mix was spread on kanamycin plates for selection of only transformed bacteria. A total of eight (8) colonies were picked from the agar plates and then these were allowed to grow in suspension. Thereafter, bacterial cells were harvested and by following the procedure of QIAprep Spin Miniprep Kit Protocol, we purified the bacterial plasmid. The DNA concentration of purified plasmid was then measured by NanoDrop Spectrophotometer and after that the plasmid was sequenced by using three different primers in order to verify the presence of the mutation. Using the forward primer M13 (-20), which binds to the priming site of the pDONR221, gave a sequence of 940 nucleotides of *preproMMP-9ΔH-HPX* in forward direction without covering the area where the desired mutation was inserted. On the other hand, the second forward primer designed from the nucleotide sequences that correspond to amino acids G195 to D205 of *preproMMP-9ΔH-HPX* covered the sequence of the mutated area and showed a correct mutation introducing a stop codon. The M13 reverse primer was used to sequence the hemopexin and hinge region of *preproMMP-9ΔH-HPX* including the mutated area (Fig.18). The obtained sequences were also analyzed to ascertain that the nucleotide sequences of the entire *preproMMP-9ΔH-HPX* ORF in the gateway entry vector (pDONR221) was in the right frame and free of unexpected mutations.

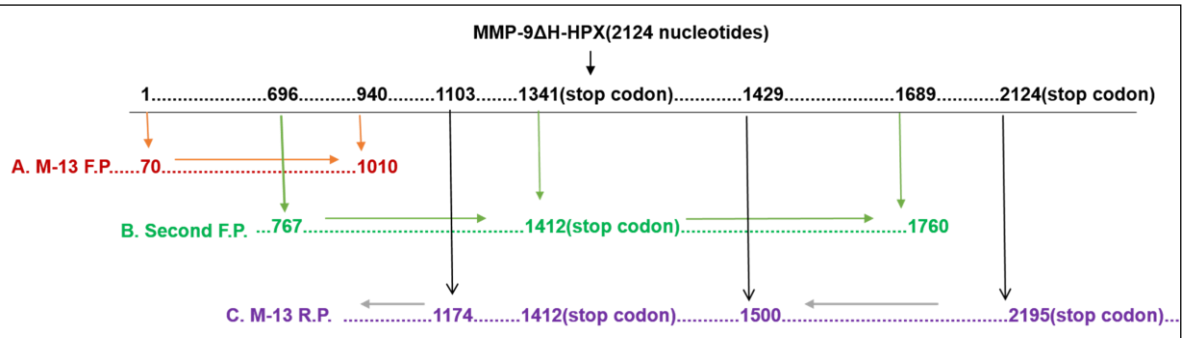

Figure 18. Analysis the sequence of *preproMMP-9ΔH-HPX*. Nucleotide sequence representation of proMMPΔH-HPX containing pDONR221 entry clone plasmid showing points of anneal of three different primers. **A**. The M-13 forward primer anneal upstream of the gateway attL sequence of the pDONR221-*preproMMP-9ΔH-HPX* vector and sequenced until about 940(1010) nucleotide bases of the MMP-9 DNA. **B**. Another forward primer which sequenced from 696(767) till 1689 (1760) nucleotide bases and **C.** The M-13 reverse primer sequenced in the reverse direction from approximately 2124 (2195) till 1103(1174) nucleotides of *preproMMP-9ΔH-HPX*.

The sequence alignment analysis showed that only a single desired mutation was produced within the entire *preproMMP-9ΔH-HPX* ORF. The mutated nucleotide was marked in the figure 19 and full sequence of *preproMMP-9ΔH-HPX* is attached in the Appendix (A1).

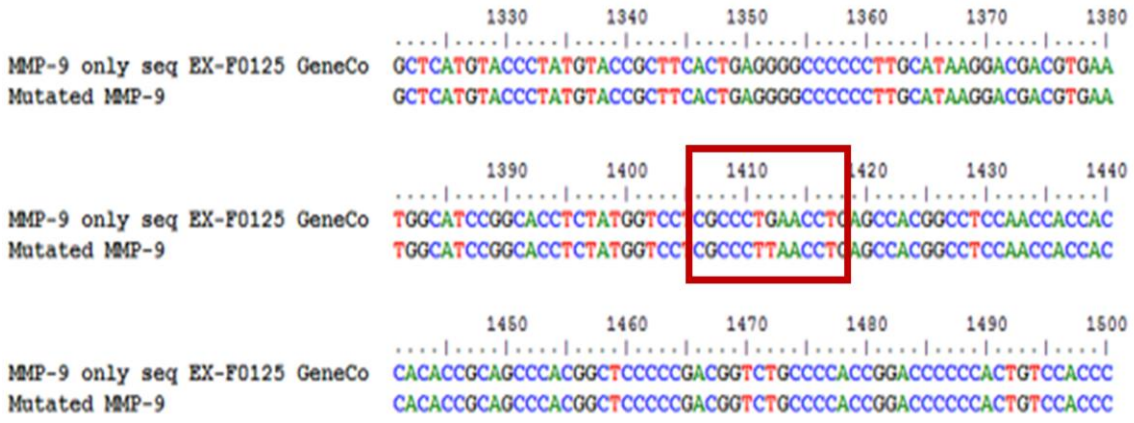

Figure 19. Sequence alignment of *preproMMP-9ΔH-HPX*. pDONR221-*preproMMP-9ΔH-HPX* was sequenced and the resulting sequence was aligned with wild-type proMMP-9. The highlighted box shows the mutation of G to T in the hinge region of MMP-9 replacing the codon GAA for glutamate to TAA a stop codon.

Generation of a recombinant Baculovirus DNA vector by Gateway LR recombination reaction

In pDONR221-MMP-9ΔH-HPX, the *preproMMP-9ΔH-HPX* ORF is flanked with attL sites. Both pDONR221-*MMP-9ΔH-HPX* and pDONR221-*proMMP-9* encoding normal full length proMMP-9, were mixed with linear Baculovirus DNA containing attR site according to the protocol of Baculo-Direct Baculovirus expression system. In order to transfer the ORFs from the pDONR221-vectors to the Baculovirus DNA, an LR recombination reaction was performed. In order to verify the successful insertion within the Baculovirus genome, PCR using polyhedrin forward and V5 reverse primer was performed with the LR recombination products as template. The amplified DNA was then subjected to 1% agarose gel electrophoresis. Analysis of the gel electrophoresis result revealed that none of the bands corresponded to the expected 2.4 kb size of the *preproMMP-9ΔH-HPX* ORF inserted into the linear Baculovirus genome (Fig. 20) (See appendix A2).

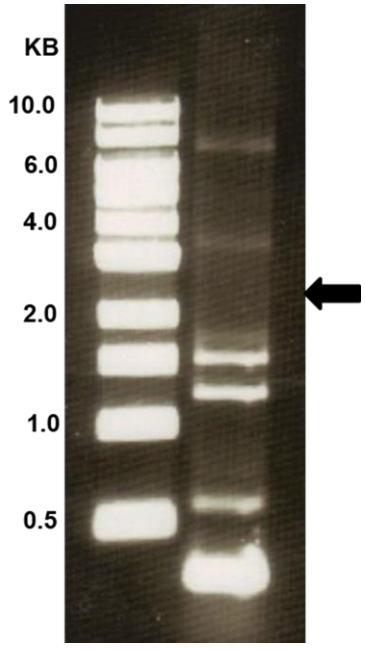

Figure 20. Agarose gel electrophoresis of LR recombination reaction product. 1% agarose gel showing the product of LR reaction where the *preproMMP-9ΔH-HPX* ORF in the Baculovirus genome was used as a template. The first lane is a 1kb DNA ladder and the second lane is the amplified LR product. An arrowhead indicates the position where the right size LR product was expected to appear.

The BaculoDirect™Baculovirus Expression System is a well-established method with an apparent 100% yield of recombinant viruses (Kost et al., 2005) and PCR is a standard method, still we were unable to obtain a PCR product of the expected size and therefore unable to verify correct insertion using this method. The failure might be due to unspecific primer binding, too low or high concentration of template or primer, or sub-optimal annealing temperature of the primers or sub-optimal primer design.

Upon closer analysis of the polyhedrin and V5 primers provided with the kit, we found that the melting temperature (Tm) of the polyhedrin forward primer was theoretically estimated to be 50ºC, whereas V5 reverse primer was 66ºC. According to protocol, the annealing temperature used for the PCR reaction at 52ºC. For a successful PCR product, it is important to have a similar Tm for both primers and ideally it is recommended to select an annealing temperature 3 to 5 degrees lower than the Tm of the primer so that both forward and reverse primers can bind to the template. In other case, going too low with the annealing temperature, the primers might anneal to nonspecific sequences leading to undesired multiple PCR products.

In our present investigation, analysis of the agarose gel result revealed at least seven bands of different sizes where four smaller bands were strong and three bigger sizes were weak bands (Fig. 20). The results indicated that the primers annealed at many different places in the template, probably due to a too low annealing temperature allowing the V5 primer to anneal un-specifically. Re-amplification with changing annealing temperature was found to be difficult because the difference of melting temperature of those two primers were so big.

However, when we observed that the transfection of Sf9 cells with LR product was successful in producing our target proteases (proMMP-9ΔH-HPX and proMMP-9), we put minor importance on the PCR amplification result and proceeded with the experiments.

Transfection of Sf9 insect cells with recombinant linear Baculovirus DNA

The Sf9 insect cell from Life Technologies are the traditional cell lines suitable for producing recombinant protein using the Baculovirus expression system protocol. Throughout the transfection procedure the Sf9 cells culture were always examined in order to be sure that cells were regular in shape and 90% confluent (monolayer culture). The percentage of cell's viability was also determined before each transfection procedure by staining with trypan blue followed by examination and counting using regular phase contrast microscopy. According to the protocol around $8x10^5$ cell/ml viable Sf9 cells were used for each transfection procedure.

For the transfection, the solutions containing recombinant Baculovirus DNA with the *preproMMP-9ΔH-HPX* and *preproMMP-9*, respectively, were added drop wise onto the Sf9 cells that were cultured in complete Grace's insect growth medium. The transfected cells were then incubated for 72 hours at 27ºC, and thereafter the cells were examined under light microscope (Leica DFC320). Floating and disrupted Sf9 cells indicated the production of recombinant viruses since high production of viral particles might lead to cell lysis. When we observed symptom of virus production, the insect growth medium was collected and named Passages of viral stock or P1. This P1 viral stock was expanded in fresh Sf9 cells to produce P2, P3 and P4 virus stock with increasing virus titre. All the (P1-P4) passages of viral stocks were analysed by Gelatin Zymography using Sodium Dodecyl Sulfate (SDS)-polyacrylamide gels copolymerized with 0.1% gelatin in order to analyse the gelatinolytic activity of the protease produced by the infected Sf9 cells.

Since LR recombination reaction was performed for insertion of *preproMMP-9* and *preproMMP-9ΔH-HPX* into Baculovirus genome and Sf9 cells were transfected with the resulted recombinant Baculovirus genome, it was expected that the Sf9 cells would produce proMMP-9 and proMMP-9ΔH-HPX proteins. Additionally, previous results from our research group have shown that Sf9 cells do not produce any gelatinases, thus any bands on the gelatin zymography gel would be an indication of MMP-9 production.

Since our aim was to produce a truncated proMMP-9, therefore, the size of the protease was expected to be smaller than the size of the full length proMMP-9. A study by Philippe E. Van den Steen, *et.al.* showed that recombinant proMMP-9 produced by Sf9 cells lacking both the hinge and hemopexin domain was around 48 kDa and the same molecular weight was observed under both reducing and non-reducing conditions (Van den Steen, 2006). In the present study, Gelatin Zymography of all Passages of viral stock revealed that gelatin degrading activity by the proteases in both the proMMP-9 and the proMMP-9ΔH-HPX sample were so strong that it was difficult to determine the accurate sizes of the protease bands in the samples (Fig. 21).

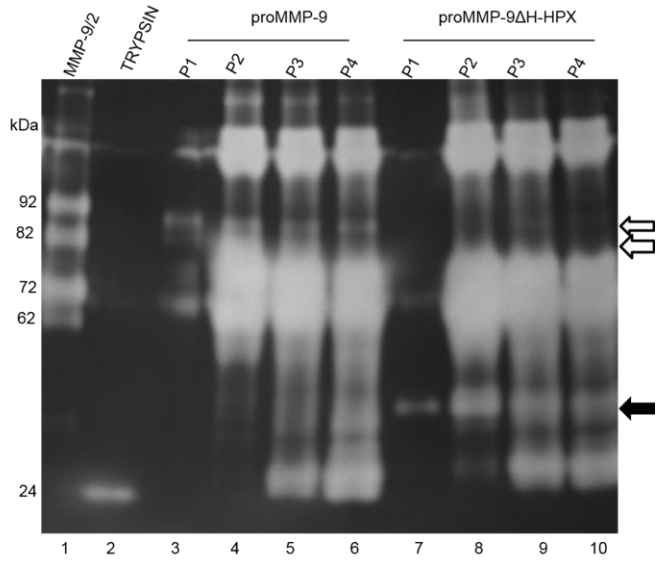

Figure 21. Gelatin zymography showing the gelatin degrading proteases in the passages of viral stock produced in Sf9 cells. All passages of viral stock were 20x diluted. Standards MMP-9/2 in the lane 1 and Trypsin in lane 2. Lane 3-6 shows the viral stock (P1-P4) of positive control containing proMMP-9 and lane 7-10 represents the viral stocks (P1-P4) of the proMMP-9ΔH-HPX protease sample. Coomassie Blue was used for staining the gel. White bands denote proteolytic activity of the proteases over the blue background which contain gelatin. Two open arrows indicate two protein bands around 85 kDa and 82 kDa in the positive control and closed arrow indicates the expected proMMP-9ΔH-HPX protease band in the proMMP-9ΔH-HPX sample.

Additionally, the many bands showing gelatinolytic activity in both samples were very similar, with only some exceptions. As shown in figure 21, it was found that the P1 viral stock of the proMMP-9 sample showed doublets bands with molecular size of around 82 and 85 kDa, whereas the P1 viral stock in the proMMP-9ΔH-HPX sample showed a single strong band of approximately 48 kDa. This could represent the proMMP-9ΔH-HPX protease as the estimated size calculated based on data from the MEROPS database and ExPASY analysis was 48 kDa. The contamination might be occurred from the P2 viral stock of both samples. The unexpected protease bands observed in P2 viral stock were also present in the following viral stocks. However, the gelatinolytic bands were not clear enough to determine their sizes. Therefore, the

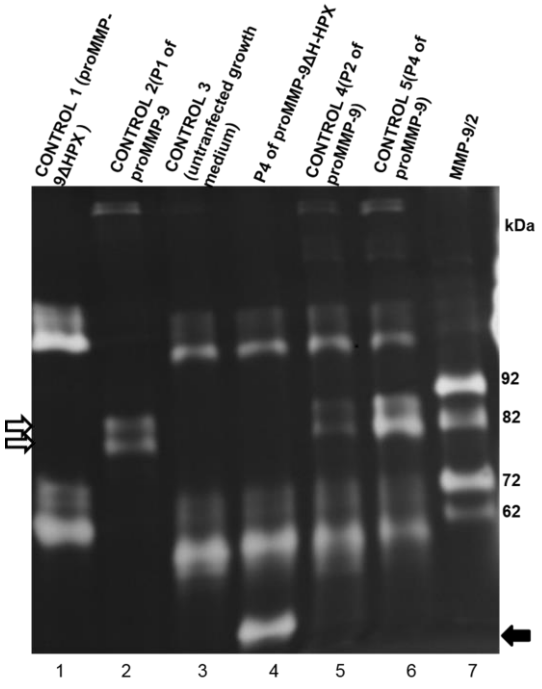

Figure 22. Gelatin degrading proteases in the medium from Sf9 cells. All samples were diluted 200x with 0.1M HEPES buffer. Control 1 was insect growth medium containing MMP-9ΔHPX protease whereas control 2, 4 and 5 were P1, P2 and P4 viral stocks of proMMP-9. In control 3, un-transfected insect growth medium of Sf9 cell. P4 viral stock from the sample containing MMP-9ΔH-HPX is shown in the lane no 4. Two open arrows indicate the molecular sizes of 82 kDa and 85 kDa protease bands in the positive control proMMP-9. Another arrow (closed) indicates the expected proMMP-9ΔH-HPX protease produced in Sf9 cells.

samples were dilute 200x and analysed by Gelatin Zymography. Several control samples were included in order to determine the sizes of the protease bands (Fig. 22). Analysing the result of the Gelatin Zymography it was observed that the activity of the two contaminating bands at approximate 60 kDa and 120 kDa in control 3, was common in other samples as well, including the negative control. Besides these common bands, additional bands around 82 kDa and 85 kDa were observed in the P4 viral stocks of the proMMP-9 sample. Based on the knowledge that proMMP-9 is heavily glycosylated, the double bands most likely represent proMMP-9 with different degree of glycosylation. In the proMMP-9ΔH-HPX sample in lane 4, a band of the expected size of 48 kDa was observed. Thus, from this we concluded that we had successfully produced proMMP-9 and proMMP-9ΔH-HPX, although with several contaminating proteins. Thus, a purification protocol was needed in order to exclude the contaminating proteins and obtain high purify of the samples.

Protein purification by Gelatin Sepharose Chromatography

Since the three fibronectin-like repeats in the catalytic domain of MMP-9 is known to have affinity for gelatin (Goldberg et al., 1992), the technique Gelatin Sepharose affinity chromatography was performed to purify the proMMP-9ΔH-HPX and proMMP-9. The binding between gelatin and the FnII module in MMP-9 is reversible, and the two MMP-9 enzymes can be detached from the column by the addition of 7.5% DMSO. During purification, along with eluted proteases, aliquots of the flow through and washing buffer with 1 M NaCl were collected. NaCl give ionic strength to the purification buffer which helps to prevent nonspecific ionic interactions between proteins and the column. Hence, aliquots from the washing step were collected to observe if the nonspecific protease passed through the column and was removed from the sample. All aliquots were subjected to gelatin zymography. The result of the zymography (Fig. 23) revealed that the eluted proMMP-9ΔH-HPX protease in lane 3 contained a strong band around 48 kDa and two weak contaminating bands around 60 kDa and 120 kDa having gelatinase activity. Eluted proMMP-9 contained bands with molecular sizes of around 82 kDa and 85 kDa along with contaminating bands of 60 kDa and 120 kDa (Fig. 23).

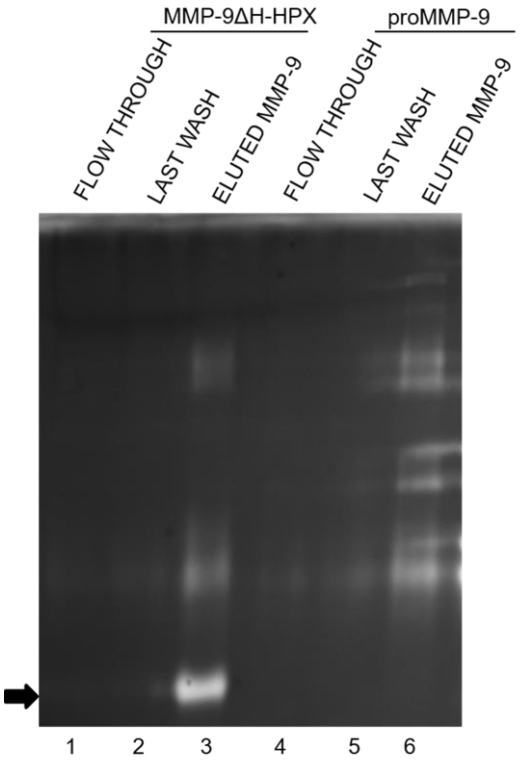

Figure 23. Gelatin Zymography showing the gelatin degrading proteases in various steps of affinity purification technique. All samples were 200x diluted except the aliquot from last wash of purification step. Lane 1-3 represent aliquots of purification steps of the truncated proMMP-9 (MMP-9ΔH-HPX) whereas lane no (4-6) represent aliquots of purification steps of positive control samples (proMMP-9). An arrow indicates the expected MMP-9ΔH-HPX protease in the partly purified sample.

Another Gelatin Sepharose Chromatography was performed for other batches of P4 viral stock of the truncated variant following the same affinity purification procedure. Aliquots of different purification steps along with eluted protease were subjected to another Gelatin Zymography. Analysis of the zymography results revealed that even though 1 M NaCl removed a lot of unspecific proteases from the Sepharose column, still the aliquots of last wash without NaCl contained large amount unspecific proteases (Fig. 24). The observations of both zymography results (Fig. 23 and 24) of aliquots from various steps of Gelatin Sepharose purification technique depicted that the different sizes of contaminating bands including around 60 kDa, 120 kDa also bind to Gelatin Sepharose column and as they also occurred in the last washing step it

might be possible to remove these impurities by introducing further washing steps of the Gelatin Sepahrose column.

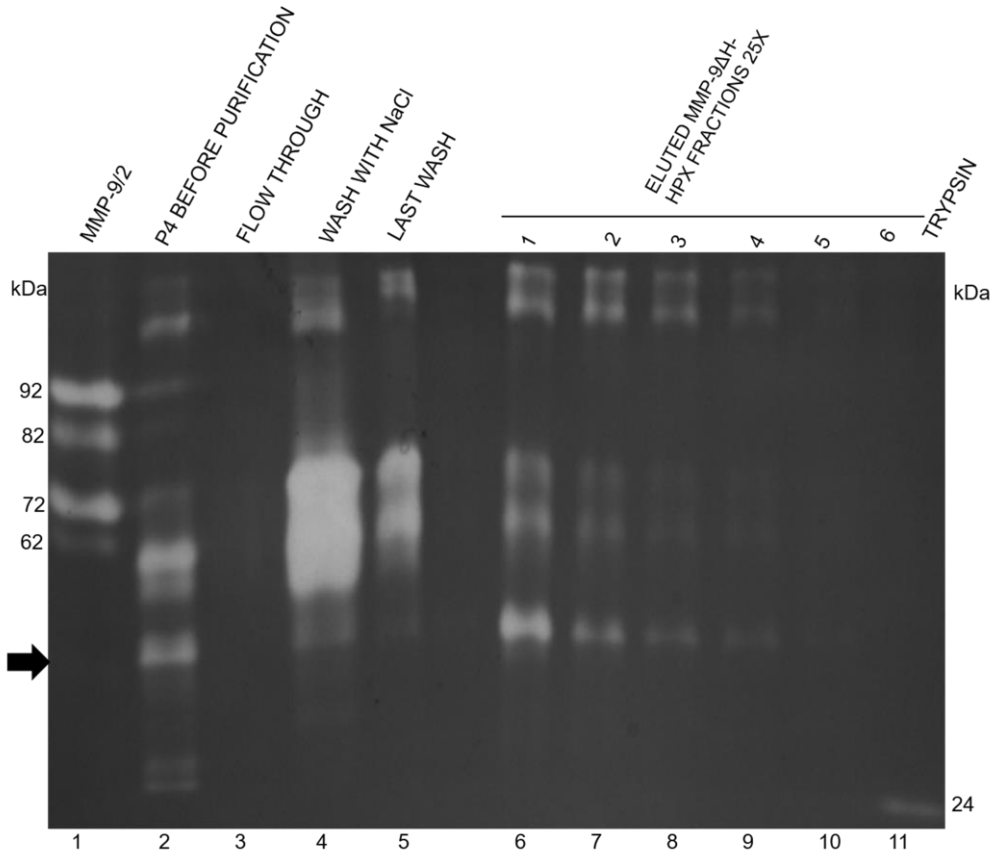

Figure 24. Gelatin degrading proteases in the aliquots of different steps of affinity purification. All samples were 100x diluted. In the lane 1, the molecular standard MMP-9/2 whereas lane no 2 represents the P4 viral stock containing the truncated proMMP-9. The aliquots of Flow through in the lane no 3 and wash with 1 M NaCl in lane no 4. Aliquots of the last wash without NaCl is shown in the lane no 5. Purified truncated proMMP-9 was collected in different fractions is represented by lane no 6-10. Trypsin is in the lane no 11. An arrow indicates the expected proMMP-9ΔH-HPX protease.

Identification of the types of protease produced by the transfected Sf9 cells

Before going through additional purification procedure, it was necessary to explore what type of protease (metallo-, serine-, and cysteine protease) that was produced by the transfected Sf9 cells. The P4 viral stock containing proMMP-9ΔH-HPX was

analysed by Gelatin Zymography together with a MMP-9/2 standard and trypsin as controls. After electrophoresis, the gel was cut into four pieces where each piece contained P4 viral stock (proMMP-9ΔH-HPX), molecular standard MMP-9/2 and trypsin. Thereafter, three pieces were treated separately with three different inhibitors, EDTA, E64, and pefabloc during the incubation and washing steps of zymography gel, while one piece of the gel was without any inhibitor in the incubating and washing step. The zymography result showed that in the control without any inhibitors, gelatin was digested by the gelatinolytic enzymes produced as previously seen in the transfected Sf9 cells. Additionally, the molecular standard MMP-9/2 and trypsin also digested gelatin as expected as there was no inhibitor added to influence the gelatinolytic activity (Fig. 25A). In contrast, the presence of the metalloprotease inhibitor EDTA (10 mM) showed almost complete eradication of the gelatinolytic activity both of the proteases produced by the Sf9 cells and the molecular standard MMP-9/2. Since trypsin is not a metalloprotease, but a serine protease, it was not affected (Fig. 25B). This finding confirmed that the proteases produced by the transfected Sf9 cells were all metalloproteases. Cysteine proteases may also have gelatinolytic activity. Using the cysteine inhibitor E-64 (5 mM) there was no noticeable effect on the gelatinolytic activity of proteases (Fig. 25C), indicating that none of the detected gelatin degrading proteases are cysteine proteases. Furthermore, Pefabloc (1mM) which inhibits serine proteases like trypsin, showed no inhibition of the protease in the Sf9-sample (Fig. 25D), but completely eradicated the trypsin activity. Therefore, the gelatin degrading proteases produced by the transfected Sf9 cells are all metalloproteases.

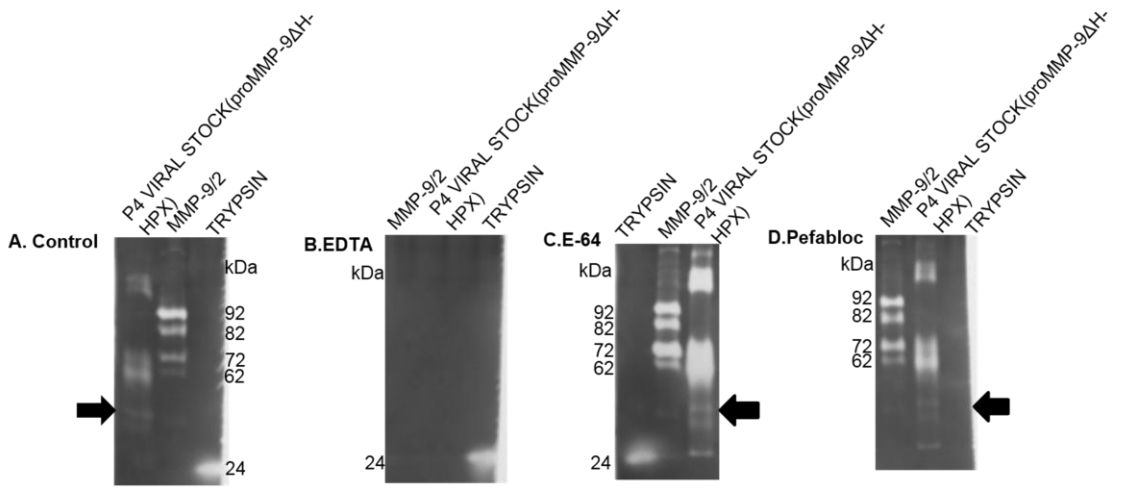

Figure 25. Detection of the type of proteases produced in Sf9 cells by using inhibitors. The P4 viral stock in the zymography was 200x diluted. **A.** Control showing the gelatinolytic activity of protease in the absence of inhibitors. **B.** The presence of metalloprotease inhibitor EDTA (10 mM). **C.** The presence of the Cysteine protease inhibitor E-64 (3.2 mM). **D.** The presence of the serine protease inhibitor pefabloc (0.5 M) only affected Trypsin activity on gelatin. The arrows in the figure indicates the expected protease produced in Sf9 cells.

Identification of proMMP-ΔH-HPX by Western blot

To further analyse the produced proMMP-9ΔH-HPX and its molecular mass, Western blot under non-reducing condition (right half), and for investigation the dimerization patterns if any, a reducing condition (left half) with 0.5 M DTT was carried out. For identification of proteases produced by Sf9 cells, reducing condition was preferred because DTT usually can dissociate the S-S bridges in the dimer or multimeric form of MMP-9. An anti-MMP-9 polyclonal antibody against purified proMMP-9 from THP-1 cells (1:2000 dilution of 5.1 mg/ml) was used as a primary antibody and a goat anti-rabbit IgG tagged with Horse Reddish Peroxidase as a secondary antibody (1:1000 of 1 mg/ml) were used to identify any MMP-9 protease in the blot, including the proMMP-9ΔH-HPX. ProMMP-9 is known to be produced as a monomer, as well as a variety of dimeric forms (Goldberg et al., 1992; Winberg et al., 2000b).The homo- and several hetero-dimer forms are SDS-resistant (Triebel et al., 1992a; Van den Steen, 2006) but reduction-sensitive (Malla et al., 2008). Under reducing conditions, DTT dissociates the S-S bridges in the dimer or multimer of the enzyme which are SDS resistant (Van

den Steen, 2006). Samples in lane 1-5 were treated with 0.5 M DTT (reducing conditions) while the same samples lanes 7-12 were untreated (non-reducing conditions) (Fig. 26). Analysis of the Western blot revealed the protein around 48 kDa was recognized by the specific anti-MMP-9 antibody in both reducing and non-reducing conditions further confirming that the protein is the expected proMMP-9ΔH-HPX protease.

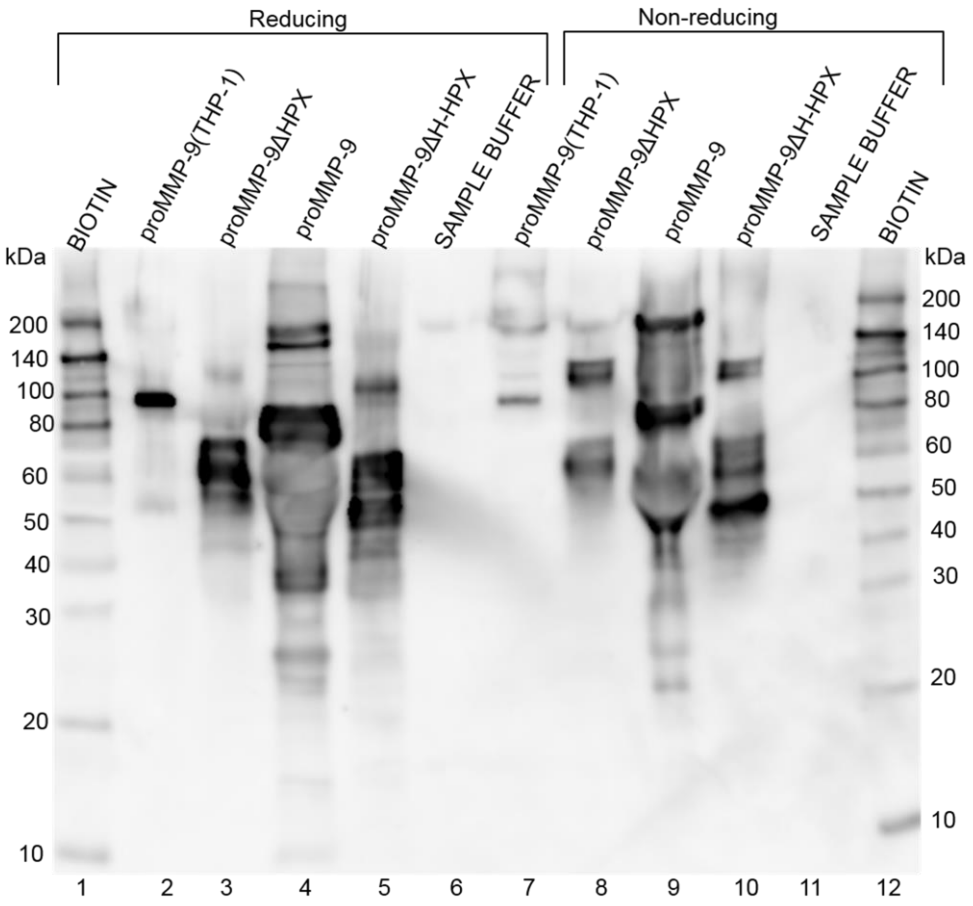

Figure 26. Western blot analysis of the target and control samples under reduced and non-reduced conditions. The technique was performed with anti-MMP-9 polyclonal antibody as primary antibody and goat anti-rabbit IgG as a secondary antibody. The reducing agent was added in the sample are represented from lane 1-6. Biotinylated molecular weight standard in lane 1 and 12. Control THP-1 derived MMP-9 (20x) and MMP-9ΔHPX is shown in the lane no 2 and 3, respectively. Another control proMMP-9 in the lane no 4 and MMP-9ΔH-HPX containing sample is represented by lane no 5. Sample buffer (5x) with (0.5 M) DTT and without DTT is shown in the lane no 6 and 11, respectively.

Actually, two important findings were observed from the above investigation; firstly, the protease around 48 kDa showed gelatinase activity in zymography analysis was

also recognized by MMP-9 specific antibody in the immuno-blotting. Secondly, besides the target size 48 kDa proMMP-9ΔH-HPX, other bands of large molecular weight were also identified by anti-MMP-9 antibody raising the question of oligomerization by proMMP-9ΔH-HPX. However, the study by Van den Steen *et. al.* showed that proMMP-9ΔH-HPX do not form homo-dimer in contrast to deletion variants of proMMP-9 containing the hinge region. Further investigations are needed to determine if these high molecular weight proteins indeed are dimers or complexes of proMMP-9ΔH-HPX.

Unexpectedly, in the present study the result of immune-blotting of the SDS-gel under reduced condition was ambiguous. It was so, because the purified sample was concentrated by vacuum centrifuging, resulting in a high concentration of salt in the samples made the samples very sticky. Therefore, the sample could not travel properly on the gel thereby leaving an inconclusive identification with respect to oligomerization.

In contrast, a single band of the control proMMP-9ΔHPX was recognized by the MMP-9 antibody under reducing conditions while it was detected as both a monomeric and a dimeric form under non reducing conditions. Control THP-1 derived proMMP-9 showed monomeric form at 92 kDa and a homo-dimer around 200 kDa that was reduction sensitive (Fig. 26) as expected from the previous studies (Malla et al., 2013; Winberg et al., 2000).

In the present study, Polyclonal primary antibody was used instead of monoclonal antibody in the western blot experiments because polyclonal antibody allows for more efficient detection by recognizing multiple epitopes on any one antigen and hence amplifying the signal from the target. In addition, it is more tolerant to small changes of the protease, such as denaturation. Conversely, polyclonal antibody has higher potentiality, for cross reactivity due to recognizing multiple epitopes.

SDS-PAGE of partly purified concentrated proMMP-9ΔH-HPX protease

Zymography is a very sensitive detection method, so to be able to detect the proteins on SDS-PAGE and Coomassie staining, the samples need to be concentrated. The sample containing partly purified proMMP-9ΔH-HPX protease was concentrated by using a spin column with a cut off of 10 kDa before performing SDS-PAGE. One hundred (100) µl of proMMP-9ΔH-HPX protease sample was span downed to 20 µl. The samples were washed with 300 µl of 0.1 M HEPES washing buffer during the concentrating procedure in order to remove DMSO from the sample. The protein concentration of the concentrated samples was then determined by NanoDrop Spectrophotometer at A_{280nm}. Using Beer-Lambert equation, proMMP-9ΔH-HPX enzyme was estimated to be 430 µM. The SDS-PAGE under non-reduced conditions (NuPAGE-4-12%, Bis-Tris Gel 1.0 mm x 12 well) was carried out with this concentrated partly purified proMMP-ΔH-HPX protease sample. The result of SDS-PAGE and subsequent Coomassie blue staining revealed a strong band of molecular size of around 50 kDa as expected to be our target size protease. Additionally, other two contaminating strong bands around 125 kDa and 120 kDa was also present in the sample. Two other contaminating weak bands around 70 kDa and 60 kDa was also observed in the sample. The intensity of the bands revealed that the 50 kDa band and the other two contaminating bands at 125 kDa and 120 kDa was present abundantly in contrast to those of 70 kDa and 60 kDa bands (Fig. 27).

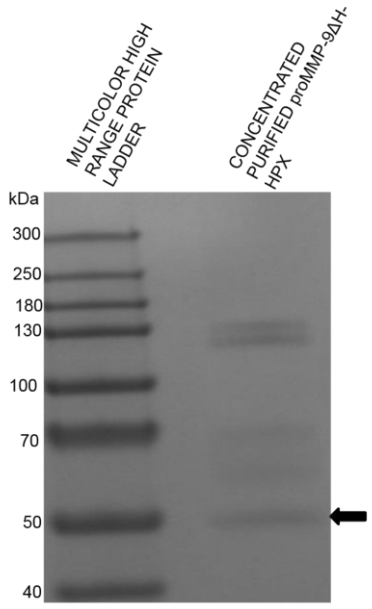

Figure 27. SDS-PAGE analysis of the partly purified concentrated sample containing proMMP-9ΔH-HPX protease. The molecular standard Multi-colour high range protein ladder was used in the lane no 1. Purified concentrated proMMP-9ΔH-HPX protease sample was used in the lane no 2. An arrow indicates the expected proMMP-9ΔH-HPX protease band.

Western blot analysis of the partly purified concentrated proMMP-9ΔH-HPX sample

For the confirmation of the production of proMMP-9ΔH-HPX protease, the concentrated sample containing target protease was subjected to Western blot again under non-reducing conditions with anti-MMP-9 polyclonal antibody (1:2000 dilution of 5.1 mg/ml) as primary antibody and goat anti-rabbit IgG linked with Horse Reddish Peroxidase as a secondary antibody (1:1000 of 1 mg/ml). The finding of western blot resembled the result of SDS-PAGE in detecting one strong band at 48 kDa and two other strong bands and two weak bands contaminating in the purified proMMP-9ΔH-HPX protease sample (Fig. 28). In previous western blot result (Fig. 26), the 48 kDa protease band was observed to be stronger than the other contaminating bands. The same findings also revealed by the present western blot analysis.

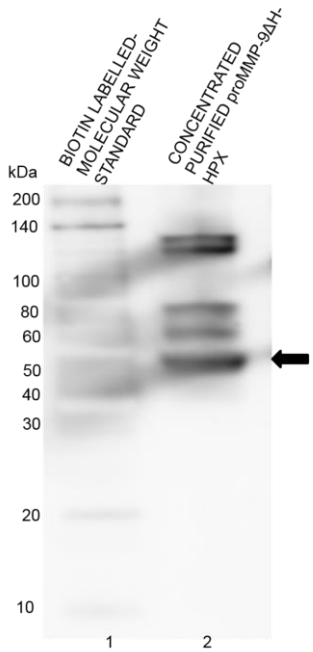

Figure 28. Identification of proMMP-9ΔH-HPX by w**estern blot.** Biotin-labelled molecular weight standard was used in the lane no 1. Purified concentrated proMMP-9ΔH-HPX in the lane no 2. Arrow in the figure indicates the expected proMMP-9ΔH-HPX protease in the sample.

Pufication of MMP-9ΔH-HPX proteinase by Gelatin Sepharose Chromatography with an extra washing step

In order to remove the contaminating high molecular weight proteins, an extra washing step was introduced. Previously we used 1.5 ml washing buffer with 1 M NaCl in the affinity chromatography to purify the protease from 1 ml P4 viral stock medium. We found that this amount was not enough to purify the protease of interest. Therefore, we decided to wash the sample with a double volume (3 ml) of washing buffer keeping the concentration of NaCl unchanged. During the chromatography, aliquots of the different steps in the purification were collected and together with the eluted proMMP-9ΔH-HPX they were subjected to gelatin zymography. The result of the zymography depicted that the eluted proMMP-9ΔH-HPX sample still contained two strong protease bands of large molecular weight of 125 and 120 kDa having gelatinase activity even

though the extra wash with NaCl removed a lot of unspecific proteins from the column. Due to a possible overflow in lane 7 from lane 6, it was difficult to determine whether the two bands in the region of 62-72 kDa was removed before the last washing step or if they was eluted during the last washing step (Fig. 29).

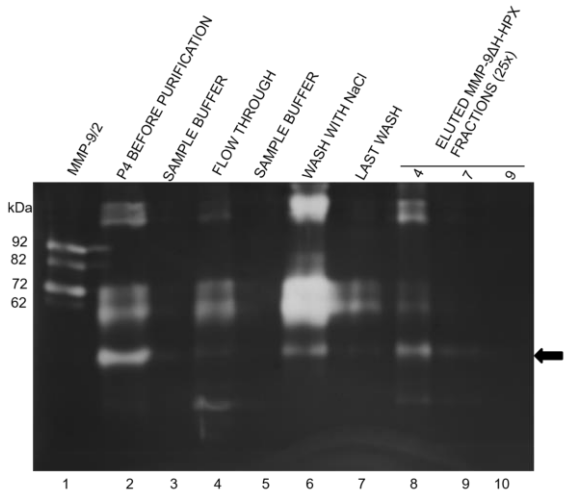

Figure 29. Gelatin degrading proteases in eluted fractions and in aliquots of double washing steps. All samples were 100x diluted. Lane no 1 shows MMP-9/2 molecular standard and un-purified P4 viral stock solution in the lane no 2. Between the protease samples, 5x sample buffer was used. Aliquots of extra washing step with NaCl and last wash is represented by the lane no 6 and 7, respectively. Eluted protein fractions are shown by lane no 8-10. An arrow shows the proMMP-9ΔH-HPX protease in the sample.

From this figure 29 it can be observed that the two contaminating bands around 70 and 60 kDa were mostly non-specifically bound proteins. Hence these were removed abundantly in the washing step.

The partly purified protease was subjected to a concentration procedure to concentrate the protease that were larger than 10 kDa. To do so, a spin column with a cut off of 10 kDa was used. The concentrated sample containing proMMP-9ΔH-HPX was then used for Gelatin Zymography and found that the purified samples still contained several protease bands having gelatinolytic activity. However, 100x dilution of the partly purified concentrated proMMP-9ΔH-HPX sample showed larger amounts

of the 48 kDa proteases than of the contaminating proteases (Fig. 30). The concentrated proMMP-9ΔH-HPX sample was determined again using NanoDrop Spectrophotometer at A_{280nm}. Using Beer-Lambert equation, the protein concentration of the proMMP-9ΔH-HPX sample was estimated to be 1.09 mM.

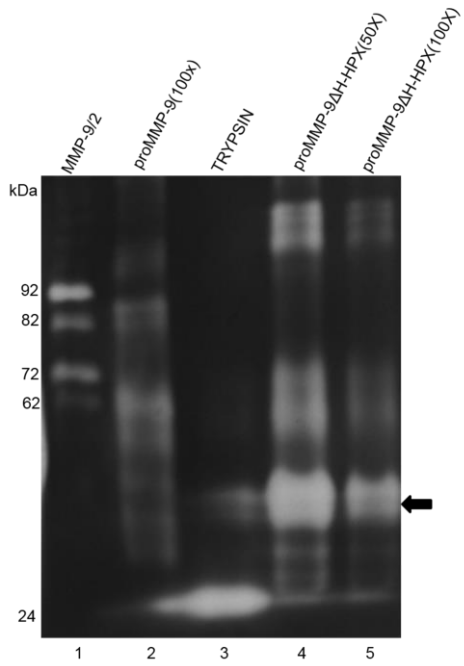

Figure 30. Gelatin degrading proteases purified with additional washing step of affinity chromatography. Molecular standard MMP-9/2 and Trypsin is represented by lane no 1 and 3, respectively. The control proMMP-9 produced in Sf9 cells is represented by the lane 2. The eluted MMP-9ΔH-HPX protease with two dilution 50x and 100x are represented by lane no 4 and 5, respectively. The expected proMMP-9ΔH-HPX protease is indicated by an arrow in the figure.

Determining the sizes of proteases removed by additional purification step

In order to see what proteases had been removed by the double washing step, the partly purified concentrated sample was subjected to SDS-PAGE. For comparing the purification efficacy an un-purified sample containing the target protease proMMP-9ΔH-HPX was also included in this investigation.

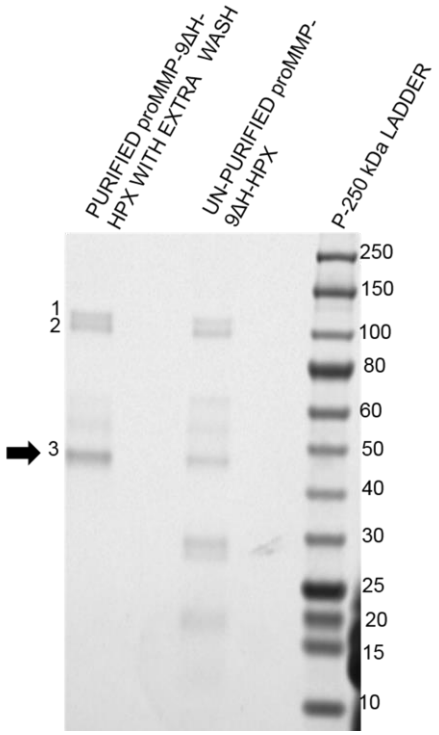

Figure 31. Determining the size of proteases purified with the double washing purification step. P-250 kDa protein ladder was used as a molecular standard and both purified concentrated proMMP-9ΔH-HPX protease sample and un-purified proMMP-9ΔH-HPX sample were used in this technique to observe the proteases removed in the extra washing step of purification technique. The expected proMMP-9ΔH-HPX protease is indicated by an arrow and three bands indicated as 1, 2, 3 were sent for Mass Spectrometry analysis.

Analysing the image of SDS-PAGE, it was found that the sample of proMMP-9ΔH-HPX protease that was purified with double washing volume contained three strong protease bands and two very weak bands. In contrast, un-purified proMMP-9ΔH-HPX protease sample contained several additional bands (Fig. 31). Additional washing was found effective to remove most of the two weak contaminating protein bands from the target sample. We still need to separate two strong contaminating protease bands of larger molecular size around 120 and 130 kDa from the sample.

Accurate determination of the molecular weight of proMMP-9ΔH-HPX protease bands

For estimating the molecular weight of both purified and un-purified proMMP-9ΔH-HPX protease bands from SDS-PAGE gel (Fig 31), and from zymography gel (Fig. 30) the relative migration distance (Rf) of the standards and proMMP-9ΔH-HPX bands were determined by dividing the migration distance of the protein by the migration distance of the dye front. A ruler (in centimetre) was used to measure the migration distance from the top of the gel for all target bands in the gel (Fig. 32A and B). By plotting the molecular weight of each band of the standard in Y axis and the Rf value obtained for the bands of the standard on the X axis using a semi logarithm sheet, a linear plot was generated. From the graph, the molecular weight of band 1 in the purified proMMP-9ΔH-HPX sample was determined to be 125 kDa, band 2 was calculated to be 120 kDa, and band 3 to be 48 kDa. The molecular weight of purified proMMP-9ΔH-HPX in zymography gel was also determined to be around 48 kDa. The molecular size of all detected protein bands in both purified as well as the crude samples in SDS-PAGE are summarised in figure 32B. In order to compare the molecular weight obtained manually from the semi logarithm sheet, the obtained data was plotted in to the computer program Sigma Plot. Here, the molecular size was only calculated for the target band of purified proMMP-9ΔH-HPX protease. The calculation resulted in a log value 1.69 for the molecular size of the target protease which corresponds to 48.9 kDa (Fig. 32A). Since both ways of calculating the molecular size of the smallest band gave a size of approximately 48 kDa, we expected that the estimation of the other protease bands would be similar to that of the manual estimation.

A

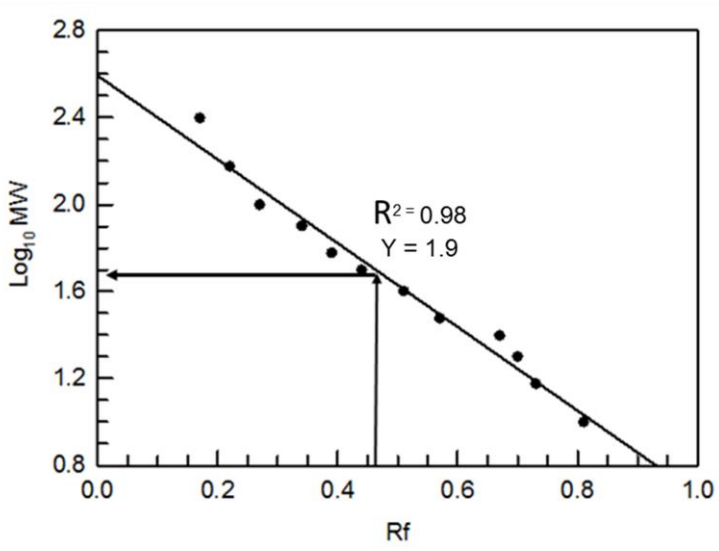

B

	molecular standard P-250 kDa				Purified MMP-9ΔH-HPX				Unpurified MMP-9ΔH-HPX			
logM.W	Distance migrated	gel length	Rf		Distance migrated	gel length	Rf	anti-logM.W	Distance migrated	gel length	Rf	anti-log M.W
2.398	1.6	9.4	0.17		2.5	9.4	0.26	125	2.5	9.3	0.26	125
2.176	2.1		0.22		2.7		0.28	120	2.7		0.29	110
2	2.6		0.27		3.6		0.38	72	3.6		0.38	72
1.903	3.2		0.34		4		0.42	60	4		0.43	58
1.778	3.7		0.39		4.4		0.46	48	4.4		0.47	47
1.699	4.2		0.44						5.5		0.59	27
1.602	4.8		0.51						5.7		0.61	24
1.477	5.4		0.57						6.6		0.7	16
1.398	6.3		0.67									
1.301	6.6		0.7									
1.176	6.9		0.73									
1	7.7		0.81									

Figure 32. Determination of the molecular size of proMMP-9ΔH-HPX protease and contaminating bands from SDS-PAGE (gel 15). A. Sigma plot shows the log value for the target smallest band of partly purified proMMP-9ΔH-HPX **B**. Table showing the Rf value and molecular size calculated for the molecular standard as well as all the protein bands detected in SDS-PAGE.

Identification of MMP-9 derived peptides in the proMMP-9ΔH-HPX sample by MS/MS

In order to analyse the identity of the proteins in both the 48 kDa band and the 120 and 125 kDa contaminating bands, the three bands in the SDS-PAGE gel (numbered 1, 2, and 3 in the figure 31) were cut out for Mass spectrometry (MS) analysis. The MS was performed by Tromsø University Proteomics Platform (TUPP). The samples

were digested by trypsin and subjected to MS-MS and the various sizes of separated peptides are analysed by computer technology using a database for protein identification and characterisation based on best matching peptide sizes of theoretical trypsin digests of proteins in the database and the investigated protein sample. We received the percentage of peptide sequence coverage for three bands from TUPP. According to their analysis, band number one (1) showed similarities to seven different type of proteins. The top listed protein was MMP-9 and it had 24% similarity of database MMP-9 peptide sequence within 366 peptide sequences. Band number two (2) showed similarity to 29 different proteins on the hit list. The highest score belonged to human keratin type II with 23% sequence similarity. The analysis of band three (3) showed peptide similarity with five proteins of which MMP-9 of *Homo sapiens* was on top of the list with a peptide similarity of 28%.

Protein sequence coverage: 24%

Matched peptides shown in ***bold red***.

```
  1 MSLWQPLVLV LLVLGCCFAA PRQRQSTLVL FPGDLRTNLT DRQLAEEYLY
 51 RYGYTRVAEM RGESKSLGPA LLLLQKQLSL PETGELDSAT LKAMRTPRCG
101 VPDLGRFQTF EGDLKWHHHN ITYWIQNYSE DLPRAVIDDA FARAFALWSA
151 VTPLTFTRVY SRDADIVIQF GVAEHGDGYP FDGKDGLLAH AFPPGPGIQG
201 DAHFDDDELW SLGKGVVVPT RFGNADGAAC HFPFIFEGRS YSACTTDGRS
251 DGLPWCSTTA NYDTDDRFGF CPSERLYTQD GNADGKPCQF PFIFQGQSYS
301 ACTTDGRSDG YRWCATTANY DRDKLFGFCP TRADSTVMGG NSAGELCVFP
351 FTFLGKEYST CTSEGRGDGR LWCATTSNFD SDKKWGFCPD QGYSLFLVAA
401 HEFGHALGLD HSSVPEALMY PMYRFTEGPP LHKDDVNGIR HLYGPRPEPE
451 PRPPTTTTPQ PTAPPTVCPT GPPTVHPSER PTAGPTGPPS AGPTGPPTAG
501 PSTATTVPLS PVDDACNVNI FDAIAEIGNQ LYLFKDGKYW RFSEGRGSRP
551 QGPFLIADKW PALPRKLDSV FEERLSKKLF FFSGRQVWVY TGASVLGPRR
601 LDKLGLGADV AQVTGALRSG RGKMLLFSGR RLWRFDVKAQ MVDPRSASEV
651 DRMFPGVPLD THDVFQYREK AYFCQDRFYW RVSSRSELNQ VDQVGYVTYD
701 ILQCPED
```

Figure 33. Mass spectrometry analysis of band number 1 from SDS-PAGE showing 24% peptide similarity with full length proMMP-9. Peptide similarity is represented by bold red colour.

Since we introduced a stop codon at the start of the hinge region our expected C-terminal end residue is P447. Additionally, our expected protease does not include the 19 amino acid of pre-domain since that is cleaved off in the ER. Therefore, total amino acid residue for the target protease was expected to be 428 instead of 707 amino acids for full length proMMP-9. The total amino acid labelled in red for band no 1 in the figure 33 was counted to be 170. For estimation of actual percentage of peptide similarity, we divided the total labelled amino acid by total amino acid of truncated proMMP-9 (170/428) and multiplied by 100. Thus the actual peptide sequence coverage appeared to be 40% for the band number 1. From the analysis of MS, it was also detected that peptide similarity was within the first 366 amino acids indicating that the contaminating band number one (1) could contain the truncated variant proMMP-9ΔH-HPX. It could be and SDS-stable and reduction stable homodimer or a heteromer with unknown partner.

The second highest score for band 2 showed 16% similarity with full length human proMMP-9 (Fig. 34) and 27% similarity if we only compare it with 428 amino acids in the truncated human proMMP-9. Here, peptide similarity was detected within first 384 amino acids of the sequence. As for the contaminating protein band number one, we cannot exclude that the contaminating protein band number two also is and SDS-stable and reduction insensitive homodimer or hetromultimer of the proMMP-9ΔH-HPX.

2.a. Keratin, type II cytoskeletal 1(Homo sapiens)

Protein sequence coverage: 23%

Matched peptides shown in ***bold red***.

```
  1 MSRQFSSRSG YRSGGGFSSG SAGIINYQRR TTSSSTRRSG GGGGRFSSCG
 51 GGGGSFGAGG GFGSRSLVNL GGSKSISISV ARGGGRGSGF GGGYGGGGFG
101 GGGFGGGGFG GGGIGGGGFG GFGSGGGGFG GGGFGGGGYG GGYGPVCPPG
151 GIQEVTINQS LLQPLNVEID PEIQKVKSRE REQIKSLNNQ FASFIDKVRF
201 LEQQNQVLQT KWELLQQVDT STRTHNLEPY FESFINNLRR RVDQLKSDQS
251 RLDSELKNMQ DMVEDYRNKY EDEINKRTNA ENEFVTIKKD VDGAYMTKVD
301 LQAKLDNLQQ EIDFLTALYQ AELSQMQTQI SETNVILSMD NNRSLDLDSI
351 IAEVKAQYED IAQKSKAEAE SLYQSKYEEL QITAGRHGDS VRNSKIEISE
401 LNRVIQRLRS EIDNVKKQIS NLQQSISDAE QRGENALKDA KNKLNDLEDA
451 LQQAKEDLAR LLRDYQELMN TKLALDLEIA TYRTLLEGEE SRMSGECAPN
501 VSVSVSTSHT TISGGGSRGG GGGGYGSGGS SYGSGGGSYG SGGGGGGGRG
551 SYGSGGSSYG SGGGSYGSGG GGGGHGSYGS GSSSGGYRGG SGGGGGGSSG
601 GRGSGGGSSG GSIGGRGSSS GGVKSSGGSS SVKFVSTTYS GVTR
```

2.b.Matrix metalloproteinase-9 (Homo sapiens)

Protein sequence coverage: 16%

Matched peptides shown in ***bold red***.

```
  1 MSLWQPLVLV LLVLGCCFAA PRQRQSTLVL FPGDLRTNLT DRQLAEEYLY
 51 RYGYTRVAEM RGESKSLGPA LLLLQKQLSL PETGELDSAT LKAMRTPRCG
101 VPDLGRFQTF EGDLKWHHHN ITYWIQNYSE DLPRAVIDDA FARAFALWSA
151 VTPLTFTRVY SRDADIVIQF GVAEHGDGYP FDGKDGLLAH AFPPGPGIQG
201 DAHFDDDELW SLGKGVVVPT RFGNADGAAC HFPFIFEGRS YSACTTDGRS
251 DGLPWCSTTA NYDTDDRFGF CPSERLYTQD GNADGKPCQF PFIFQGQSYS
301 ACTTDGRSDG YRWCATTANY DRDKLFGFCP TRADSTVMGG NSAGELCVFP
351 FTFLGKEYST CTSEGRGDGR LWCATTSNFD SDKKWGFCPD QGYSLFLVAA
401 HEFGHALGLD HSSVPEALMY PMYRFTEGPP LHKDDVNGIR HLYGPRPEPE
451 PRPPTTTTPQ PTAPPTVCPT GPPTVHPSER PTAGPTGPPS AGPTGPPTAG
501 PSTATTVPLS PVDDACNVNI FDAIAEIGNQ LYLFKDGKYW RFSEGRGSRP
551 QGPFLIADKW PALPRKLDSV FEERLSKKLF FFSGRQVWVY TGASVLGPRR
601 LDKLGLGADV AQVTGALRSG RGKMLLFSGR RLWRFDVKAQ MVDPRSASEV
651 DRMFPGVPLD THDVFQYREK AYFCQDRFYW RVSSRSELNQ VDQVGYVTYD
701 ILQCPED
```

Figure 34. Mass spectrometry analysis of band number 2 from SDS-PAGE. 2a represents the peptide sequence matched with Keratin, type II cytoskeletal 1 whereas 2b shows peptide similarity with proMMP-9.

Band no 3 showed 46% peptide sequence similarity with human proMMP-9 if we only count the 428 amino acids in proMMP-9ΔH-HPX (Fig. 35). All identified peptides matched proMMP-9 within the first 447 amino acids which corresponds to the part of proMMP-9 included in the produced truncated proMMP-9.

Based on the above findings, it can be said that bands number 1 and 2 might be a homodimers or heteromeric forms of proMMP-9ΔH-HPX that is not reduction sensitive. The band number three (3) appeared as proMMP-9ΔH-HPX with maximum peptide similarity and the peptide similarity was observed within first 447 amino acids. Therefore, we conclude that band number three is our expected monomeric form of the proMMP-9ΔH-HPX protease.

3. Matrix metalloproteinase-9 (Homo sapiens)

Protein sequence coverage: 28%

Matched peptides shown in ***bold red***.

```
  1 MSLWQPLVLV LLVLGCCFAA PRQRQSTLVL FPGDLRTNLT DRQLAEEYLY
 51 RYGYTRVAEM RGESKSLGPA LLLLQKQLSL PETGELDSAT LKAMRTPRCG
101 VPDLGRFQTF EGDLKWHHHN ITYWIQNYSE DLPRAVIDDA FARAFALWSA
151 VTPLTFTRVY SRDADIVIQF GVAEHGDGYP FDGKDGLLAH AFPPGPGIQG
201 DAHFDDDELW SLGKGVVVPT RFGNADGAAC HFPFIFEGRS YSACTTDGRS
251 DGLPWCSTTA NYDTDDRFGF CPSERLYTQD GNADGKPCQF PFIFQGQSYS
301 ACTTDGRSDG YRWCATTANY DRDKLFGFCP TRADSTVMGG NSAGELCVFP
351 FTFLGKEYST CTSEGRGDGR LWCATTSNFD SDKKWGFCPD QGYSLFLVAA
401 HEFGHALGLD HSSVPEALMY PMYRFTEGPP LHKDDVNGIR HLYGPRPEPE
451 PRPPTTTTPQ PTAPPTVCPT GPPTVHPSER PTAGPTGPPS AGPTGPPTAG
501 PSTATTVPLS PVDDACNVNI FDAIAEIGNQ LYLFKDGKYW RFSEGRGSRP
551 QGPFLIADKW PALPRKLDSV FEERLSKKLF FFSGRQVWVY TGASVLGPRR
601 LDKLGLGADV AQVTGALRSG RGKMLLFSGR RLWRFDVKAQ MVDPRSASEV
651 DRMFPGVPLD THDVFQYREK AYFCQDRFYW RVSSRSELNQ VDQVGYVTYD
701 ILQCPED
```

Figure 35. Mass spectrometry analysis of band number 3 from SDS-PAGE. Peptide sequence similarity with 28% represented by bold in red colour for full length proMMP-9.

Gelatin Sepharose Chromatography with a pre-elution step

Although the 125 and 120 kDa bands were shown to contain MMP-9, their exact identity is unknown. Thus, further attempts were done to remove both the 125 and the 120 kDa proteins from the 48 kDa pro MMP-9ΔH-HPX. Various hydrophobic compounds such as DMSO (Murphy, 1995.; Strongin et al., 1993), Brij-35 (0.05%), and triton X-100 (0.5%) have been previously used for elution of MMP-9 (Malla et al., 2008). A study revealed that 5% DMSO was able to separate proMMP-9 from gelatin (Fini et al., 1991). Additionally, MMP-9 has also been observed to elute with increasing concentration of up to 10% DMSO in the presence of 0.05% Brij-35 when it is in monomeric form, but at a lower DMSO concentration when it is in a heteromeric form (Malla et al., 2008). Hence, we introduced a pre-elution step in the purification protocol of the Gelatin Sepharose affinity chromatography, where this step contained the elution buffer, bit instead of 7.5% DMSO the buffer contained 0.1% DMSO. Gelatin zymography revealed that the proteinase eluted with 0.1% DMSO contained large amount MMP-9 protease of molecular sizes of 48 kDa, 62 kDa, and also 72 kDa respectively. Those sizes of protease were also removed in huge amount after additional wash with NaCl (Fig. 36) indicating that large amount of protease bands of those sizes were loosely bounded to gelatin. Additionally, the 125 kDa size protease was observed to be eluted in 7.5% DMSO which was also removed by NaCl in large amount. From the above observations, we concluded that even though huge amount of loosely bound proteins was removed in various steps of the purification technique, still eluted protease sample contained two contaminating proteases around 125 kDa and 120 kDa along with the 48 kDa proMMP-9ΔH-HPX protease.

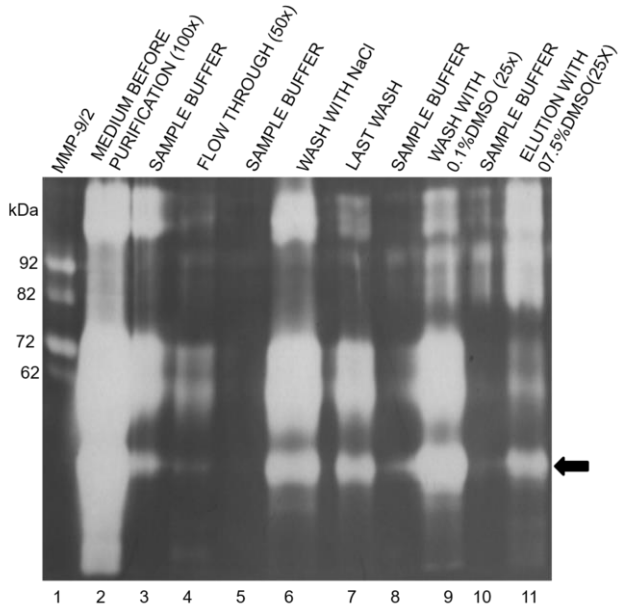

Figure 36. Gelatin degrading proteases purified with a pre-elution step of affinity chromatography. Additional pre- elution step was performed with elution buffer containing 0.1% DMSO. Molecular standard MMP-9/2 in the lane no 1 and 100x diluted un-purified protease sample in the lane no 2. 5x sample buffer was loaded in between the protein samples. Flow through and wash with NaCl is represented by lane no 4 and 6, respectively. The protease pre-eluted with 0.1% DMSO in the lane no 9 and protease eluted with 7.5% DMSO is resented by lane 11. An arrow indicates the 48 kDa proMMP-9ΔH-HPX protease in the figure.

SDS-PAGE analysis of proteases purified with a pre-elution purification step

Analysis of SDS-PAGE of eluted protease showed the expected 48 kDa protease bands along with two strong contaminating bands (Fig. 37). These three bands were also observed in the previous SDS-PAGE (Fig. 31) indicating that the pre-elution step with 0.1% DMSO was not an effective step to remove the two contaminating bands around 120 and 130 kDa from the column. We therefore tested if it was possible to remove these two contaminating bands form the 48 kDa target protease by size exclusion chromatography.

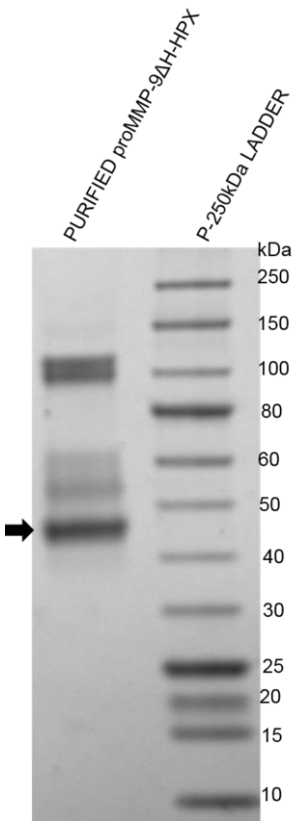

Figure 37. SDS-PAGE showing proMMP-9ΔH-HPX protease eluted after a pre-elution purification step. Molecular weight standard P-250 kDa protein ladder was used to determine the sizes of protease bands present in the sample containing proMMP-9ΔH-HPX protease. A black in the figure indicates the 48 kDa protease.

Size exclusion chromatography for purification of the 48 kDa proMMP-9ΔH-HPX protease

Gel filtration chromatography is a technique used for separation of chemical substances by size, based on their migration through a stationary bed of porous Sephadex gel.

Determination of the separation properties of Sephadex G-75 column

Before doing the experiment with our protease sample, the separation properties of the Sephadex G-75 column was determined by using Blue dextran 2000 (2 mg/ml)

and potassium dichromate (0.6 mg/ml). A 10 ml pipet was filled with 6 ml Sephadex gel carefully avoiding air bubble. After washing and equilibrating the column with 0.1 M Hepes buffer, $CaCl_2$, pH 7.5, the Void volume (V_0) was determined by blue dextran and total volume (V_t) by potassium dichromate. Blue dextran came out between 2.5-4 ml with a peak at 3 ml. This is the void volume of the column (V_0). Potassium chromate came out from the column in 4-5 ml with a peak at 4.5 ml. This determines the total volume (V_t) of the column.

Separation of target size MMP-9ΔH-HPX (48kDa) using Sephadex G-75 size exclusion chromatography

In an attempt to separate the 48 kDa proMMP-9ΔH-HPX from the two contaminating proteases with molecular size of 120 kDa and 125 kDa, 100 µl of partly concentrated purified proMMP-9ΔH-HPX from Gelatin Sepharose Chromatography was applied to the Sephadex G-75 column. It was expected that the contaminating proteases should occur in the void volume and the 48 kDa proMMP-9ΔH-HPX should be eluted after the void volume. The first 1.5 ml solution was discarded and then the solution was collected in 500 µl fractions up to 8 ml. A Gelatin Zymography was performed on the eluted fractions using aliquots diluted 25x to explore at what volumes the 48 kDa protease could be found. Gelatin Zymography revealed that our 48 kDa proMMP-9ΔH-HPX came out of the column between 2.5 and 7 ml (Fig. 38, lane 4-13). The 48 kDa proMMP-9ΔH-HPX came out of the column already in the void along with other contaminating proteases, suggesting that a part of proMMP-9ΔH-HPX has occurred as a complex.

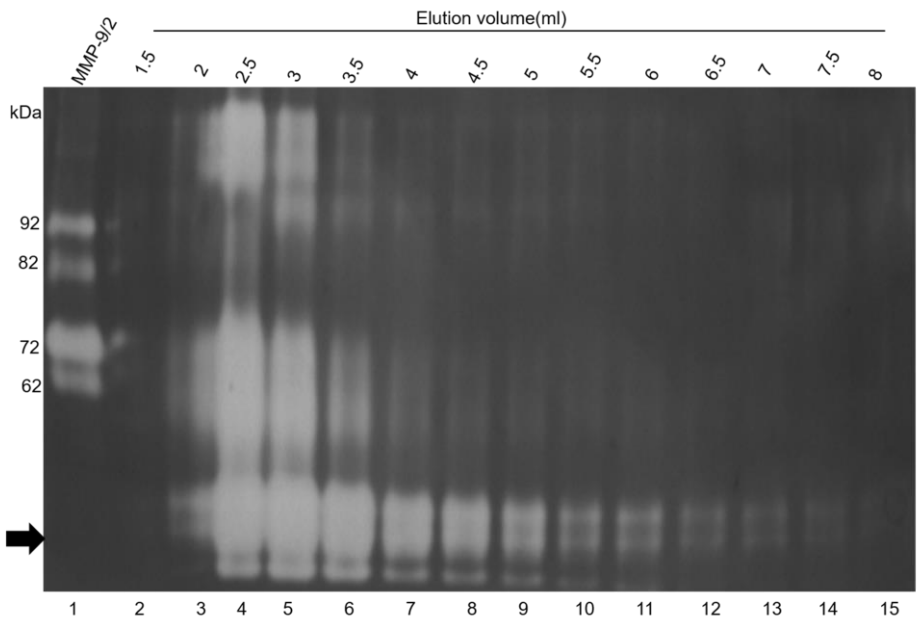

Figure 38. Gelatin Zymography showing gelatin degrading proteases in the eluted fractions in Sephadex G-75 size exclusion chromatography. 25x diluted purified sample containing proMMP-9ΔH-HPX was used for the Zymography. The molecular weight standard MMP-9/2 is in the lane 1. Lane 2, 3, show only Hepes buffer. The expected protease came out at 2.5 ml solution along with other larger molecules. The pure 48 kDa proMMP-9ΔH-HPX protease came out of the column is shown in the following elution fractions. The 48 kDa proMMP-9ΔH-HPX protease is indicated by an arrow in the figure.

In order to verify the purity of the 48 kDa proMMP-9ΔH-HPX that occurred in the fractions after the void volume, fractions 6-8 contained the highest protease activity (Fig. 38) were pooled together. This pooled fraction was subjected to SDS-PAGE under reducing and non-reducing conditions. A single band of around 48 kDa was observed under both reducing and non-reducing conditions (Fig. 39). Thus, we could then conclude that we were able to separate the expected 48 kDa protease from the contaminating proteases using a Sephadex G-75 size exclusion chromatography column (Fig.39).

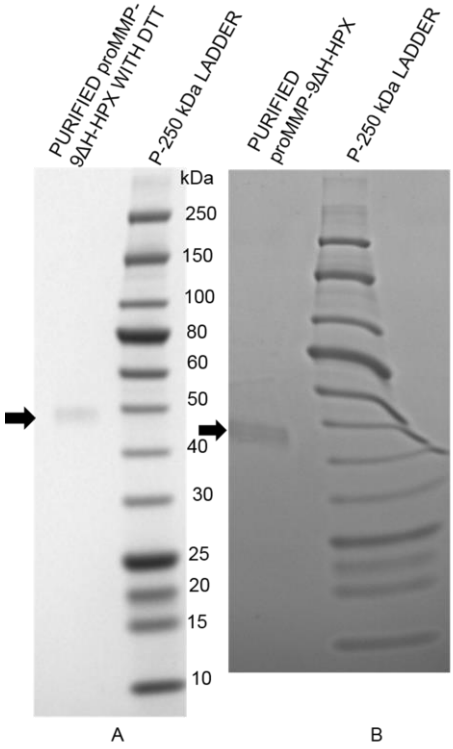

Figure 39. SDS-PAGE analysis of purified 48 kDa proMMP-9ΔH-HPX protease. A. Under reducing condition a single 48 kDa protease was detected and **B**. Under non-reducing condition the same 48 kDa protease was also detected. Protein marker P-250 kDa was used to estimate the molecular size of purified protease. The expected 48 kDa of protease is indicated by arrows in the figure.

In conclusion, a diagram is outlined to show all the techniques used in the present study to produce and purify the recombinant proMMP-9ΔH-HPX. The analytical tools used for verifying the production, activity and purity of proMMP-9ΔH-HPX was also summarized in the diagram.

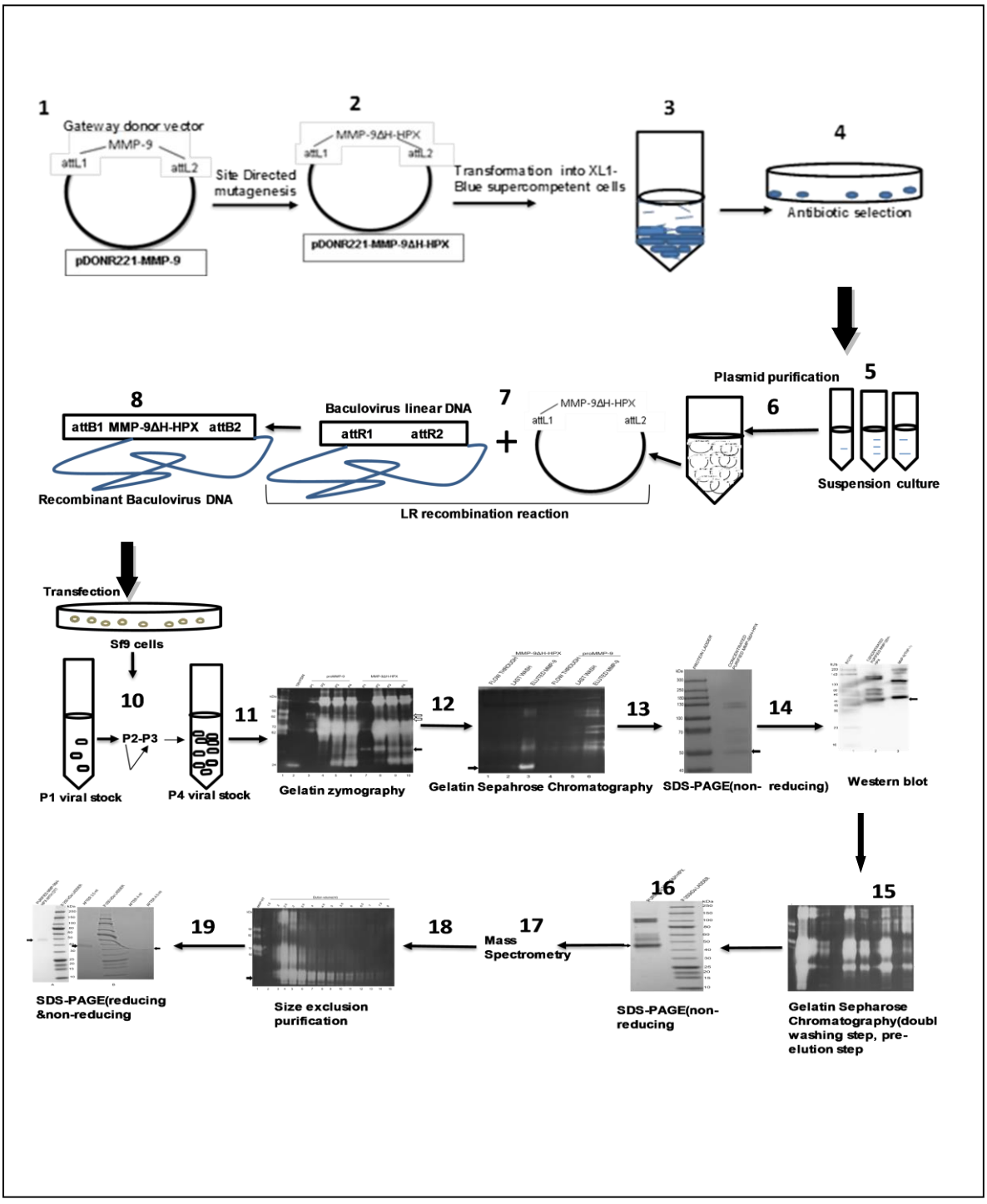

Figure 40. A diagram summarizing the different steps of proMMP-9ΔH-HPX production and purification.

Furthermore, a flow chart of proposed purification procedure of proMMP-9ΔH-HPX is given below:

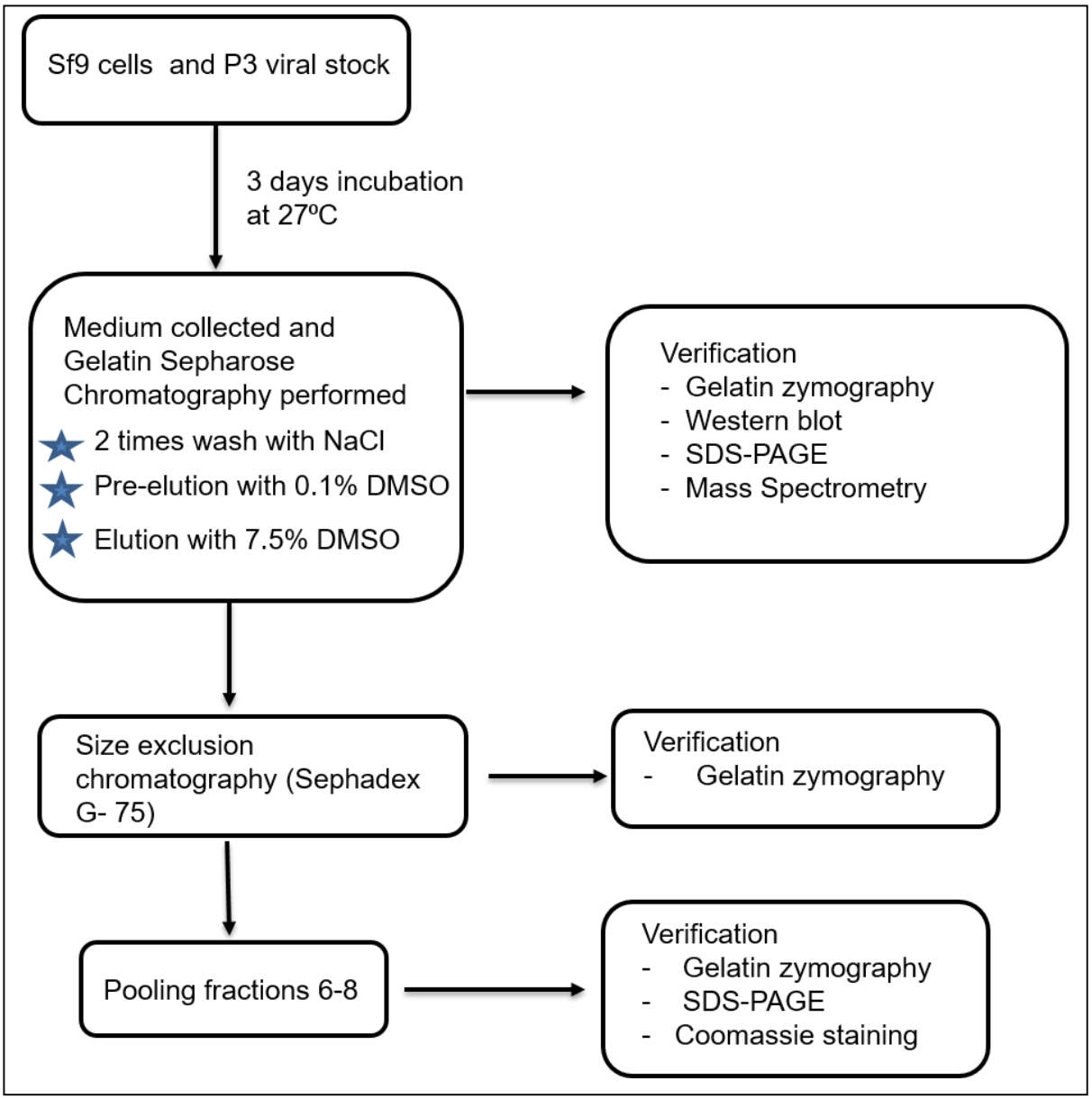

Figure 41. A flow chart of proposed purification procedure of proMMP-9ΔH-HPX.

Concluding remarks

In conclusion, we were able to produce and purify the expected 48 kDa proMMP-9ΔH-HPX protease, however in small quantity. The identity of the protease was confirmed by Western blot with an anti-MMP-9 antibody and by Mass spectrometry. The activity of the protease was confirmed by Gelatin Zymography. The purity of the expected protease was determined by SDS-PAGE and Coomassie blue protein staining for visualisation.

Future prospective

Even though at the end of the current project we were able to produce purified proMMP-9ΔH-HPX protease in Sf9 insect cells, the yield of the purified protease was not sufficient for further investigations. Therefore, the purification procedure needs to be optimized for large scale proMMP-9ΔH-HPX production.

Since full length MMP-9 has numerous roles in both physiological and pathological conditions, the truncated MMP-9ΔH-HPX in combination with full length MMP-9 can be useful in studying these conditions *in vitro*. The MMP-9ΔH-HPX protein can also be used to explore the influence of the hinge and the hemopexin domain on cleavage of a number of known substrates of MMP-9 since both domains contain secondary binding sites (exosites) for many substrates. TIMP-1 is known to bind to the C-terminal hemopexin domain and play significant role in MMP-9 activation (O'Connell et al., 1994). The deletion variant can be used to study the binding sites of the TIMP-1.

MMP-9 is found to bind to the low-density lipoprotein receptor-related protein-1(LRP-1) and to the membrane bound receptor, the DNA repair protein Ku by hemopexin domain (Monferran et al., 2004). In addition, the hinge region has been shown to be involved in proper orientation of the hemopexin domain (Van den Steen, 2006). Therefore, the deletion variant of proMMP-9 can be used for more detailed studies of the role of the hemopexin domain and hinge region in endocytosis of MMP-9. Full length MMP-9 is involved in many physiological process such as cell migration, wound healing, tissue remodelling etc. Using the MMP-9ΔH-HPX protease, the role of the hinge and hemopexin domain in these process can be elucidated.

References:

Alberts, B., J.A., Lewis J, et al. (2002). Molecular Biology of the Cell. In the Extracellular Matrix of Animals. 4th edition, New York Garland Science, 1-19.

Arnold, M. S. and Kaufman, R. J. (2003). Protein synthesis, folding, modification, and secretion in mammalian cells. New Comprehensive Biochemistry, *38*, 411-432.

Bannikov, G.A., Karelina, T.V., Collier, I.E., Marmer, B.L., and Goldberg, G.I. (2002). Substrate binding of gelatinase B induces its enzymatic activity in the presence of intact propeptide. J Biol Chem *277*, 16022-16027.

Bieniossek, C., Imasaki, T., Takagi, Y., and Berger, I. (2012). MultiBac: expanding the research toolbox for multiprotein complexes. Trends Biochem Sci *37*, 49-57.

Bouchard, F., Belanger, S.D., Biron-Pain, K., and St-Pierre, Y. (2010). EGR-1 activation by EGF inhibits MMP-9 expression and lymphoma growth. Blood *116*, 759-766.

Bourguet, E., et al (2012). Pharmacomodulation of Broad Spectrum Matrix Metalloproteinase Inhibitors Towards Regulation of Gelatinases, Enzyme Inhibition and Bioapplications.

Brzezinska, A. A., Johnson, J.L., Munafo, D.B., Crozat, K., Beutler, B., Kiosses, W.B., Ellis, B.A., and Catz, S.D. (2008). The Rab27a effectors JFC1/Slp1 and Munc13-4 regulate exocytosis of neutrophil granules. Traffic *9*, 2151-2164.

Burg-Roderfeld, M., Roderfeld, M., Wagner, S., Henkel, C., Grotzinger, J., and Roeb, E. (2007). MMP-9-hemopexin domain hampers adhesion and migration of colorectal cancer cells. Int J Oncol *30*, 985-992.

Busti, C., Falcinelli, E., Momi, S., and Gresele, P. (2010). Matrix metalloproteinases and peripheral arterial disease. Internal and emergency medicine *5*, 13-25.

Butler, G.S., Apte, S.S., Willenbrock, F., and Murphy, G. (1999). Human tissue inhibitor of metalloproteinases 3 interacts with both the N- and C-terminal domains of gelatinases A and B - Regulation by polyanions. J Biol Chem *274*, 10846-10851.

Cauwe, B., and Opdenakker, G. (2010). Intracellular substrate cleavage: a novel dimension in the biochemistry, biology and pathology of matrix metalloproteinases. Crit Rev Biochem Mol *45*, 351-423.

Cawston, T.E., and Young, D.A. (2010). Proteinases involved in matrix turnover during cartilage and bone breakdown. Cell Tissue Res *339*, 221-235.

Cha, H., Kopetzki, E., Huber, R., Lanzendorfer, M., and Brandstetter, H. (2002a). Structural basis of the adaptive molecular recognition by MMP9. J Mol Biol *320*, 1065-1079.

Cheshenko, N., Krougliak, N., Eisensmith, R.C., and Krougliak, V.A. (2001). A novel system for the production of fully deleted adenovirus vectors that does not require helper adenovirus. Gene Ther *8*, 846-854.

Descamps, F.J., Van den Steen, P.E., Martens, E., Ballaux, F., Geboes, K., and Opdenakker, G. (2003). Gelatinase B is diabetogenic in acute and chronic pancreatitis by cleaving insulin. Faseb Journal *17*, 887-9.

Dufour, A., Sampson, N.S., Li, J., Kuscu, C., Rizzo, R.C., DeLeon, J.L., Zhi, J., Jaber, N., Liu, E., Zucker, S., *et al.* (2011). Small-Molecule Anticancer Compounds Selectively Target the Hemopexin Domain of Matrix Metalloproteinase-9. Cancer Res *71*, 4977-4988.

Dufour, A., Sampson, N.S., Zucker, S., and Cao, J. (2008a). Role of the Hemopexin Domain of Matrix Metalloproteinases in Cell Migration. J Cell Physiol *217*, 643-651.

Dufour, A., Sampson, N.S., Zucker, S., and Cao, J. (2008b). Role of the hemopexin domain of matrix metalloproteinases in cell migration. Journal of cellular physiology *217*, 643-651.

Dwek, M.V., Brooks, S.A., and Schumacher, U. (2012). Metastasis research protocols, 2nd edn (New York: Humana Press : Springer).

Dwek, R.A. (1996). Glycobiology: Toward Understanding the Function of Sugars. Chemical reviews *96*, 683-720.

Elkins, P.A., Ho, Y.S., Smith, W.W., Janson, C.A., D'Alessio, K.J., McQueney, M.S., Cummings, M.D., Romanic, A.M. (2002). Crystal structure of human matrix metalloproteinase MMP9 (gelatinase B). Acta Crystallogr,SectD *58*, 1182-1192.

Estella, C., Herrer, I., Atkinson, S.P., et.al. (2012). Inhibition of histone deacetylase activity in human endometrial stromal cells promotes extracellular matrix remodelling and limits embryo invasion. PloS one *7*, e30508.

Fahling, M., Steege, A., Perlewitz, A., Nafz, B., Mrowka, R., Persson, P.B., and Thiele, B.J. (2005). Role of nucleolin in posttranscriptional control of MMP-9 expression. Biochimica et biophysica acta *1731*, 32-40.

Farina, A.R., and Mackay, A.R. (2014). Gelatinase B/MMP-9 in Tumour Pathogenesis and Progression. Cancers *6*, 240-296.

Feng, X., Liu, X., Luo, Q., and Liu, B.F. (2008). Mass spectrometry in systems biology: an overview. Mass Spectrom Rev *27*, 635-660.

Fini, M.E., Cui, T.Y., Mouldovan, A., Grobelny, D., Galardy, R.E., and Fisher, S.J. (1991). An Inhibitor of the Matrix Metalloproteinase Synthesized by Rabbit Corneal Epithelium. Invest Ophth Vis Sci *32*, 2997-3001.

Flannery, C.R. (2006). MMPs and ADAMTSs: functional studies. Frontiers in bioscience : a journal and virtual library *11*, 544-569.

Fouad, A., Zouein, A. D., YuanTian, Jared A. White, Yu-Fang Jin and Merry L. Lindsey (2015). Matrix Metalloproteinase 9 (MMP-9).The Middle-Man of Post-myocardial Infarction Extracellular Matrix Remodeling. Advances in Biochemistry in Health and Disease *13,*237-259.

Frantz, C., Stewart, K.M., and Weaver, V.M. (2010). The extracellular matrix at a glance. J Cell Sci *123*, 4195-4200.

George, F.R. (2013). Baculovirus Molecular Biology, 3rd edition (Bethesda: National Center for Biotechnology Information (US).

Georgia Papavasiliou, S.S.a.M.T. (2012). Synthetic PEG Hydrogels as Extracellular Matrix Mimics for Tissue Engineering Applications, chapter 8, Reda Helmy Sammour, ISBN 978-953-51-0151-22012.

Geurts, N., Martens, E., Van Aelst, I., Proost, P., Opdenakker, G., and Van den Steen, P.E. (2008). beta-hematin interaction with the hemopexin domain of gelatinase B/MMP-9 provokes autocatalytic processing of the propeptide, thereby priming activation by MMP-3. Biochemistry-Us *47*, 2689-2699.

Ghosh, S., Parvez, M.K., Banerjee, K., Sarin, S.K., and Hasnain, S.E. (2002). Baculovirus as mammalian cell expression vector for gene therapy: An emerging strategy. Mol Ther *6*, 5-11.

Ghulam, Md. A. and Ishfaq A. S.(2013). Role of Matrix Metalloproteinases in Cancer. OMICS Group eBooks 731 Gull Ave, Foster City. CA 94404, USA.

Giraudo, E., Inoue, M., and Hanahan, D. (2004). An amino-bisphosphonate targets MMP-9-expressing macrophages and angiogenesis to impair cervical carcinogenesis. J Clin Invest *114*, 623-633.

Glick, B.R., Pasternak, J.J. Patten, C.L. . (2010). Molecular biotechnology, principles and applications of recombinant DNA (American society for microbiology), pp. 47-95, 261-271, 290-302, 677-678, 948, 965.

Goldberg, G.I., Strongin, A., Collier, I.E., Genrich, L.T., and Marmer, B.L. (1992). Interaction of 92-Kda Type-Iv Collagenase with the Tissue Inhibitor of Metalloproteinases Prevents Dimerization, Complex-Formation with Interstitial Collagenase, and Activation of the Proenzyme with Stromelysin. J Biol Chem *267*, 4583-4591.

Golub, L.M., Ramamurthy, N.S., Mcnamara, T.F., Greenwald, R.A., and Rifkin, B.R. (1991). Tetracyclines Inhibit Connective-Tissue Breakdown - New Therapeutic Implications for an Old Family of Drugs. Crit Rev Oral Biol M *2*, 297-322.

Gong, Y., Chippada-Venkata, U.D., and Oh, W.K. (2014). Roles of matrix metalloproteinases and their natural inhibitors in prostate cancer progression. Cancers *6*, 1298-1327.

Gum, R., Lengyel, E., Juarez, J., Chen, J.H., Sato, H., Seiki, M., and Boyd, D. (1996). Stimulation of 92-kDa gelatinase B promoter activity by ras is mitogen-activated protein kinase kinase 1-independent and requires multiple transcription factor binding sites including closely spaced PEA3/ets and AP-1 sequences. J Biol Chem *271*, 10672-10680.

Gupta, S.P., ed. (2012). Matrix-metalloproteinase inhibitors (Heidelberg New York Dordrecht London: Springer Basal).

Hadler-Olsen, E., Fadnes, B., Sylte, I., Uhlin-Hansen, L., and Winberg, J.O. (2011). Regulation of matrix metalloproteinase activity in health and disease. FEBS J *278*, 28-45.

Hanania, R., Sun, H.S., Xu, K., Pustylnik, S., Jeganathan, S., and Harrison, R.E. (2012). Classically activated macrophages use stable microtubules for matrix metalloproteinase-9 (MMP-9) secretion. J Biol Chem *287*, 8468-8483.

Harvima, I.T. (2008). Induction of matrix metalloproteinase-9 in keratinocytes by histamine. The Journal of investigative dermatology *128*, 2748-2750.

Hay, E.D., ed. (1991). Cell Biology of Extracellular Matrix, 2nd edn (New York and London: Plenum Press).

Hefferon, K.L., and Miller, L.K. (2002). Reconstructing the replication complex of AcMNPV. Eur J Biochem *269*, 6233-6240.

Hibbs, M.S., Hasty, K.A., Seyer, J.M., Kang, A.H., and Mainardi, C.L. (1985). Biochemical and immunological characterization of the secreted forms of human neutrophil gelatinase. J Biol Chem *260*, 2493-2500.

Hieronymus, H., and Silver, P.A. (2004). A systems view of mRNP biology. Genes & development *18*, 2845-2860.

Hobeika, M.J., Thompson, R.W., Muhs, B.E., Brooks, P.C., and Gagne, P.J. (2007a). Matrix metalloproteinases in peripheral vascular disease. Journal of vascular surgery *45*, 849-857.

Hobeika, M.J., Thompson, R.W., Muhs, B.E., Brooks, P.C., and Gagne, P.J. (2007b). Matrix metalloproteinases in peripheral vascular disease. J Vasc Surg *45*, 849-857.

Hu, J., Fiten, P., Van den Steen, P.E., Chaltin, P., and Opdenakker, G. (2005). Simulation of evolution-selected propeptide by high-throughput selection of a peptidomimetic inhibitor on a capillary DNA sequencer platform. Anal Chem *77*, 2116-2124.

Hu, J.L., Van den Steen, P.E., Sang, Q.X.A., and Opdenakker, G. (2007). Matrix metalloproteinase inhibitors as therapy for inflammatory and vascular diseases. Nat Rev Drug Discov *6*, 480-498.

Homo sapiens Annotation Release 107, GRCh38.p2 (NCBI).

Jarvelainen, H., Sainio, A., Koulu, M., Wight, T.N., and Penttinen, R. (2009). Extracellular matrix molecules: potential targets in pharmacotherapy. Pharmacol Rev *61*, 198-223.

Jodele, S., Blavier, L., Yoon, J.M., and DeClerck, Y.A. (2006). Modifying the soil to affect the seed: role of stromal-derived matrix metalloproteinases in cancer progression. Cancer metastasis reviews *25*, 35-43.

Jovanovic, D.V., Martel-Pelletier, J., Di Battista, J.A., Mineau, F., Jolicoeur, F.C., Benderdour, M., and Pelletier, J.P. (2000). Stimulation of 92-kd gelatinase (matrix metalloproteinase 9) production by interleukin-17 in human monocyte/macrophages - A possible role in rheumatoid arthritis. Arthritis Rheum *43*, 1134-1144.

Khan, M.M., Simizu, S., Suzuki, T., Masuda, A., Kawatani, M., Muroi, M., Dohmae, N., and Osada, H. (2012). Protein disulfide isomerase-mediated disulfide bonds regulate the gelatinolytic activity and secretion of matrix metalloproteinase-9. Experimental cell research *318*, 904-914.

Kost, T.A., Condreay, J.P., and Jarvis, D.L. (2005). Baculovirus as versatile vectors for protein expression in insect and mammalian cells. Nat Biotechnol *23*, 567-575.

Kotra, L.P., Zhang, L., Fridman, R., Orlando, R., and Mobashery, S. (2002). N-Glycosylation pattern of the zymogenic form of human matrix metalloproteinase-9. Bioorganic chemistry *30*, 356-370.

Kovacs, G.R., Guarino, L.A., and Summers, M.D. (1991). Novel Regulatory Properties of the Ie1 and Ie0 Transactivators Encoded by the Baculovirus Autographa-Californica Multicapsid Nuclear Polyhedrosis-Virus. J Virol *65*, 5281-5288.

Lamar, J.M., Pumiglia, K.M., and DiPersio, C.M. (2008). An immortalization-dependent switch in integrin function up-regulates MMP-9 to enhance tumor cell invasion. Cancer Res *68*, 7371-7379.

Landy, A. (1989). Dynamic, structural, and regulatory aspects of lambda site-specific recombination. Annual review of biochemistry *58*, 913-949.

Lee, J.H., and Welch, D.R. (1997). Suppression of metastasis in human breast carcinoma MDA-MB-435 cells after transfection with the metastasis suppressor gene, KiSS-1. Cancer Res *57*, 2384-2387.

Lin, C.Y., Tsai, P.H., Kandaswami, C.C., Lee, P.P., Huang, C.J., Hwang, J.J., and Lee, M.T. (2011). Matrix metalloproteinase-9 cooperates with transcription factor Snail to induce epithelial-mesenchymal transition. Cancer Sci *102*, 815-827.

Mackay, A.R., Ballin, M., Pelina, M.D., Farina, A.R., Nason, A.M., Hartzler, J.L., and Thorgeirsson, U.P. (1992). Effect of phorbol ester and cytokines on matrix metalloproteinase and tissue inhibitor of metalloproteinase expression in tumor and normal cell lines. Invasion & metastasis *12*, 168-184.

Malla, N., Berg, E., Theocharis, A.D., Svineng, G., Uhlin-Hansen, L., and Winberg, J.O. (2013). Invitro reconstitution of complexes between pro-matrix metalloproteinase-9 and the proteoglycans serglycin and versican. Febs Journal *280*, 2870-2887.

Malla, N., Berg, E., Uhlin-Hansen, L., and Winberg, J.O. (2008). Interaction of pro-matrix metalloproteinase-9/proteoglycan heteromer with gelatin and collagen. J Biol Chem *283*, 13652-13665.

Maolood, N., Hardin-Pouzet, H., and Grange-Messent, V. (2008). Matrix metalloproteinases MMP2 and MMP9 are upregulated by noradrenaline in the mouse neuroendocrine hypothalamus. The European journal of neuroscience *27*, 1143-1152.

Massova, I., Kotra, L.P., Fridman, R., and Mobashery, S. (1998). Matrix metalloproteinases: structures, evolution, and diversification. FASEB journal : official publication of the Federation of American Societies for Experimental Biology *12*, 1075-1095.

Mayo, M.W., Denlinger, C.E., Broad, R.M., Yeung, F., Reilly, E.T., Shi, Y., and Jones, D.R. (2003). Ineffectiveness of histone deacetylase inhibitors to induce apoptosis involves the transcriptional activation of NF-kappa B through the Akt pathway. The Journal of biological chemistry *278*, 18980-18989.

McQuibban, G.A., Gong, J.H., Wong, J.P., Wallace, J.L., Clark-Lewis, I., and Overall, C.M. (2002). Matrix metalloproteinase processing of monocyte chemoattractant proteins generates CC chemokine receptor antagonists with anti-inflammatory properties in vivo. Blood *100*, 1160-1167.

Mehta, P.B., Jenkins, B.L., McCarthy, L., Thilak, L., Robson, C.N., Neal, D.E., and Leung, H.Y. (2003). MEK5 overexpression is associated with metastatic prostate cancer, and stimulates proliferation, MMP-9 expression and invasion. Oncogene *22*, 1381-1389.

Monferran, S., Paupert, J., Dauvillier, S., Salles, B., and Muller, C. (2004). The membrane form of the DNA repair protein Ku interacts at the cell surface with metalloproteinase 9. Embo J *23*, 3758-3768.

Murphy, G., and Crabbe, T. (1995). Gelatinases A and B. Methods Enzymol *248*, 470-484.

Murphy, G., Houbrechts, A., Cockett, M.I., Williamson, R.A., Oshea, M., and Docherty, A.J.P. (1991). The N-Terminal Domain of Tissue Inhibitor of Metalloproteinases Retains Metalloproteinase Inhibitory Activity. Biochemistry *30*, 8097-8101.

Murphy, G.a.T.C. (1995). Gelatinase-A and Gelatinase-B. Proteolytic Enzymes: Aspartic and Metallo Peptidases. *248*, 470-484.

Nagase, H., Visse, R., and Murphy, G. (2006). Structure and function of matrix metalloproteinases and TIMPs. Cardiovascular research *69*, 562-573.

O'Connell, J.P., Willenbrock, F., Docherty, A.J., Eaton, D., and Murphy, G. (1994). Analysis of the role of the COOH-terminal domain in the activation, proteolytic activity, and tissue inhibitor of metalloproteinase interactions of gelatinase B. The Journal of biological chemistry *269*, 14967-14973.

O'Farrell, T.J., and Pourmotabbed, T. (1998). The fibronectin-like domain is required for the type V and XI collagenolytic activity of gelatinase B. Arch Biochem Biophys *354*, 24-30.

O'Reilly, D.R., Miller, L. K. and Luckow, V. A. (1994). Baculovirus expression vectors: A laboratory manual.Oxford University press, ISBN 0-29-509131-0.

Oconnell, J.P., Willenbrock, F., Docherty, A.J.P., Eaton, D., and Murphy, G. (1994). Analysis of the Role of the Cooh-Terminal Domain in the Activation, Proteolytic Activity, and Tissue Inhibitor of Metalloproteinase Interactions of Gelatinase-B. J Biol Chem *269*, 14967-14973.

Okada, Y., Gonoji, Y., Naka, K., Tomita, K., Nakanishi, I., Iwata, K., Yamashita, K., and Hayakawa, T. (1992). Matrix metalloproteinase 9 (92-kDa gelatinase/type IV collagenase) from HT 1080 human fibrosarcoma cells. Purification and activation of the precursor and enzymic properties. J Biol Chem *267*, 21712-21719.

Olson, M.W., Bernardo, M.M., Pietila, M., Gervasi, D.C., Toth, M., Kotra, L.P., Massova, I., Mobashery, S., and Fridman, R. (2000). Characterization of the monomeric and dimeric forms of latent and active matrix metalloproteinase-9. Differential rates for activation by stromelysin 1. J Biol Chem *275*, 2661-2668.

Opdenakker, G., Van den Steen, P.E., Dubois, B., Nelissen, I., Van Coillie, E., Masure, S., Proost, P., and Van Damme, J. (2001a). Gelatinase B functions as regulator and effector in leukocyte biology. Journal of leukocyte biology *69*, 851-859.

Opdenakker, G., Van den Steen, P.E., and Van Damme, J. (2001b). Gelatinase B: a tuner and amplifier of immune functions. Trends Immunol *22*, 571-579.

Opdenakker, G., Van den Steen, P.E., and Van Damme, J. (2001c). Gelatinase B: a tuner and amplifier of immune functions. Trends in immunology *22*, 571-579.

Ra, H.J., and Parks, W.C. (2007). Control of matrix metalloproteinase catalytic activity. Matrix biology : journal of the International Society for Matrix Biology *26*, 587-596.

Rawlings, N.D., Waller, M., Barrett, A.J., and Bateman, A. (2014). MEROPS: the database of proteolytic enzymes, their substrates and inhibitors. Nucleic Acids Res *42*, D503-D509.

Roeb, E., Schleinkofer, K., Kernebeck, T., Potsch, S., Jansen, B., Behrmann, I., Matern, S., and Grotzinger, J. (2002). The matrix metalloproteinase 9 (MMP-9) hemopexin domain is a novel gelatin binding domain and acts as an antagonist. J Biol Chem *277*, 50326-50332.

Rosenblum, G., Van den Steen, P.E., Cohen, S.R., Grossmann, J.G., Frenkel, J., Sertchook, R., Slacks, N., Strange, R.W., Opdenakker, G., and Sagi, I. (2007). Insights into the structure and domain flexibility of full-length pro-matrix metalloproteinase-9/gelatinase B. Structure *15*, 1227-1236.

Roy, R., Yang, J., and Moses, M.A. (2009). Matrix Metalloproteinases As Novel Biomarkers and Potential Therapeutic Targets in Human Cancer. J Clin Oncol *27*, 5287-5297.

Salo, T., Soini, Y., Oiva, J., Kariylitalo, Nissinen, A., Biancari, F., Juvonen, T., and Satta, J. (2006). Chemically modified tetracyclines (CMT-3 and CMT-8) enable control of the pathologic remodellation of human aortic valve stenosis via MMP-9 and VEGF inhibition. International journal of cardiology *111*, 358-364.

Sans-Fons, M.G., Sole, S., Sanfeliu, C., and Planas, A.M. (2010). Matrix metalloproteinase-9 and cell division in neuroblastoma cells and bone marrow macrophages. The American journal of pathology *177*, 2870-2885.

Sato, N., Maehara, N., Su, G.H., and Goggins, M. (2003). Effects of 5-aza-2'-deoxycytidine on matrix metalloproteinase expression and pancreatic cancer cell invasiveness. Journal of the National Cancer Institute *95*, 327-330.

Schaefer, L., and Schaefer, R.M. (2010). Proteoglycans: from structural compounds to signaling molecules. Cell Tissue Res *339*, 237-246.

Sheikh, G.M.A.a.I.A., ed. (2013). Role of Matrix Metalloproteinases in Cancer (OMICS Group eBooks 731 Gull Ave, Foster City. CA 94404, USA).

Shimajiri, S., Arima, N., Tanimoto, A., Murata, Y., Hamada, T., Wang, K.Y., and Sasaguri, Y. (1999). Shortened microsatellite d(CA)21 sequence down-regulates promoter activity of matrix metalloproteinase 9 gene. FEBS letters *455*, 70-74.

Sier, C.F.M., Casetta, G., Verheijen, J.H., Tizzani, A., Agape, V., Kos, J., Blasi, F., and Hanemaaijer, R. (2000). Enhanced urinary gelatinase activities (matrix metalloproteinases 2 and 9) are associated with early-stage bladder carcinoma: A comparison with clinically used tumor markers. Clin Cancer Res *6*, 2333-2340.

Snoek-van Beurden, P.A.M., and Von den Hoff, J.W. (2005). Zymographic techniques for the analysis of matrix metalloproteinases and their inhibitors. Biotechniques *38*, 73-83.

Springman, E.B., Angleton, E.L., Birkedal-Hansen, H., and Van Wart, H.E. (1990). Multiple modes of activation of latent human fibroblast collagenase: evidence for the role of a Cys73 active-site zinc complex in latency and a "cysteine switch" mechanism for activation. Proceedings of the National Academy of Sciences of the United States of America *87*, 364-368.

St-Pierre, Y., Couillard, J., and Van Themsche, C. (2004). Regulation of MMP-9 gene expression for the development of novel molecular targets against cancer and inflammatory diseases. Expert opinion on therapeutic targets *8*, 473-489.

Steenport, M., Khan, K.M., Du, B., Barnhard, S.E., Dannenberg, A.J., and Falcone, D.J. (2009). Matrix metalloproteinase (MMP)-1 and MMP-3 induce macrophage MMP-9: evidence for the role of TNF-alpha and cyclooxygenase-2. Journal of immunology *183*, 8119-8127.

Sternlicht, M.D., and Werb, Z. (2001). How matrix metalloproteinases regulate cell behavior. Annu Rev Cell Dev Bi *17*, 463-516.

Strongin, A.Y., Collier, I.E., Krasnov, P.A., Genrich, L.T., Marmer, B.L., and Goldberg, G.I. (1993). Human 92 kDa type IV collagenase: functional analysis of fibronectin and carboxyl-end domains. Kidney Int *43*, 158-162.

Takagi, S., Simizu, S., and Osada, H. (2009). RECK negatively regulates matrix metalloproteinase-9 transcription. Cancer Res *69*, 1502-1508.

Thieringer, F.R., Maass, T., Anthon, B., Meyer, E., Schirmacher, P., Longerich, T., Galle, P.R., Kanzler, S., and Teufel, A. (2012). Liver-specific overexpression of matrix metalloproteinase 9 (MMP-9) in transgenic mice accelerates development of hepatocellular carcinoma. Mol Carcinogen *51*, 439-448.

Triebel, S., Blaser, J., Reinke, H., and Tschesche, H. (1992a). A 25 Kda Alpha-2-Microglobulin-Related Protein Is a Component of the 125-Kda Form of Human Gelatinase. Febs Lett *314*, 386-388.

Triebel, S., Blaser, J., Reinke, H., and Tschesche, H. (1992b). A 25 kDa alpha 2-microglobulin-related protein is a component of the 125 kDa form of human gelatinase. FEBS letters *314*, 386-388.

Vakonakis, I., and Campbell, I.D. (2007). Extracellular matrix: from atomic resolution to ultrastructure. Curr Opin Cell Biol *19*, 578-583.

Van den Steen, P., Rudd, P.M., Dwek, R.A., and Opdenakker, G. (1998). Concepts and principles of O-linked glycosylation. Crit Rev Biochem Mol Biol *33*, 151-208.

Van den Steen, P.E., Dubois, B. Nelissen, I. Rudd, P. M. Dwek, R. A. Opdenakker, G. (2002a). Biochemistry and molecular biology of gelatinase B or matrix metalloproteinase-9 (MMP-9). Crit Rev Biochem Mol *37*, 375-536.

Van den Steen, P.E., Van Aelst, I., Hvidberg, V., Piccard, H., Fiten, P., Jacobsen, C., Moestrup, S.K., Fry, S., Royle, L., Wormald, M.R*., et al.* (2006). The hemopexin and O-glycosylated domains tune gelatinase B/MMP-9 bioavailability via inhibition and binding to cargo receptors. J Biol Chem *281*, 18626-18637.

Van den Steen, P.E.D., B. Nelissen, I. Rudd, P. M. Dwek, R. A. Opdenakker, G. (2002b). Biochemistry and molecular biology of gelatinase B or matrix metalloproteinase-9 (MMP-9). Crit Rev Biochem Mol Biol *37*, 375-536.

Van den Steen, P.E.V.A., I. Hvidberg, V. Piccard, H. Fiten, P. Jacobsen, C. Moestrup, S. K. Fry, S. Royle, L. Wormald, M. R. Wallis, R. Rudd, P. M. Dwek, R. A. Opdenakker, G. (2006). The hemopexin and O-glycosylated domains tune gelatinase B/MMP-9 bioavailability via inhibition and binding to cargo receptors. J Biol Chem *281*, 18626-18637.

Vanderwilk, F., Vanlent, J.W.M., and Vlak, J.M. (1987). Immunogold Detection of Polyhedrin, P10 and Virion Antigens in Autographa-Californica Nuclear Polyhedrosis Virus-Infected Spodoptera-Frugiperda Cells. J Gen Virol *68*, 2615-2623.

Vandooren, J., Geurts, N., Martens, E., Van den Steen, P.E., Jonghe, S.D., Herdewijn, P., and Opdenakker, G. (2011). Gelatin degradation assay reveals MMP-9 inhibitors and function of O-glycosylated domain. World journal of biological chemistry *2*, 14-24.

Vandooren, J., Van den Steen, P.E., and Opdenakker, G. (2013). Biochemistry and molecular biology of gelatinase B or matrix metalloproteinase-9 (MMP-9): the next decade. Crit Rev Biochem Mol Biol *48*, 222-272.

Vandooren, J.V.d.S., P. E. Opdenakker, G. (2013). Biochemistry and molecular biology of gelatinase B or matrix metalloproteinase-9 (MMP-9): The next decade. Crit Rev Biochem Mol *48*, 222-272.

Walker, J.M. (1984). Methods in Molecular Biology (Clifton, New jersey: Humana Press).

Wang, B.Q., Zhang, C.M., Gao, W., Wang, X.F., Zhang, H.L., and Yang, P.C. (2011). Cancer-derived matrix metalloproteinase-9 contributes to tumor tolerance. J Cancer Res Clin Oncol *137*, 1525-1533.

Watabe, T., Yoshida, K., Shindoh, M., Kaya, M., Fujikawa, K., Sato, H., Seiki, M., Ishii, S., and Fujinaga, K. (1998). The Ets-1 and Ets-2 transcription factors activate the promoters for invasion-associated urokinase and collagenase genes in response to epidermal growth factor. International journal of cancer Journal international du cancer *77*, 128-137.

Whitford, M., Stewart, S., Kuzio, J., and Faulkner, P. (1989). Identification and Sequence-Analysis of a Gene Encoding-Gp67, an Abundant Envelope Glycoprotein of the Baculovirus Autographa-Californica Nuclear Polyhedrosis-Virus. J Virol *63*, 1393-1399.

Wilhelm, S.M., Collier, I.E., Marmer, B.L., Eisen, A.Z., Grant, G.A., and Goldberg, G.I. (1989). Sv40-Transformed Human-Lung Fibroblasts Secrete a 92-Kda Type-Iv Collagenase Which Is Identical to That Secreted by Normal Human Macrophages. J Biol Chem *264*, 17213-17221.

Winberg, J.O., Berg, E., Kolset, S.O., and Uhlin-Hansen, L. (2003). Calcium-induced activation and truncation of promatrix metalloproteinase-9 linked to the core protein of chondroitin sulfate proteoglycans. Eur J Biochem *270*, 3996-4007.

Winberg, J.O., Kolset, S.O., Berg, E., and Uhlin-Hansen, L. (2000). Macrophages secrete matrix metalloproteinase 9 covalently linked to the core protein of chondroitin sulphate proteoglycans. J Mol Biol *304*, 669-680.

Wu, X., and Brewer, G. (2012). The regulation of mRNA stability in mammalian cells: 2.0. Gene *500*, 10-21.

Yabluchanskiy, A., Ma, Y., Iyer, R.P., Hall, M.E., and Lindsey, M.L. (2013). Matrix metalloproteinase-9: Many shades of function in cardiovascular disease. Physiology *28*, 391-403.

Yan, W., Zhang, W., Sun, L., Liu, Y., You, G., Wang, Y., Kang, C., You, Y., and Jiang, T. (2011). Identification of MMP-9 specific microRNA expression profile as potential targets of anti-invasion therapy in glioblastoma multiforme. Brain Res *1411*, 108-115.

Yang, E.V., Sood, A.K., Chen, M., Li, Y., Eubank, T.D., Marsh, C.B., Jewell, S., Flavahan, N.A., Morrison, C., Yeh, P.E.*, et al.* (2006). Norepinephrine up-regulates the expression of vascular endothelial growth factor, matrix metalloproteinase (MMP)-2, and MMP-9 in nasopharyngeal carcinoma tumor cells. Cancer research *66*, 10357-10364.

Yu, Q., and Stamenkovic, I. (2000). Cell surface-localized matrix metalloproteinase-9 proteolytically activates TGF-beta and promotes tumor invasion and angiogenesis. Genes & development *14*, 163-176.

Zhang, B., Ye, S., Herrmann, S.M., Eriksson, P., de Maat, M., Evans, A., Arveiler, D., Luc, G., Cambien, F., Hamsten, A.*, et al.* (1999). Functional polymorphism in the regulatory region of gelatinase B gene in relation to severity of coronary atherosclerosis. Circulation *99*, 1788-1794.

Zhang, P.F., Klutch, M., Muller, J., and Marcus-Sekura, C.J. (1994). Susceptibility of the Sf9 insect cell line to infection with adventitious viruses. Biologicals *22*, 205-213.

Zhao, W.J., Zhang, W., Li, G.L., Cui, Y., Shi, Z.F., and Yuan, F. (2012). Differential expression of MMP-9 and AQP4 in human glioma samples. Folia neuropathologica / Association of Polish Neuropathologists and Medical Research Centre, Polish Academy of Sciences *50*, 176-186.

Appendix

A1. Nucleotide sequences of *proMMP-9ΔH-HPX* aligned with wild type proMMP-9 by three different primers (mutated nucleotide was outlined in red colour)

***proMMP-9ΔH-HPX* Sequenced by M-13 forward primer**

```
                    70        80        90        100       110       120
                    |....|....|....|....|....|....|....|....|....|....|....|....|
MMP-9 geneCopoeia   ----------ATGAGCCTCTGGCAGCCCCTGGTCCTGGTGCTCCTGGTGCTGGGCTGCTG
Mutated MMP-9       AGATAGAACCATGAGCCTCTGGCAGCCCCTGGTCCTGGTGCTCCTGGTGCTGGGCTGCTG

                    130       140       150       160       170       180
                    |....|....|....|....|....|....|....|....|....|....|....|....|
MMP-9 geneCopoeia   CTTTGCTGCCCCCAGACAGCGCCAGTCCACCCTTGTGCTCTTCCCTGGAGACCTGAGAAC
Mutated MMP-9       CTTTGCTGCCCCCAGACAGCGCCAGTCCACCCTTGTGCTCTTCCCTGGAGACCTGAGAAC

                    190       200       210       220       230       240
                    |....|....|....|....|....|....|....|....|....|....|....|....|
MMP-9 geneCopoeia   CAATCTCACCGACAGGCAGCTGGCAGAGGAATACCTGTACCGCTATGGTTACACTCGGGT
Mutated MMP-9       CAATCTCACCGACAGGCAGCTGGCAGAGGAATACCTGTACCGCTATGGTTACACTCGGGT

                    250       260       270       280       290       300
                    |....|....|....|....|....|....|....|....|....|....|....|....|
MMP-9 geneCopoeia   GGCAGAGATGCGTGGAGAGTCGAAATCTCTGGGGCCTGCGCTGCTGCTTCTCCAGAAGCA
Mutated MMP-9       GGCAGAGATGCGTGGAGAGTCGAAATCTCTGGGGCCTGCGCTGCTGCTTCTCCAGAAGCA

                    310       320       330       340       350       360
                    |....|....|....|....|....|....|....|....|....|....|....|....|
MMP-9 geneCopoeia   ACTGTCCCTGCCCGAGACCGGTGAGCTGGATAGCGCCACGCTGAAGGCCATGCGAACCCC
Mutated MMP-9       ACTGTCCCTGCCCGAGACCGGTGAGCTGGATAGCGCCACGCTGAAGGCCATGCGAACCCC

                    370       380       390       400       410       420
                    |....|....|....|....|....|....|....|....|....|....|....|....|
MMP-9 geneCopoeia   ACGGTGCGGGGTCCCAGACCTGGGCAGATTCCAAACCTTTGAGGGCGACCTCAAGTGGCA
Mutated MMP-9       ACGGTGCGGGGTCCCAGACCTGGGCAGATTCCAAACCTTTGAGGGCGACCTCAAGTGGCA

                    430       440       450       460       470       480
                    |....|....|....|....|....|....|....|....|....|....|....|....|
MMP-9 geneCopoeia   CCACCACAACATCACCTATTGGATCCAAAACTACTCGGAAGACTTGCCGCGGGCGGTGAT
Mutated MMP-9       CCACCACAACATCACCTATTGGATCCAAAACTACTCGGAAGACTTGCCGCGGGCGGTGAT

                    490       500       510       520       530       540
                    |....|....|....|....|....|....|....|....|....|....|....|....|
MMP-9 geneCopoeia   TGACGACGCCTTTGCCCGCGCCTTCGCACTGTGGAGCGCGGTGACGCCGCTCACCTTCAC
Mutated MMP-9       TGACGACGCCTTTGCCCGCGCCTTCGCACTGTGGAGCGCGGTGACGCCGCTCACCTTCAC

                    550       560       570       580       590       600
                    |....|....|....|....|....|....|....|....|....|....|....|....|
MMP-9 geneCopoeia   TCGCGTGTACAGCCGGGACGCAGACATCGTCATCCAGTTTGGTGTCGCGGAGCACGGAGA
Mutated MMP-9       TCGCGTGTACAGCCGGGACGCAGACATCGTCATCCAGTTTGGTGTCGCGGAGCACGGAGA

                    610       620       630       640       650       660
                    |....|....|....|....|....|....|....|....|....|....|....|....|
MMP-9 geneCopoeia   CGGGTATCCCTTCGACGGGAAGGACGGGCTCCTGGCACACGCCTTTCCTCCTGGCCCCGG
Mutated MMP-9       CGGGTATCCCTTCGACGGGAAGGACGGGCTCCTGGCACACGCCTTTCCTCCTGGCCCCGG
```

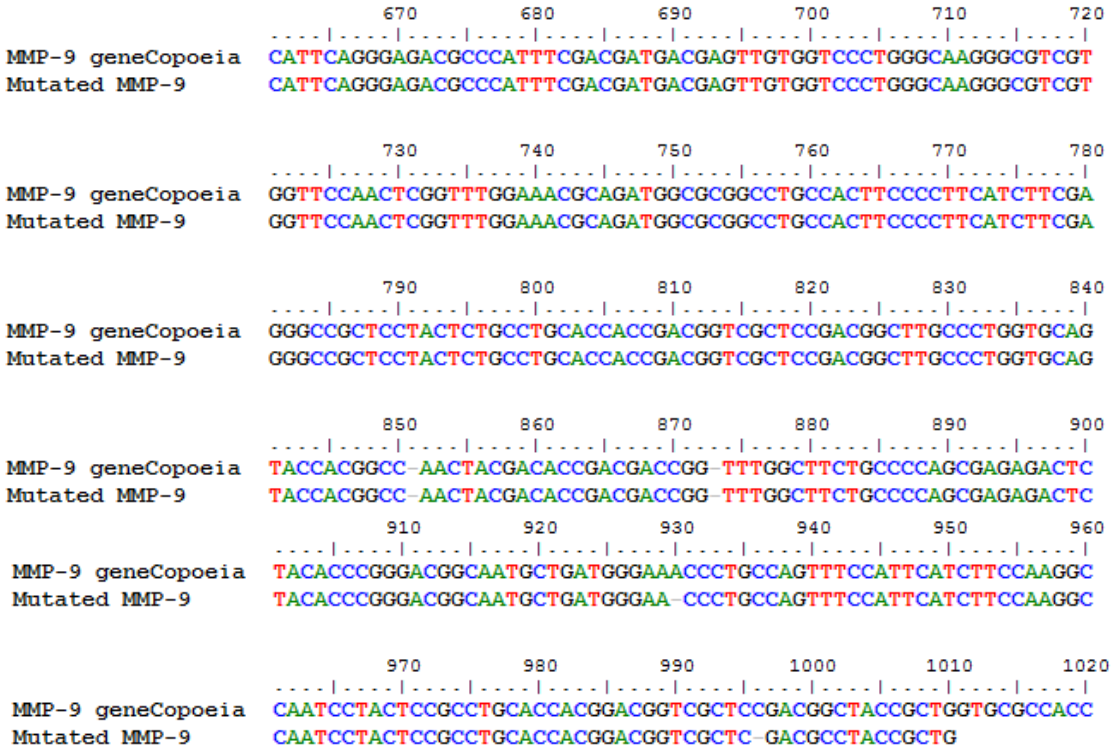
670 680 690 700 710 720
MMP-9 geneCopoeia CATTCAGGGAGACGCCCATTTCGACGATGACGAGTTGTGGTCCCTGGGCAAGGGCGTCGT
Mutated MMP-9 CATTCAGGGAGACGCCCATTTCGACGATGACGAGTTGTGGTCCCTGGGCAAGGGCGTCGT
730 740 750 760 770 780
MMP-9 geneCopoeia GGTTCCAACTCGGTTTGGAAACGCAGATGGCGCGGCCTGCCACTTCCCCTTCATCTTCGA
Mutated MMP-9 GGTTCCAACTCGGTTTGGAAACGCAGATGGCGCGGCCTGCCACTTCCCCTTCATCTTCGA
790 800 810 820 830 840
MMP-9 geneCopoeia GGGCCGCTCCTACTCTGCCTGCACCACCGACGGTCGCTCCGACGGCTTGCCCTGGTGCAG
Mutated MMP-9 GGGCCGCTCCTACTCTGCCTGCACCACCGACGGTCGCTCCGACGGCTTGCCCTGGTGCAG
850 860 870 880 890 900
MMP-9 geneCopoeia TACCACGGCC-AACTACGACACCGACGACCGG-TTTGGCTTCTGCCCCAGCGAGAGACTC
Mutated MMP-9 TACCACGGCC-AACTACGACACCGACGACCGG-TTTGGCTTCTGCCCCAGCGAGAGACTC
910 920 930 940 950 960
MMP-9 geneCopoeia TACACCCGGGACGGCAATGCTGATGGGAAACCCTGCCAGTTTCCATTCATCTTCCAAGGC
Mutated MMP-9 TACACCCGGGACGGCAATGCTGATGGGAA-CCCTGCCAGTTTCCATTCATCTTCCAAGGC
970 980 990 1000 1010 1020
MMP-9 geneCopoeia CAATCCTACTCCGCCTGCACCACGGACGGTCGCTCCGACGGCTACCGCTGGTGCGCCACC
Mutated MMP-9 CAATCCTACTCCGCCTGCACCACGGACGGTCGCTC-GACGCCTACCGCTG

proMMP-9ΔH-HPX Sequenced by second forward primer

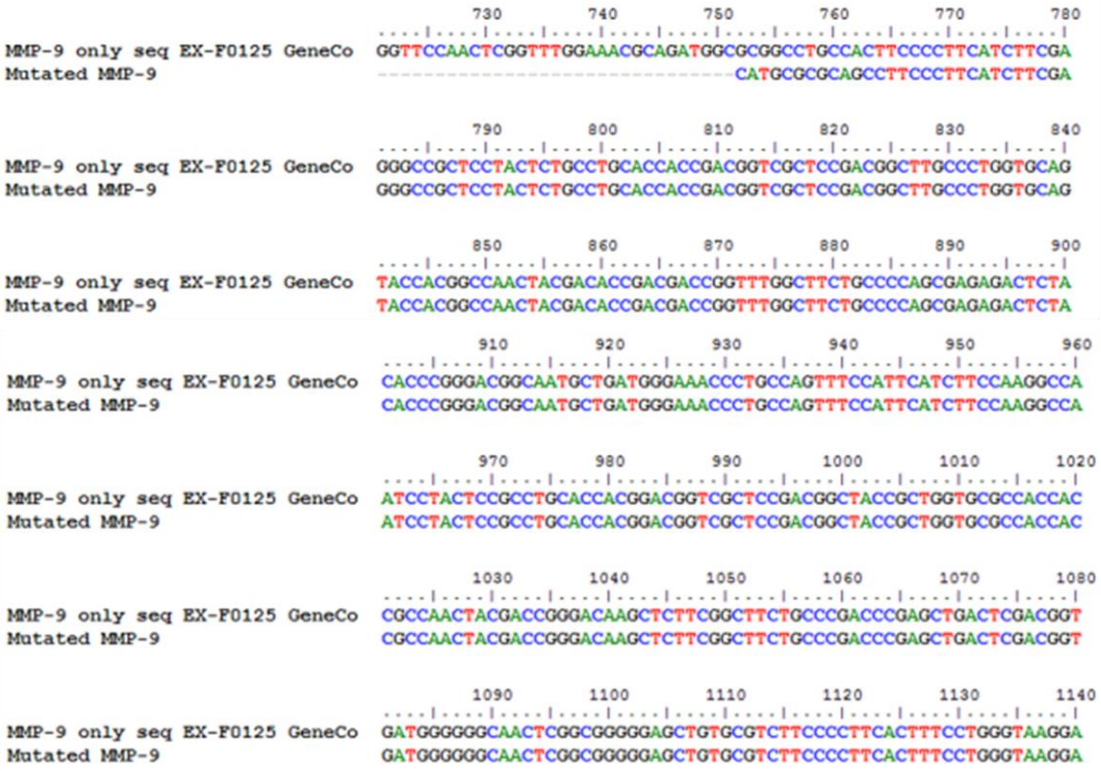

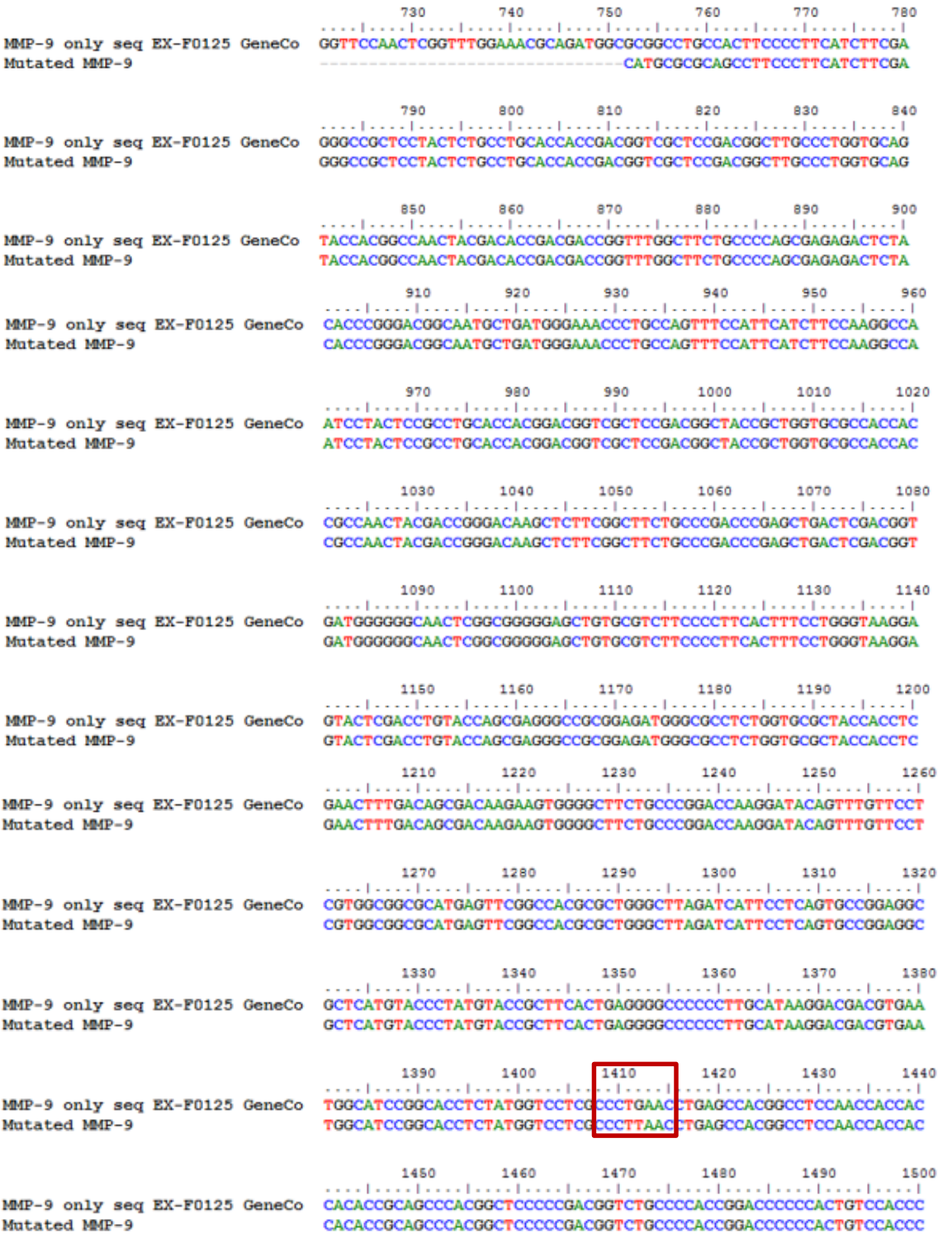
730 740 750 760 770 780
MMP-9 only seq EX-F0125 GeneCo GGTTCCAACTCGGTTTGGAAACGCAGATGGCGCGGCCTGCCACTTCCCCTTCATCTTCGA
Mutated MMP-9 CATGCGCGCAGCCTTCCCTTCATCTTCGA
790 800 810 820 830 840
MMP-9 only seq EX-F0125 GeneCo GGGCCGCTCCTACTCTGCCTGCACCACCGACGGTCGCTCCGACGGCTTGCCCTGGTGCAG
Mutated MMP-9 GGGCCGCTCCTACTCTGCCTGCACCACCGACGGTCGCTCCGACGGCTTGCCCTGGTGCAG
850 860 870 880 890 900
MMP-9 only seq EX-F0125 GeneCo TACCACGGCCAACTACGACACCGACGACCGGTTTGGCTTCTGCCCCAGCGAGAGACTCTA
Mutated MMP-9 TACCACGGCCAACTACGACACCGACGACCGGTTTGGCTTCTGCCCCAGCGAGAGACTCTA
910 920 930 940 950 960
MMP-9 only seq EX-F0125 GeneCo CACCCGGGACGGCAATGCTGATGGGAAACCCTGCCAGTTTCCATTCATCTTCCAAGGCCA
Mutated MMP-9 CACCCGGGACGGCAATGCTGATGGGAAACCCTGCCAGTTTCCATTCATCTTCCAAGGCCA
970 980 990 1000 1010 1020
MMP-9 only seq EX-F0125 GeneCo ATCCTACTCCGCCTGCACCACGGACGGTCGCTCCGACGGCTACCGCTGGTGCGCCACCAC
Mutated MMP-9 ATCCTACTCCGCCTGCACCACGGACGGTCGCTCCGACGGCTACCGCTGGTGCGCCACCAC
1030 1040 1050 1060 1070 1080
MMP-9 only seq EX-F0125 GeneCo CGCCAACTACGACCGGGACAAGCTCTTCGGCTTCTGCCCGACCCGAGCTGACTCGACGGT
Mutated MMP-9 CGCCAACTACGACCGGGACAAGCTCTTCGGCTTCTGCCCGACCCGAGCTGACTCGACGGT
1090 1100 1110 1120 1130 1140
MMP-9 only seq EX-F0125 GeneCo GATGGGGGGCAACTCGGCGGGGGAGCTGTGCGTCTTCCCCTTCACTTTCCTGGGTAAGGA
Mutated MMP-9 GATGGGGGGCAACTCGGCGGGGGAGCTGTGCGTCTTCCCCTTCACTTTCCTGGGTAAGGA
1150 1160 1170 1180 1190 1200
MMP-9 only seq EX-F0125 GeneCo GTACTCGACCTGTACCAGCGAGGGCCGCGGAGATGGGCGCCTCTGGTGCGCTACCACCTC
Mutated MMP-9 GTACTCGACCTGTACCAGCGAGGGCCGCGGAGATGGGCGCCTCTGGTGCGCTACCACCTC
1210 1220 1230 1240 1250 1260
MMP-9 only seq EX-F0125 GeneCo GAACTTTGACAGCGACAAGAAGTGGGGCTTCTGCCCGGACCAAGGATACAGTTTGTTCCT
Mutated MMP-9 GAACTTTGACAGCGACAAGAAGTGGGGCTTCTGCCCGGACCAAGGATACAGTTTGTTCCT
1270 1280 1290 1300 1310 1320
MMP-9 only seq EX-F0125 GeneCo CGTGGCGGCGCATGAGTTCGGCCACGCGCTGGGCTTAGATCATTCCTCAGTGCCGGAGGC
Mutated MMP-9 CGTGGCGGCGCATGAGTTCGGCCACGCGCTGGGCTTAGATCATTCCTCAGTGCCGGAGGC
1330 1340 1350 1360 1370 1380
MMP-9 only seq EX-F0125 GeneCo GCTCATGTACCCTATGTACCGCTTCACTGAGGGGCCCCCCTTGCATAAGGACGACGTGAA
Mutated MMP-9 GCTCATGTACCCTATGTACCGCTTCACTGAGGGGCCCCCCTTGCATAAGGACGACGTGAA
1390 1400 1410 1420 1430 1440
MMP-9 only seq EX-F0125 GeneCo TGGCATCCGGCACCTCTATGGTCCTCGCCCTGAACCTGAGCCACGGCCTCCAACCACCAC
Mutated MMP-9 TGGCATCCGGCACCTCTATGGTCCTCGCCCTTAACCTGAGCCACGGCCTCCAACCACCAC
1450 1460 1470 1480 1490 1500
MMP-9 only seq EX-F0125 GeneCo CACACCGCAGCCCACGGCTCCCCCGACGGTCTGCCCCACCGGACCCCCCACTGTCCACCC
Mutated MMP-9 CACACCGCAGCCCACGGCTCCCCCGACGGTCTGCCCCACCGGACCCCCCACTGTCCACCC

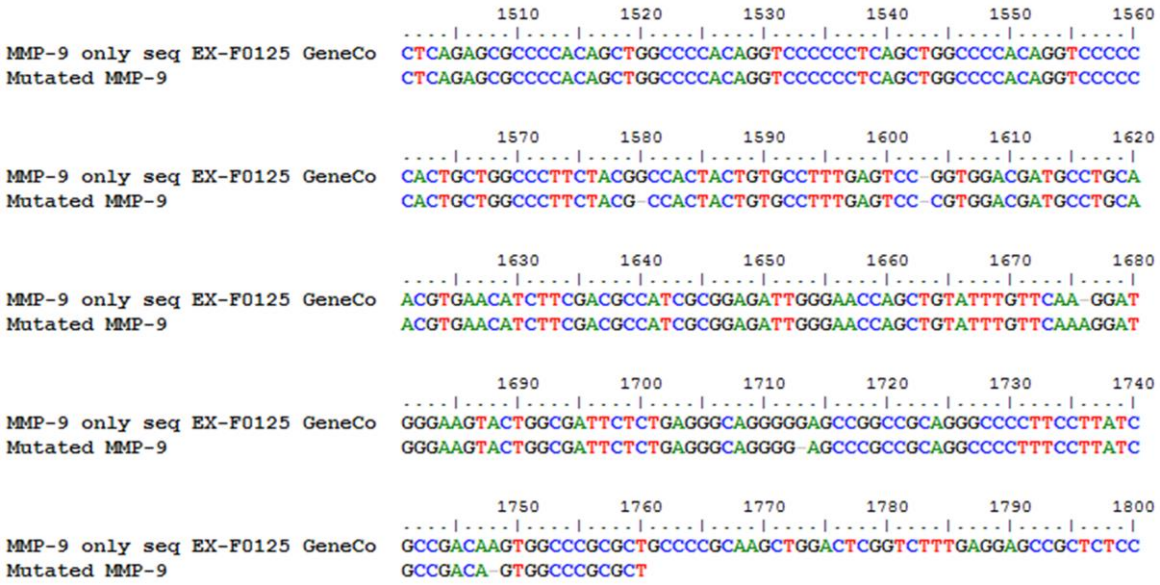

pro MMP-9ΔH-HPX sequenced by M-13 Reverse primer

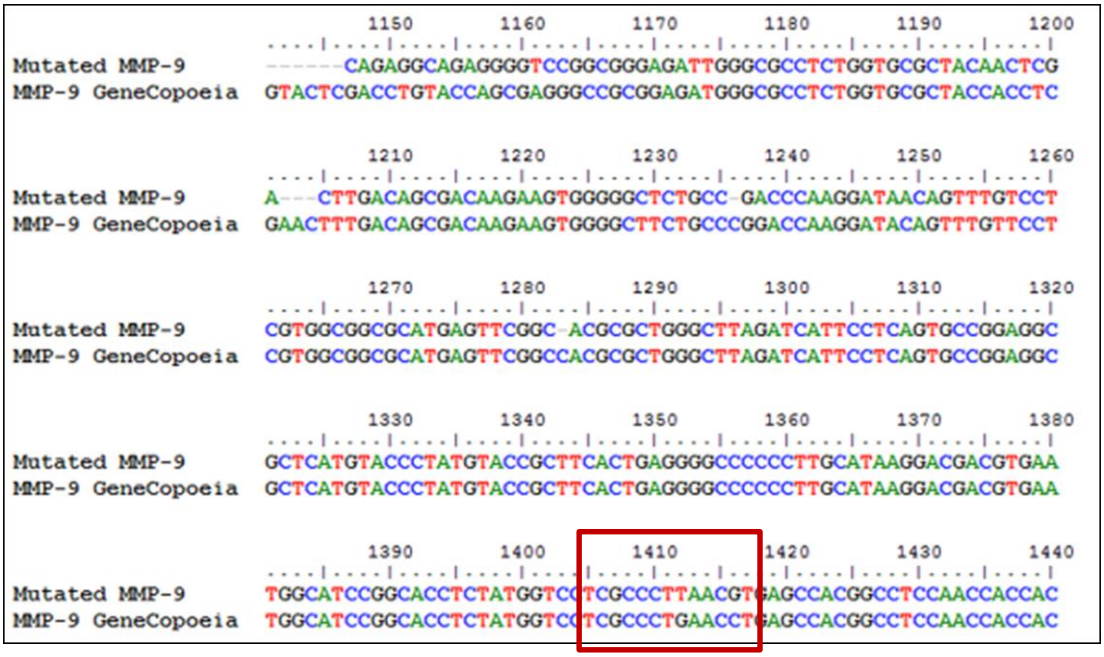

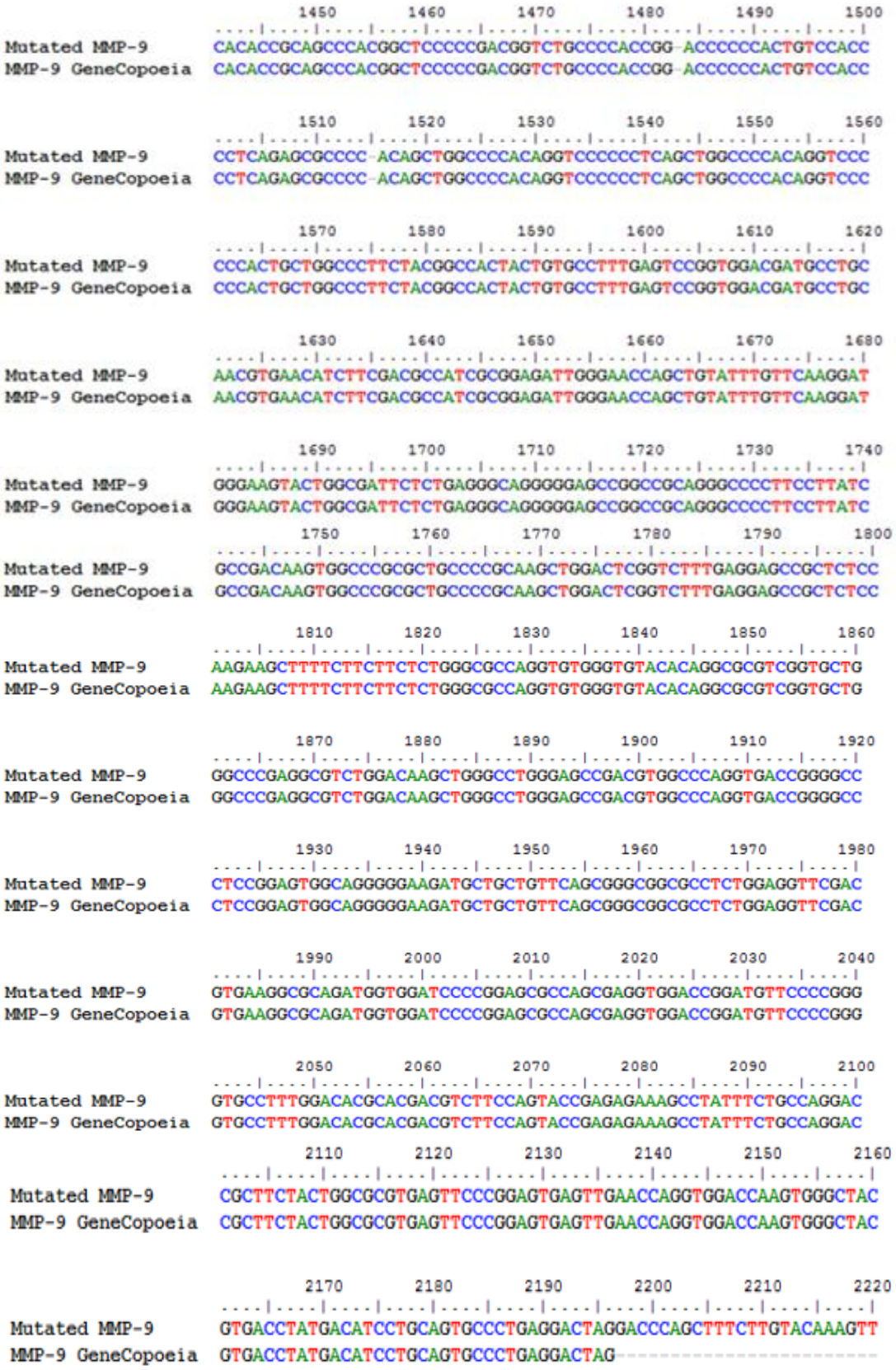
1450 1460 1470 1480 1490 1500
Mutated MMP-9 CACACCGCAGCCCACGGCTCCCCCGACGGTCTGCCCCACCGG-ACCCCCCCACTGTCCACC
MMP-9 GeneCopoeia CACACCGCAGCCCACGGCTCCCCCGACGGTCTGCCCCACCGG-ACCCCCCCACTGTCCACC
1510 1520 1530 1540 1550 1560
Mutated MMP-9 CCTCAGAGCGCCCC-ACAGCTGGCCCCACAGGTCCCCCCTCAGCTGGCCCCACAGGTCCC
MMP-9 GeneCopoeia CCTCAGAGCGCCCC-ACAGCTGGCCCCACAGGTCCCCCCTCAGCTGGCCCCACAGGTCCC
1570 1580 1590 1600 1610 1620
Mutated MMP-9 CCCACTGCTGGCCCTTCTACGGCCACTACTGTGCCTTTGAGTCCGGTGGACGATGCCTGC
MMP-9 GeneCopoeia CCCACTGCTGGCCCTTCTACGGCCACTACTGTGCCTTTGAGTCCGGTGGACGATGCCTGC
1630 1640 1650 1660 1670 1680
Mutated MMP-9 AACGTGAACATCTTCGACGCCATCGCGGAGATTGGGAACCAGCTGTATTTGTTCAAGGAT
MMP-9 GeneCopoeia AACGTGAACATCTTCGACGCCATCGCGGAGATTGGGAACCAGCTGTATTTGTTCAAGGAT
1690 1700 1710 1720 1730 1740
Mutated MMP-9 GGGAAGTACTGGCGATTCTCTGAGGGCAGGGGGAGCCGGCCGCAGGGCCCCTTCCTTATC
MMP-9 GeneCopoeia GGGAAGTACTGGCGATTCTCTGAGGGCAGGGGGAGCCGGCCGCAGGGCCCCTTCCTTATC
1750 1760 1770 1780 1790 1800
Mutated MMP-9 GCCGACAAGTGGCCCGCGCTGCCCCGCAAGCTGGACTCGGTCTTTGAGGAGCCGCTCTCC
MMP-9 GeneCopoeia GCCGACAAGTGGCCCGCGCTGCCCCGCAAGCTGGACTCGGTCTTTGAGGAGCCGCTCTCC
1810 1820 1830 1840 1850 1860
Mutated MMP-9 AAGAAGCTTTTCTTCTTCTCTGGGCGCCAGGTGTGGGTGTACACAGGCGCGTCGGTGCTG
MMP-9 GeneCopoeia AAGAAGCTTTTCTTCTTCTCTGGGCGCCAGGTGTGGGTGTACACAGGCGCGTCGGTGCTG
1870 1880 1890 1900 1910 1920
Mutated MMP-9 GGCCCGAGGCGTCTGGACAAGCTGGGCCTGGGAGCCGACGTGGCCCAGGTGACCGGGGCC
MMP-9 GeneCopoeia GGCCCGAGGCGTCTGGACAAGCTGGGCCTGGGAGCCGACGTGGCCCAGGTGACCGGGGCC
1930 1940 1950 1960 1970 1980
Mutated MMP-9 CTCCGGAGTGGCAGGGGGAAGATGCTGCTGTTCAGCGGGCGGCGCCTCTGGAGGTTCGAC
MMP-9 GeneCopoeia CTCCGGAGTGGCAGGGGGAAGATGCTGCTGTTCAGCGGGCGGCGCCTCTGGAGGTTCGAC
1990 2000 2010 2020 2030 2040
Mutated MMP-9 GTGAAGGCGCAGATGGTGGATCCCCGGAGCGCCAGCGAGGTGGACCGGATGTTCCCCGGG
MMP-9 GeneCopoeia GTGAAGGCGCAGATGGTGGATCCCCGGAGCGCCAGCGAGGTGGACCGGATGTTCCCCGGG
2050 2060 2070 2080 2090 2100
Mutated MMP-9 GTGCCTTTGGACACGCACGACGTCTTCCAGTACCGAGAGAAAGCCTATTTCTGCCAGGAC
MMP-9 GeneCopoeia GTGCCTTTGGACACGCACGACGTCTTCCAGTACCGAGAGAAAGCCTATTTCTGCCAGGAC
2110 2120 2130 2140 2150 2160
Mutated MMP-9 CGCTTCTACTGGCGCGTGAGTTCCCGGAGTGAGTTGAACCAGGTGGACCAAGTGGGCTAC
MMP-9 GeneCopoeia CGCTTCTACTGGCGCGTGAGTTCCCGGAGTGAGTTGAACCAGGTGGACCAAGTGGGCTAC
2170 2180 2190 2200 2210 2220
Mutated MMP-9 GTGACCTATGACATCCTGCAGTGCCCTGAGGACTAGGACCCAGCTTTCTTGTACAAAGTT
MMP-9 GeneCopoeia GTGACCTATGACATCCTGCAGTGCCCTGAGGACTAG----------

A2. The recombination region of the recombinant BaculoDirect™Baculovirus C-term linear DNA. LR recombination reaction between Baculovirus linear DNA and *preproMMP-9ΔH-HPX* resulted in recombinant Baculovirus containing *preproMMP-9ΔH-HPX* in the genome. Shaded region corresponds to the DNA sequence transferred from pDNOR221- *preproMMP-9ΔH-HPX* whereas the non-shaded region denote Baculovirus C-terminal linear DNA. LR product expected to include the nucleotides from the polyhedron forward primer binding site to and V5 reverse priming site including nucleotide sequence of *preproMMP-9ΔH-HPX*.